

LECTURE 11: PRESSURE SENSITIVE PAINT (PSP) & TEMPERATURE SENSITIVE PAINT (TSP) - PART 02

Dr. Hui Hu

*Martin C. Jischke Professor in Aerospace Engineering
Dept. of Aerospace Engineering, Iowa State University*

537 Bissell Road, Ames, Iowa 50011-1096, USA.

Tel: 515-294-0094 (O) / Fax: 515-294-3262 (O)

Email: huhui@iastate.edu



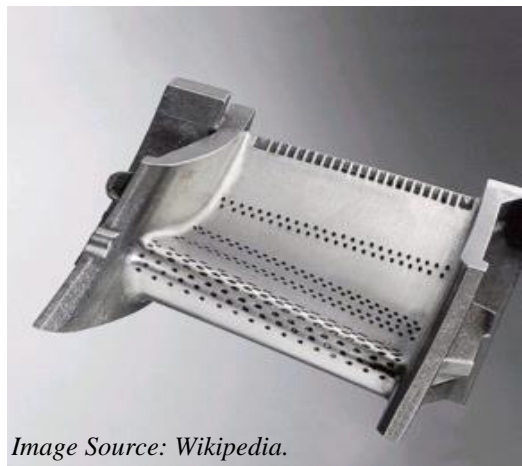
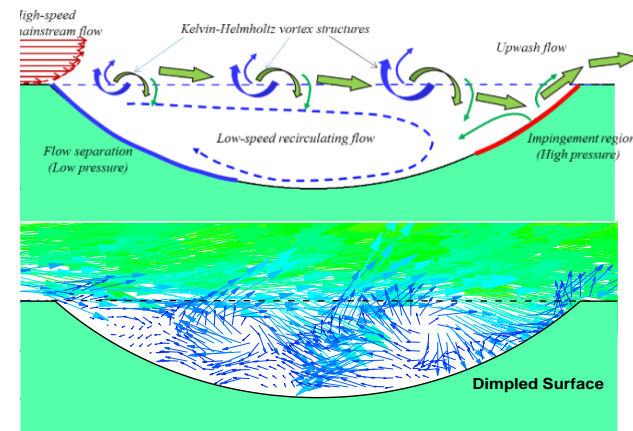
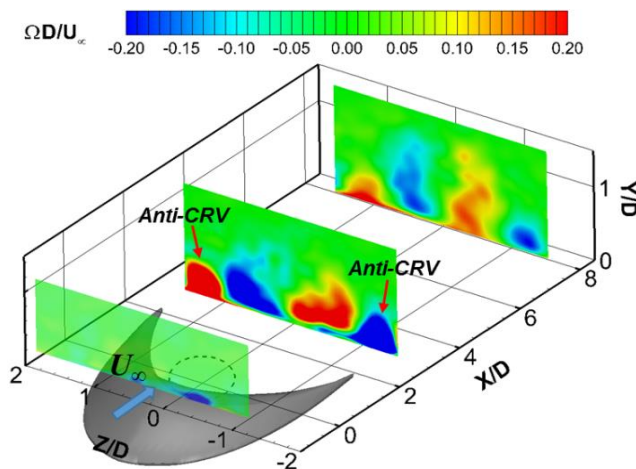


Image Source: Wikipedia.



A PSP APPLICATION TO EVALUATE NOVEL COOLING DESIGNS FOR BETTER PROTECTION OF GAS TURBINE BLADES

Dr. Hui HU

Martin C. Jischke Professor and Director

Advanced Flow Diagnostics and Experimental Aerodynamics Laboratory

Department of Aerospace Engineering, Iowa State University

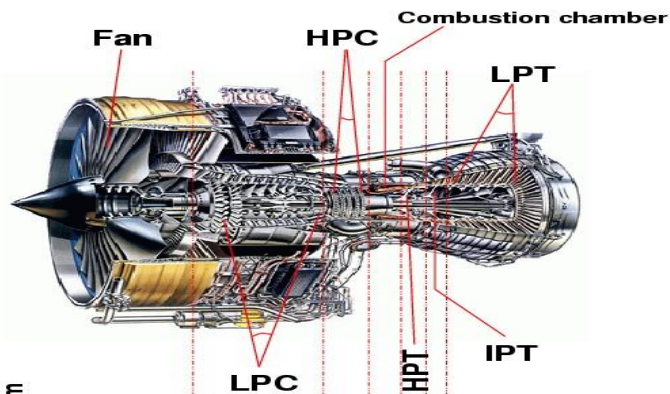
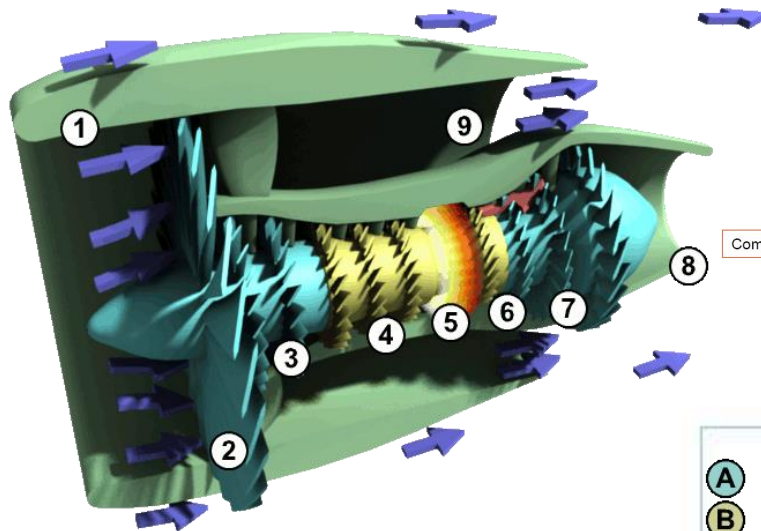
2251 Howe Hall, Ames, IA 50011-2271

Email: huhui@iastate.edu



IOWA STATE UNIVERSITY

Gas Turbines and Turbine Inlet Temperature



Temperature / °C Pressure / atm

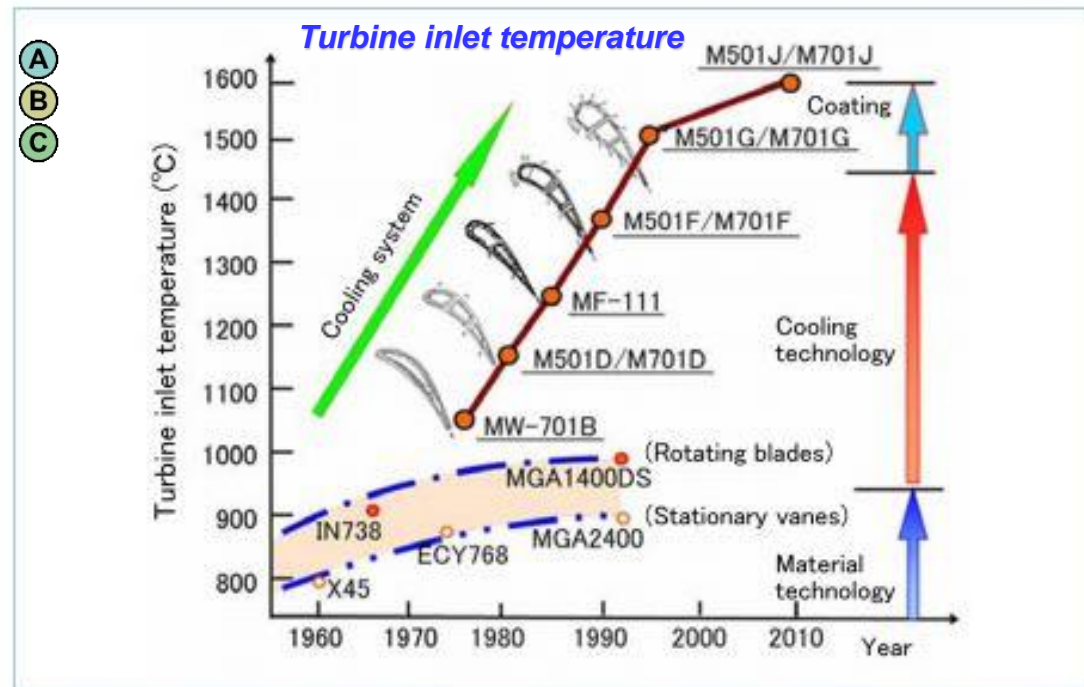
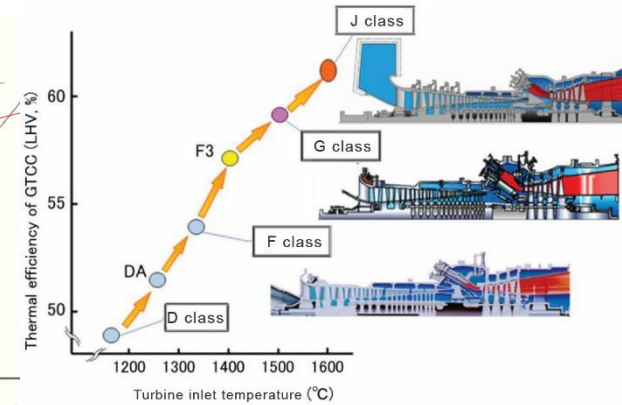
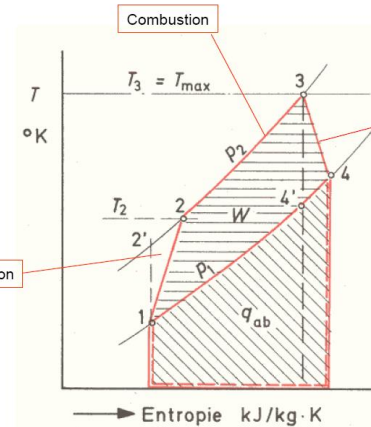
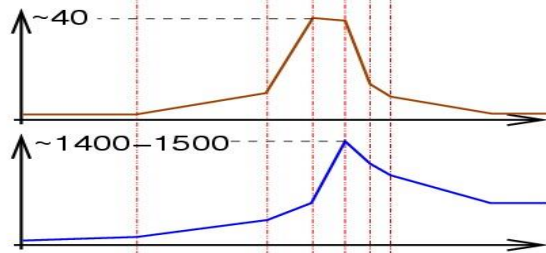


Figure 1 Increase in the turbine inlet temperature and transition of applied materials and technologies

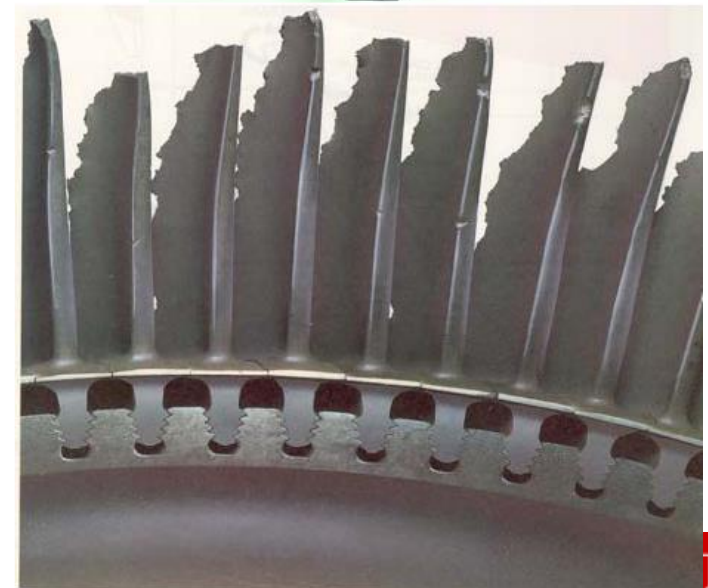
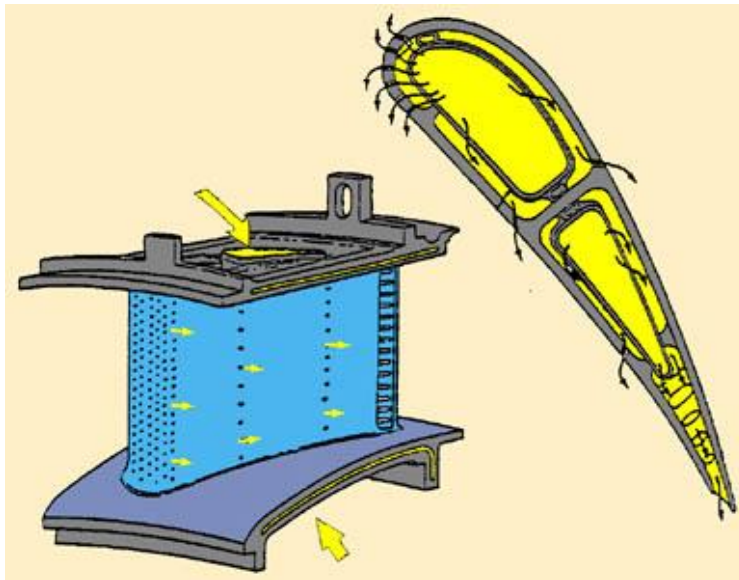
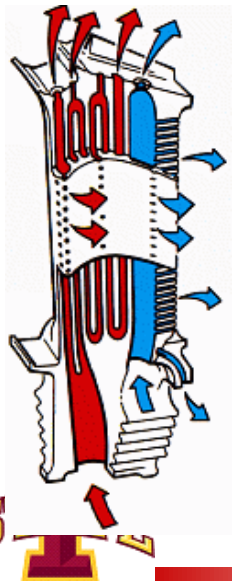
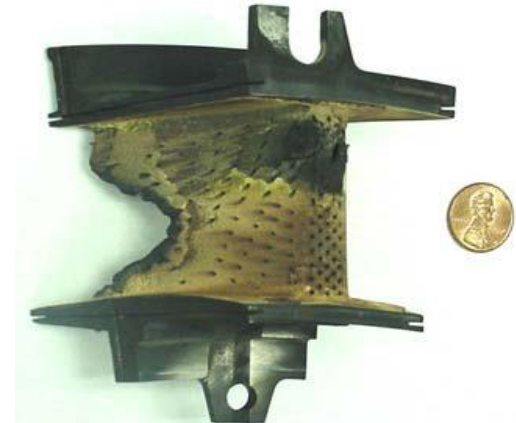
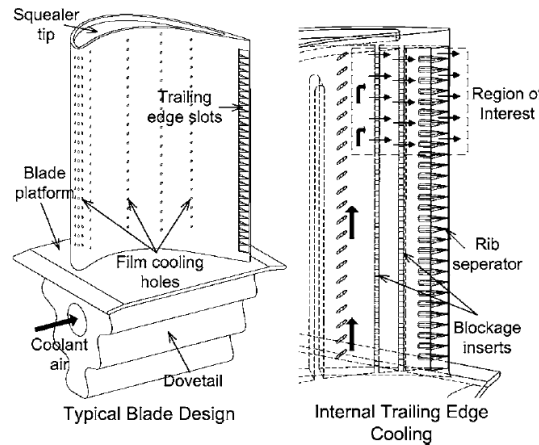
Cooling Technologies for Gas Turbine Blades



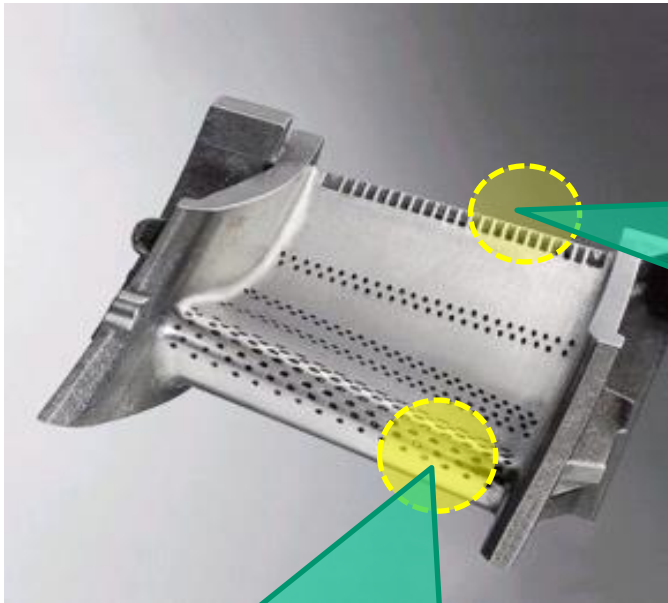
- *Turbine entry temperature:* $\sim > 3000^{\circ}\text{F}$ ($> 1650^{\circ}\text{C}$)
- *Melting point of metal:* $\sim 2400^{\circ}\text{F}$ (1300°C)

Protect turbine blades from damage:

- *New material to endure higher temperature*
- *State-of-art cooling techniques for film cooling and trailing edge cooling.*



Cooling of Gas Turbine Blades

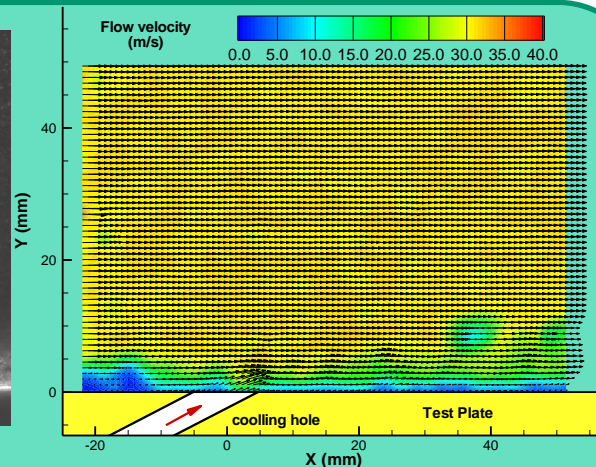


Trailing edge cooling

- Heat transfer
- Mass transfer
- Momentum transfer
-

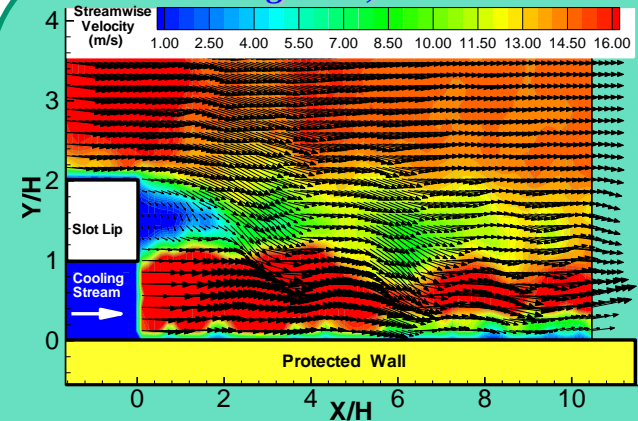
Film cooling

PIV raw image
Blowing ratio $M=0.7$

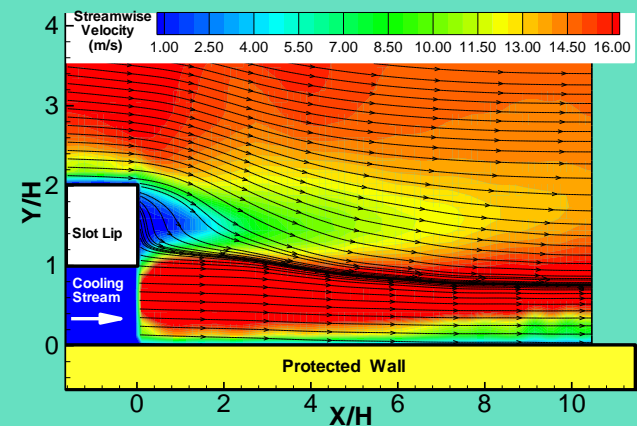


Instantaneous velocity distribution

Blowing ratio, $M=1.60$



Instantaneous velocity distributions



Time-averaged velocity distribution

Background of Film Cooling Effectiveness



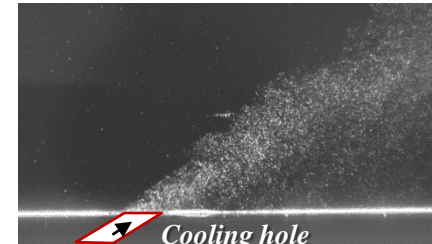
- Traditionally, the film cooling efficiency is defined based on *temperature ratio*:

$$\eta = \frac{T_{\infty} - T_{aw}}{T_{\infty} - T_c}$$

T_{aw} : *adiabatic wall temperature*
 T_{∞} : *the mainstream temperature*
 T_c : *the temperature of coolant.*

- Film cooling effectiveness is greatly affected by following factors

<i>Coolant/mainstream conditions</i>	<i>Hole geometry and configuration</i>	<i>Blade geometry (Cascade)</i>
Mass flux ratio $M = \rho_c V_c / \rho_{\infty} V_{\infty}$	Shape of hole	Cooling hole location and distribution
Density ratio $DR = \rho_c / \rho_{\infty}$	Injection angle and compound angle	Leading edge and blade tip, so on
Momentum flux ratio $I = \rho_c V_c^2 / \rho_{\infty} V_{\infty}^2 = M^2 / DR$	Hole spacing and entry length	Surface roughness
Mach number	Spacing between rows	Curvature of blade
Rotation		



Film Cooling Effectiveness – Conventional Measurement Techniques



- Film cooling effectiveness is defined by the ratio of the temperature differences

$$\eta = \frac{T_{\infty} - T_{aw}}{T_{\infty} - T_c}$$

where T_{aw} is the adiabatic wall temperature
 T_{∞} is the mainstream temperature
 T_c is the temperature of the coolant



- Traditionally, the film cooling effectiveness is determined by conducting heat transfer experiments to directly measure these three temperatures with various thermal measurement techniques, such as :
 - Surface thermocouple measurements
 - IR Thermography
 - Thermochromic crystals
 - Temperature-Sensitive Paint (TSP)
- Since it is very difficult, if not impossible, to ensure that T_{aw} can be measured accurately due to **heat conduction within the solid test models**. The measured **cooling effectiveness** from heat transfer experiments are always **over-predicted**.



Mass Transfer Analogy to Quantify Film Cooling Effectiveness

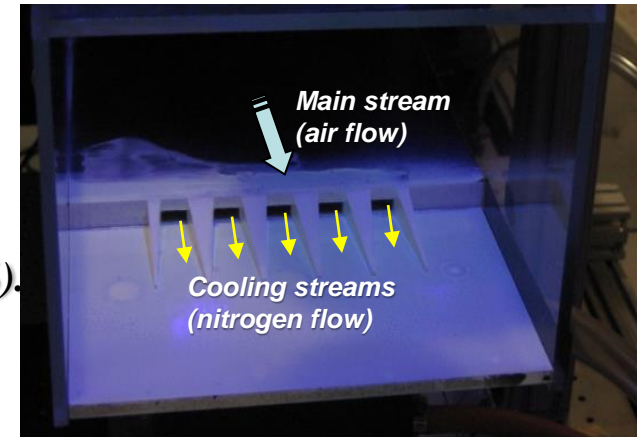


- **Mass Transfer Analogy:** the cooling effectiveness can be expressed in terms of the concentration distribution of some species on the protected surface through mass transfer.

➤ For example, **oxygen concentration on the protected surface measured by using PSP technique** (Wright et al, 2005; Han et al, 2005)

$$\eta = \frac{T_{\infty} - T_{aw}}{T_{\infty} - T_c} = \frac{C_{\infty} - C_{mix}}{C_{\infty} - C_c}$$

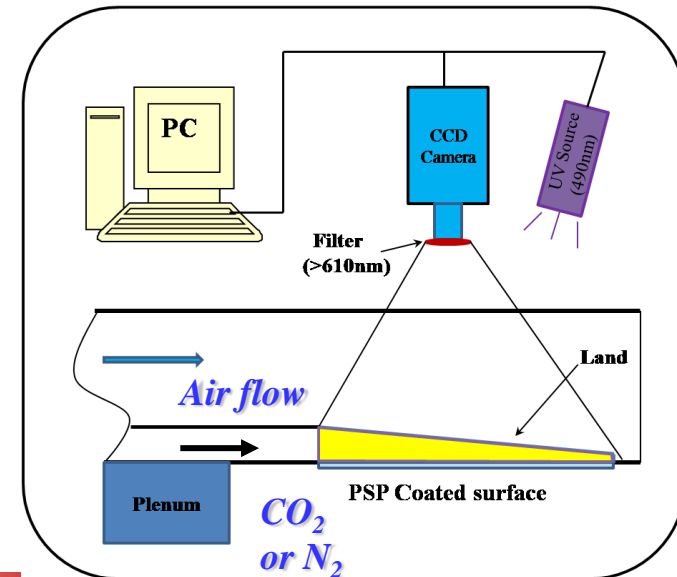
- C_{mix} : Oxygen concentration on the test surface (between 0 ~ 21%).
- C_{∞} : Oxygen concentrations of the main stream flow (~ 21%).
- C_c : Oxygen concentration of the coolant flow.



- According to Charbonnier et al. (2009), if main stream is airflow, and CO_2 or N_2 is used as coolant stream, then :

$$\eta = \frac{T_{\infty} - T_{aw}}{T_{\infty} - T_c} = \frac{C_{\infty} - C_{mix}}{C_{\infty} - C_c} = \frac{(P_{O_2})_{air} - (P_{O_2})_{mix}}{(P_{O_2})_{air}}$$

$$= 1 - \frac{1}{\left[\frac{(P_{O_2})_{air}}{(P_{O_2})_{mix}} - 1 \right] \frac{\rho_{coolant}}{\rho_{air}} + 1}$$



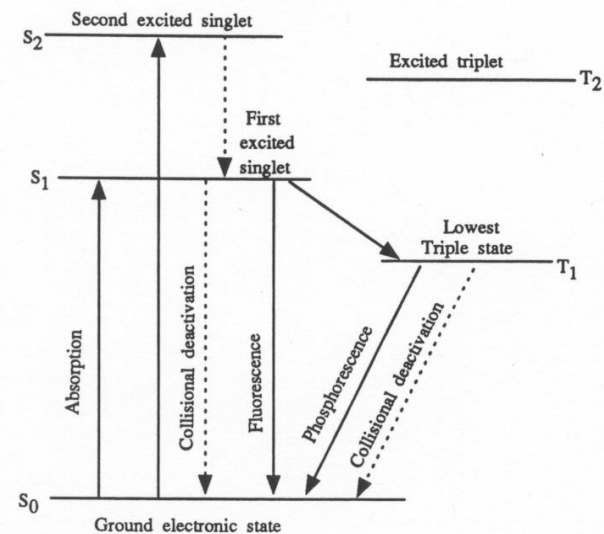
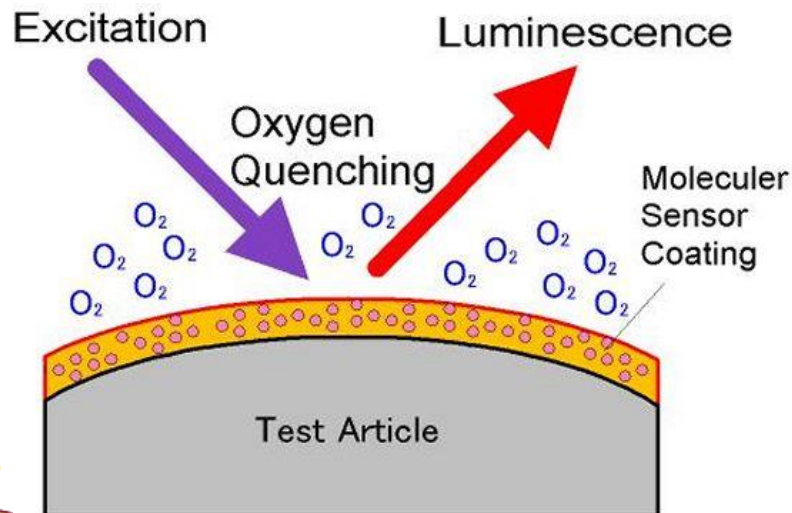
Basic Principles of Pressure Sensitive Paint (PSP)



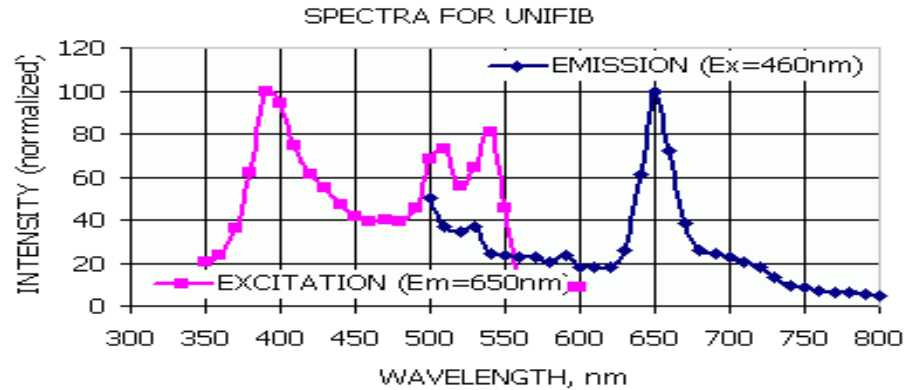
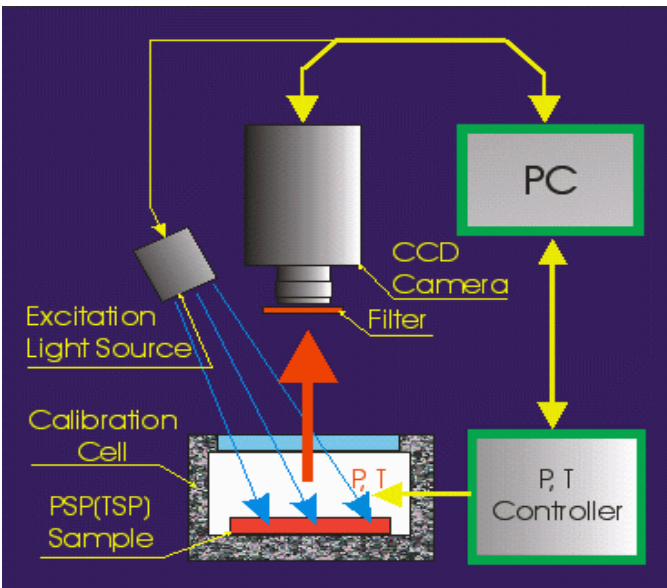
- *PSP is based on the sensitivity of certain luminescent molecules to the presence of oxygen.*
 - *For some materials, oxygen can interact with the molecule so that the transition to the ground state is radiationless, this process is known as oxygen quenching.*
 - *For oxygen quenching, the intensity decrease can be described by the **Stern-Volmer equation**:*

$$\frac{\tau_0}{\tau} = 1 + K_{SV}Q \quad \text{or} \quad \frac{\tau_0}{\tau_{O_2}} = \frac{I_0}{I_{O_2}} = 1 + K_{SV}P_{O_2}$$

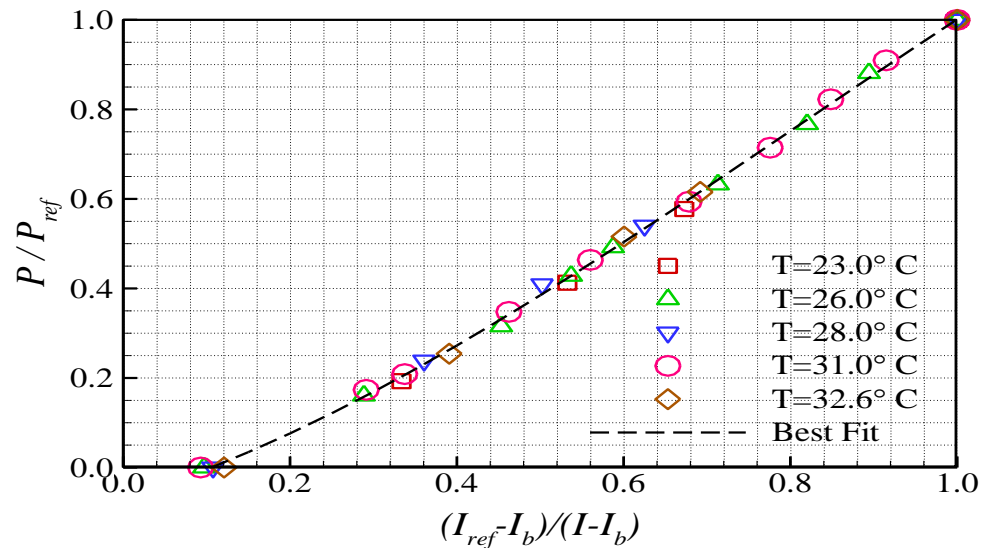
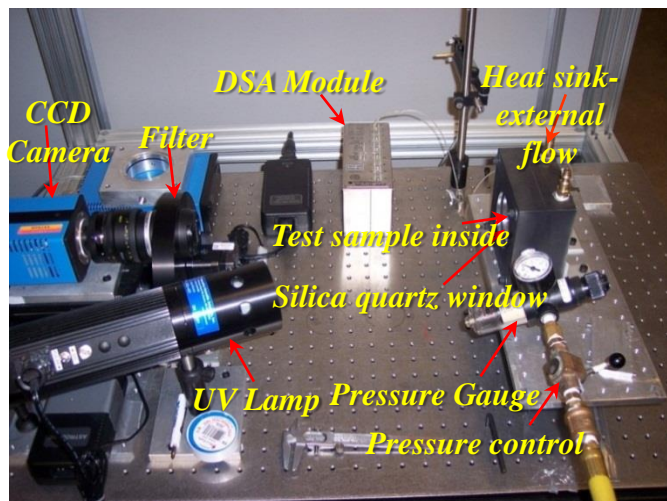
- *Volume fraction of oxygen in air is fixed at 20.95%, higher partial pressure or concentration of oxygen would indicate higher local air pressure.*
- *The air pressure distribution on the painted surface can be determined based on the intensity distribution of the acquired image of the oxygen sensitive molecules.*



Calibration procedure for PSP Measurements

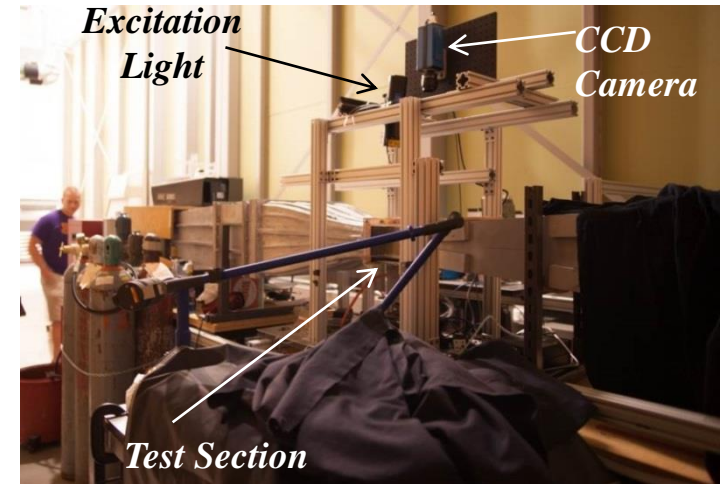
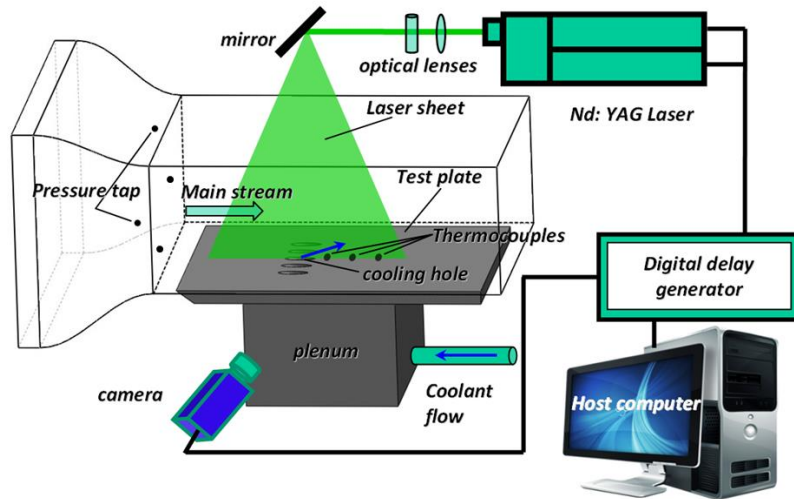


- *PSP paint illuminated (excited) by using 390 nm LED light source;*
- *Emission light isolated by using 610 nm long-pass filter.*



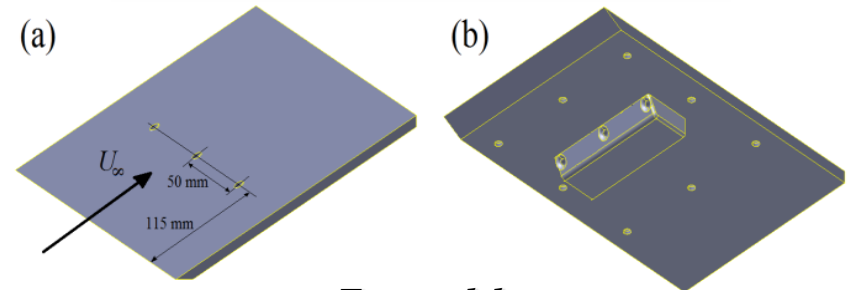
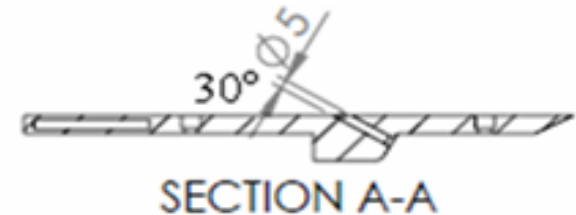
- *N₂ flush to gather zero O₂-pressure calibration point.*
- *Under appropriate normalization, the calibration curve is almost temperature-independent.*

Experimental Setup for PIV and PSP Measurements



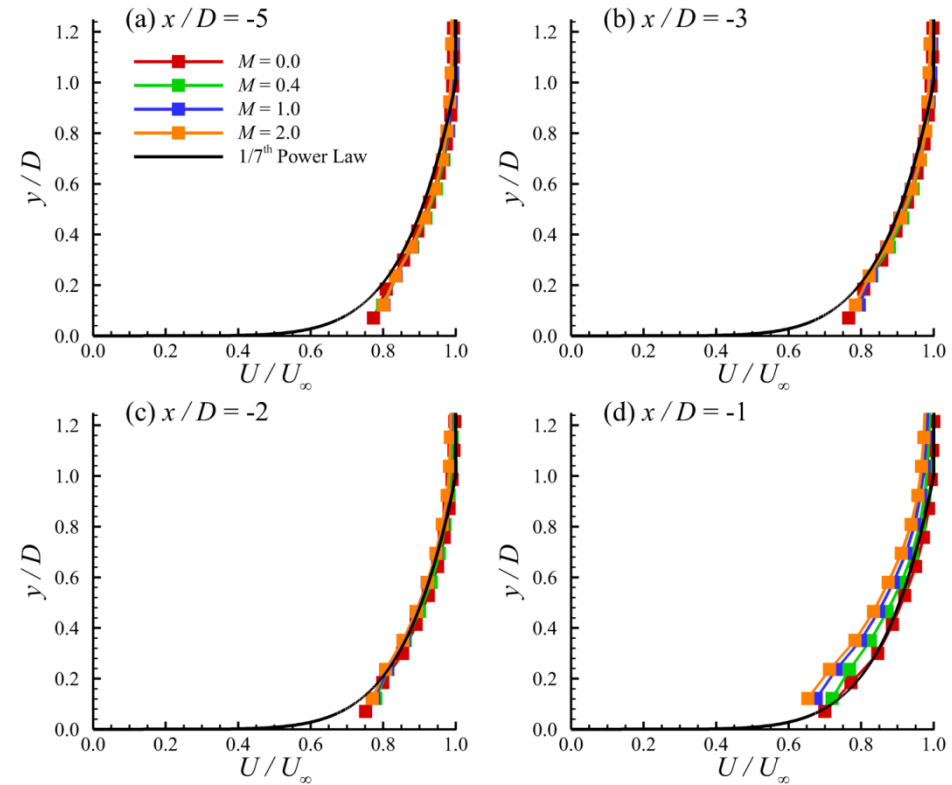
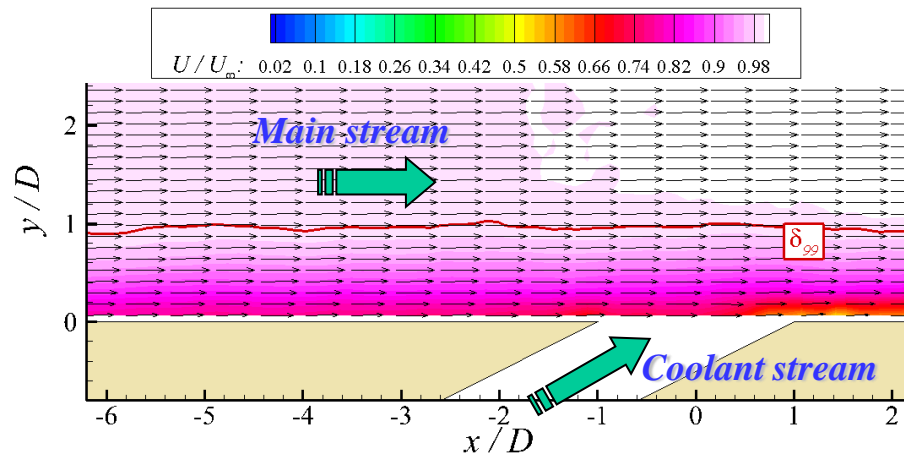
Experimental Setup for PIV measurements

- *Open-circuit wind tunnel for main flow ($U_\infty = 0 \sim 40$ m/s)*
- *Test plate model, painted with PSP, as the floor of test section*
- *Compressed gas system drives coolant jet (air, N_2 , or CO_2)*
- *Blowing Rate: $M = (\rho V)_{jet} / (\rho U)_\infty$ of $0 \sim 2.0$*
- *Flow conditions essentially isothermal (coolant and mainstream at ambient temperature)*



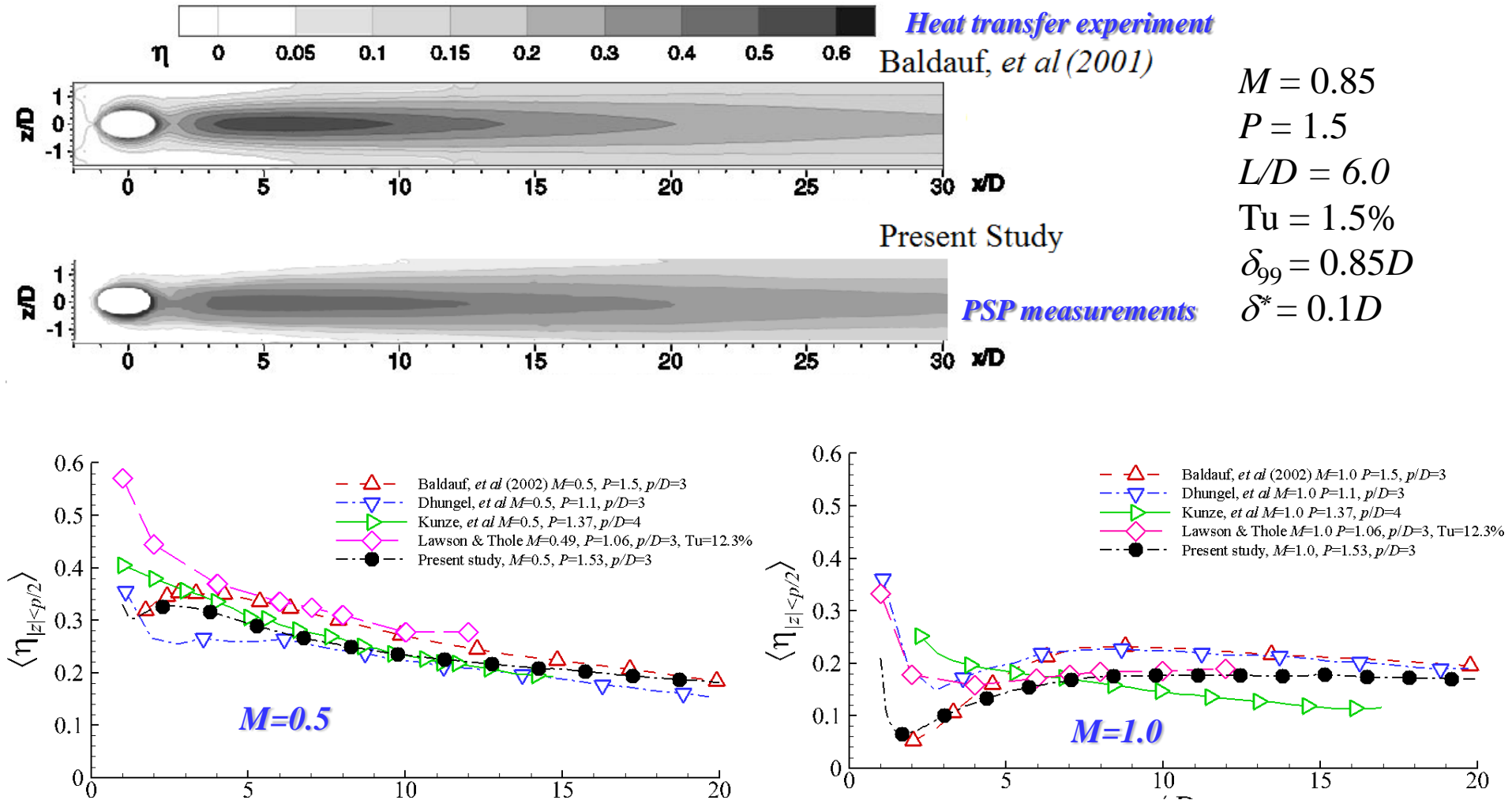
Test model

Boundary Layer Condition of the Oncoming Flow



- In the absence of coolant flow ($M = 0$), a $1/7^{\text{th}}$ power law closely approximates the oncoming flow at the leading edge of the coolant hole ($x/D = -1$)
- Main stream turbulence intensity is $\sim 1\%$
- Boundary layer thickness δ_{99} measured at $X/D = -1.0$ was found to be about $0.85D$.
- Displacement thickness δ^* measured at $X/D = -1.0$ was found to be about $0.10D$.
- The oncoming flow conditions approximately match those of Baldauf et al. (2001)
- Increasing M causes the BL to thicken, adding to the velocity deficit, especially close to the hole.

Film Cooling Effectiveness: PSP vs. Conventional IR Thermography



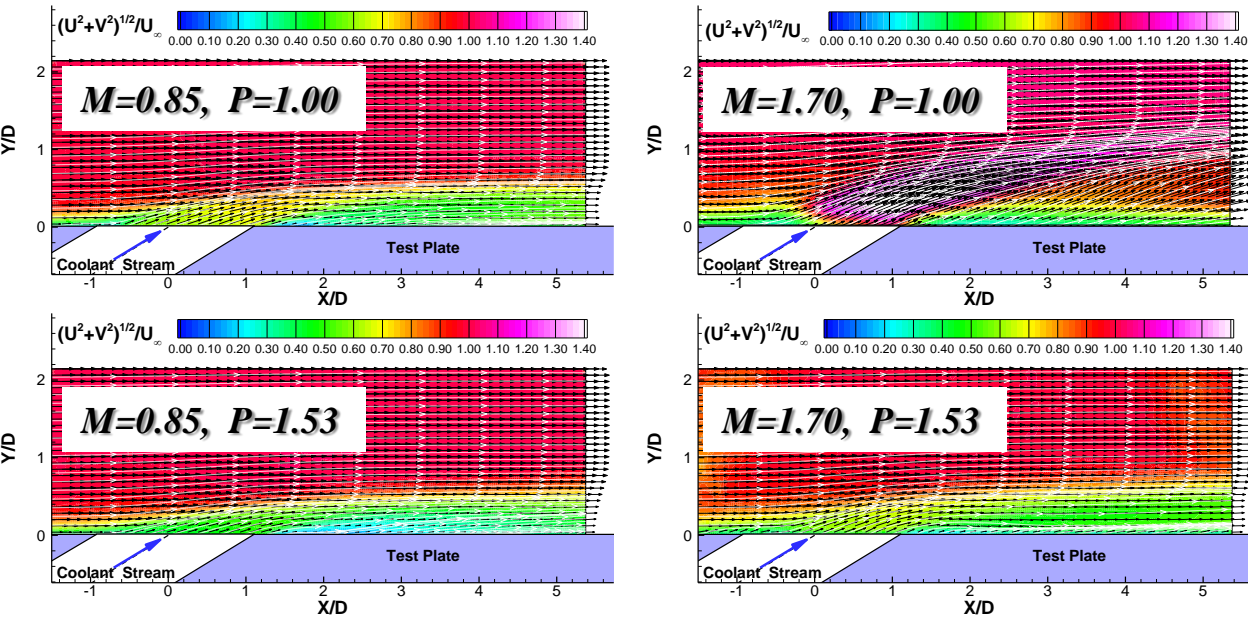
PSP results vs. conventional IR Thermography results available in literature



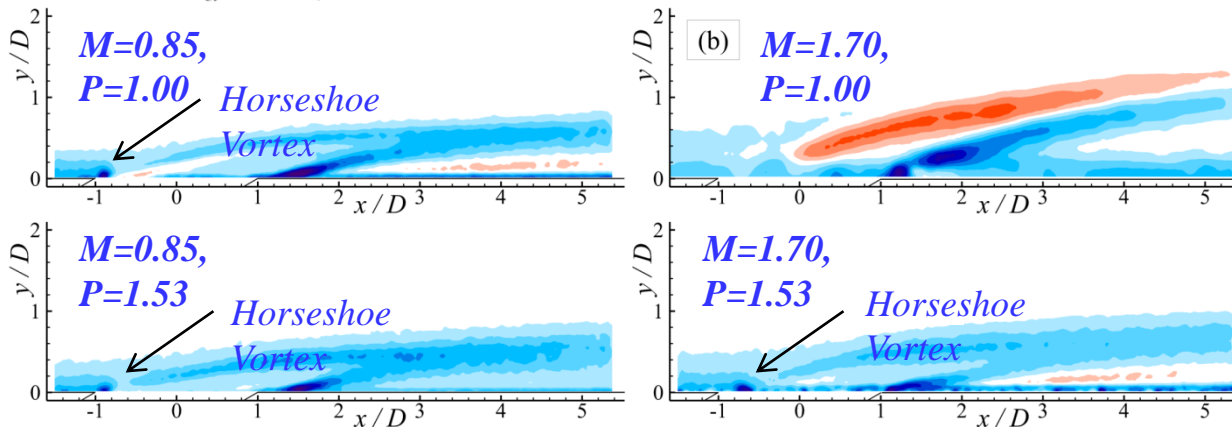
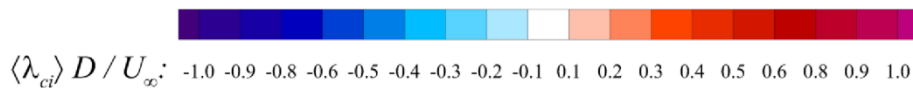
Baldauf, S., Schulz, A., and Wittig, S. 2001. "High-Resolution Measurements of Local Effectiveness from Discrete Hole Film Cooling." *Journal of Turbomachinery*. Vol. 123, pp. 758–765.

IOWA STATE UNIVERSITY

Density Ratio (P) Effect: Mean Velocity Field and Swirling Strength



- Jet lift-off (separation) is observed at $M=1.70$ for $P=1.00$ (air as coolant jet) but not for $P=1.53$ (CO_2 jet).
- Increase in P for $M=0.85$ results in slower flow within the coolant sublayer.
- Lower M for fixed P results in slower flow velocity throughout the coolant sublayer for jets that remain attached.



- λ_{ci} is imaginary part of eigenvalue of velocity gradient tensor, signed by w_z
- Negative swirl (blue) indicates clockwise rotational motion
- Horseshoe vortex noted for all cases except $P=1.00$ & $M=1.70$ case
- That case also shows strong counter-clockwise rotation in leading-edge shear layer

Swirling Strength $\langle \lambda_{ci} \rangle$

Density Ratio (P) Effect: Film Cooling Effectiveness



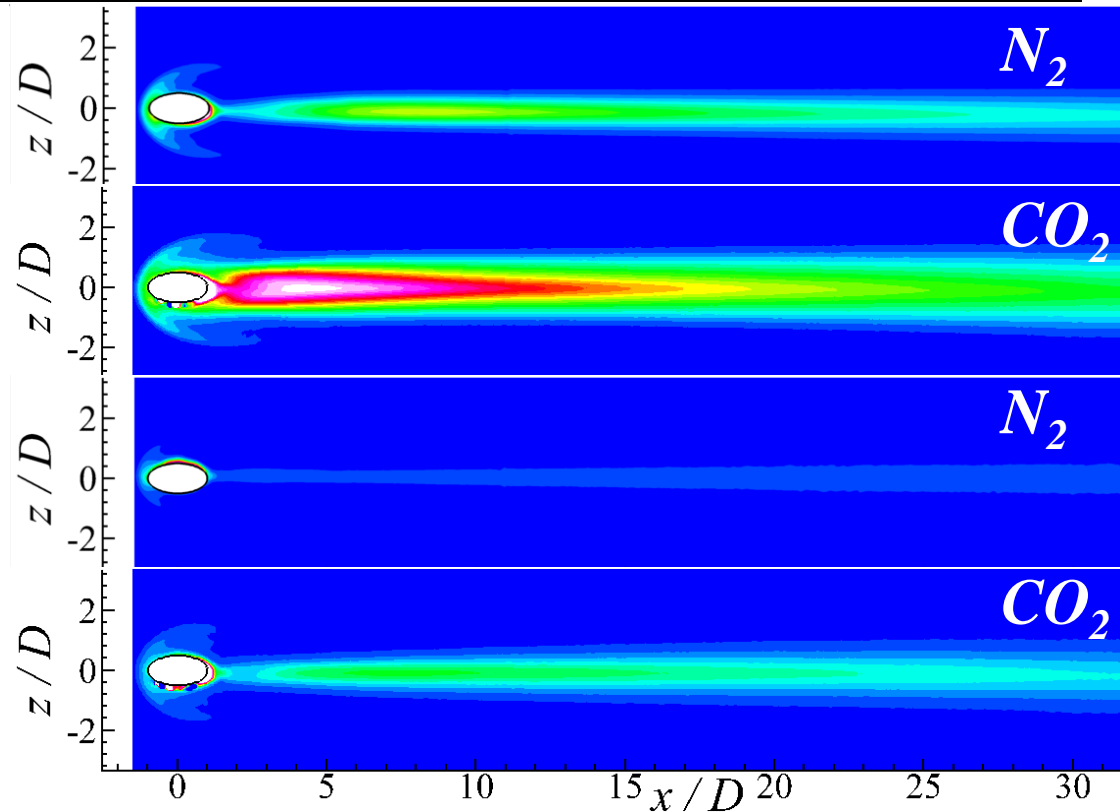
$\langle \eta \rangle$: 0.03 0.06 0.09 0.12 0.15 0.18 0.21 0.24 0.27 0.30 0.33 0.36 0.39 0.42 0.45 0.48 0.51 0.54 0.57 0.60 0.63 0.66

$M=0.85, P=0.97$

$M=0.85, P=1.53$

$M=1.70, P=0.97$

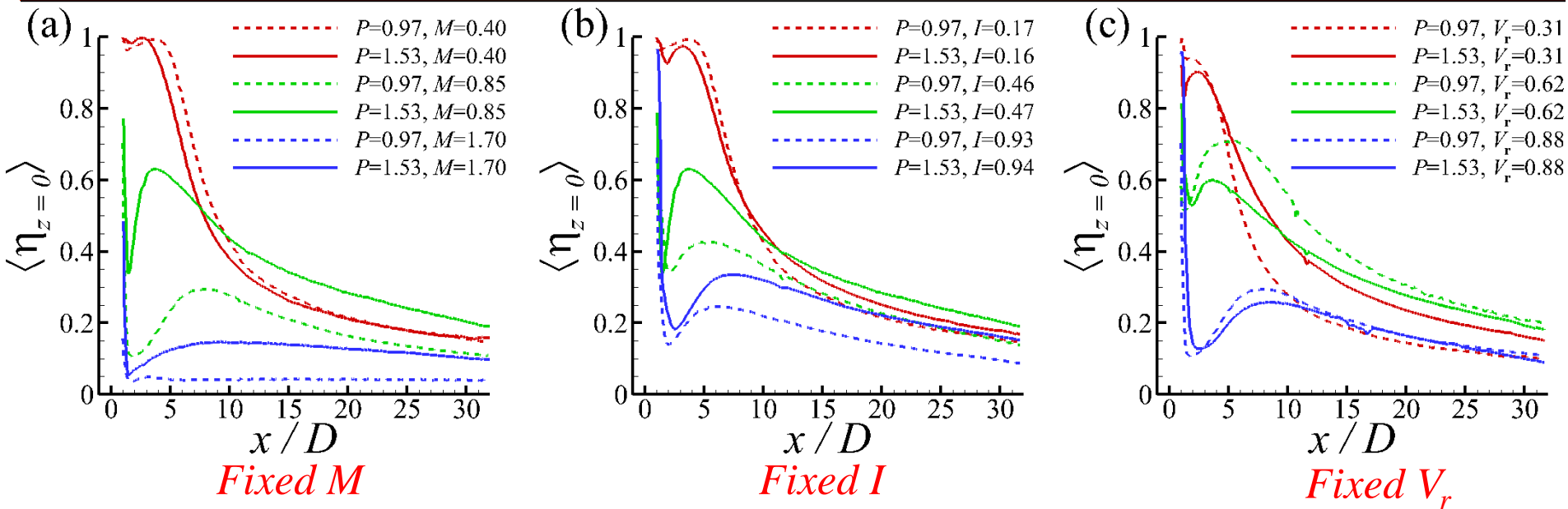
$M=1.70, P=1.53$



- Higher P significantly increases effectiveness for fixed M
- M may not be an ideal scaling quantity
- Jet that separates provides very little cooling
- Horseshoe vortex causes coolant advection “halos”



Comparison of Scaling Parameters for Varying P



Density Ratio: $P = \rho_{\text{coolant}} / \rho_{\infty}$

Velocity Ratio: $V_r = V_{\text{coolant}} / U_{\infty}$

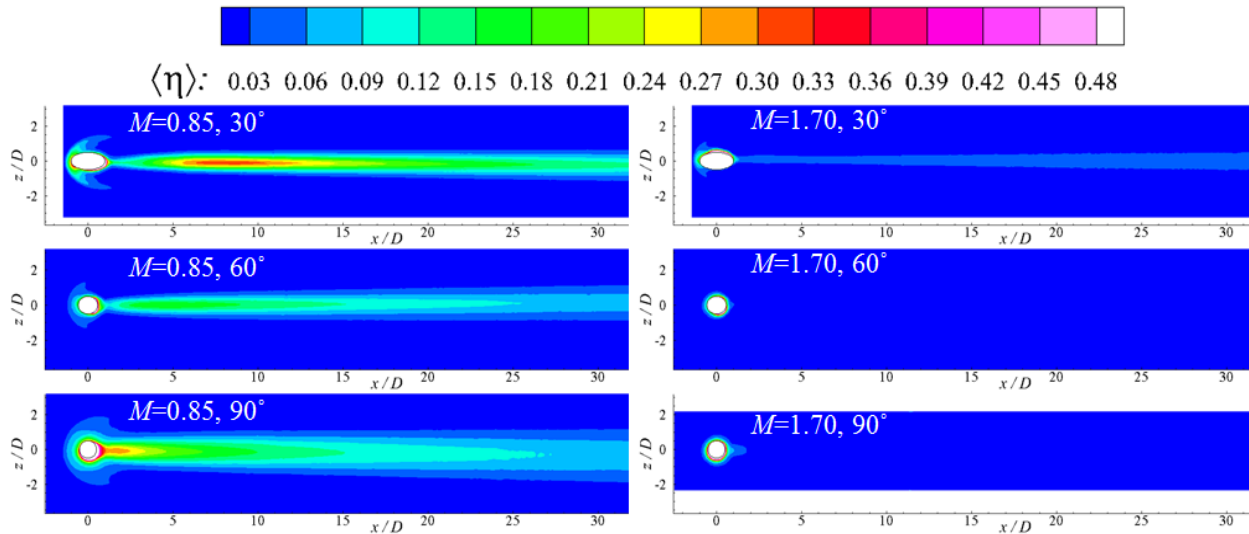
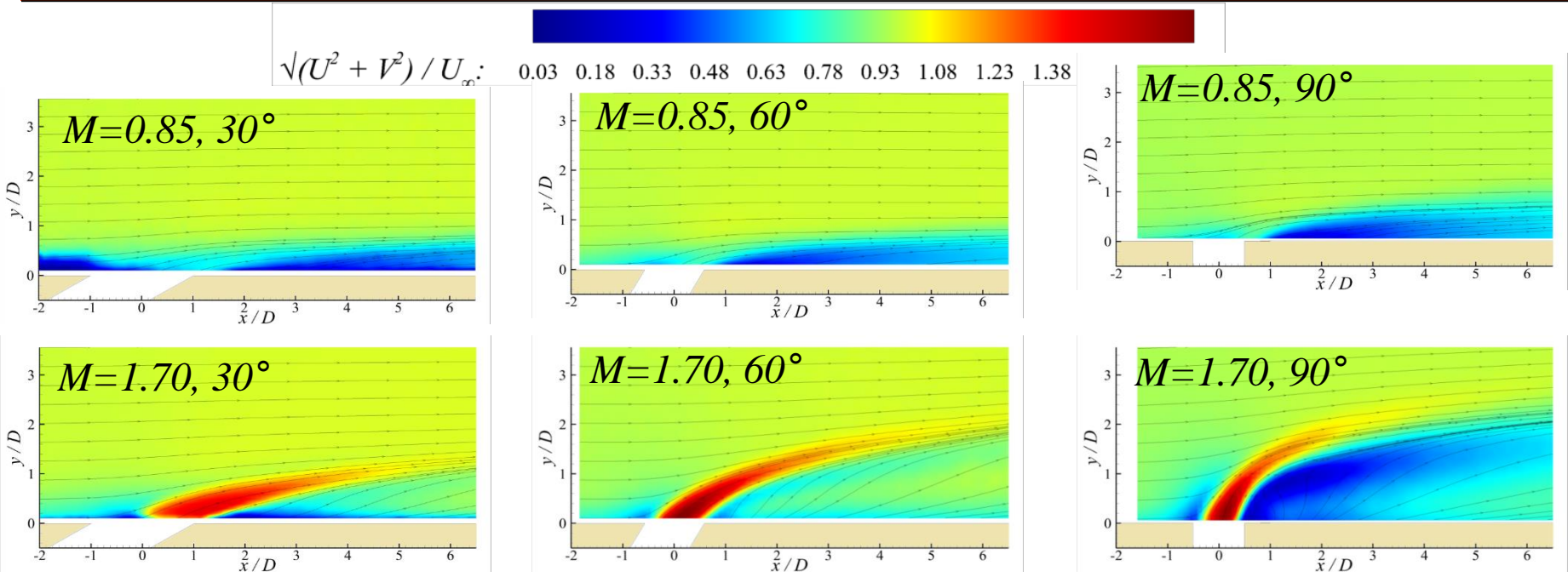
Momentum Flux Ratio: $I = P V_r^2 = M^2 / P$

Blowing Rate (mass flux ratio): $M = P V_r$

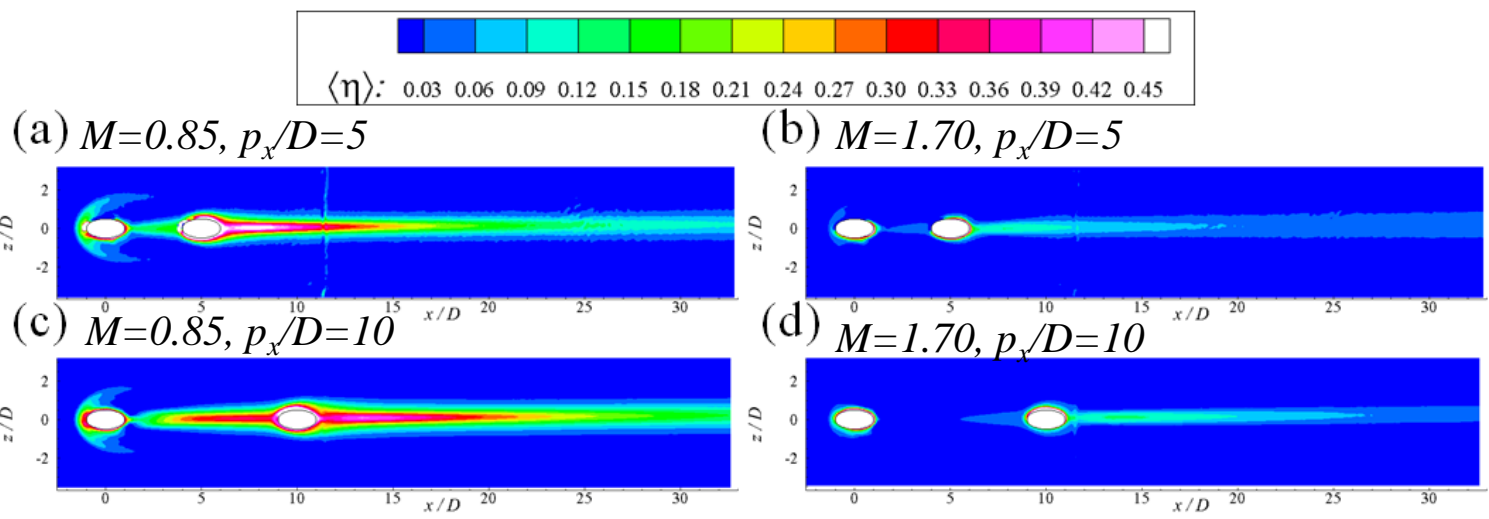
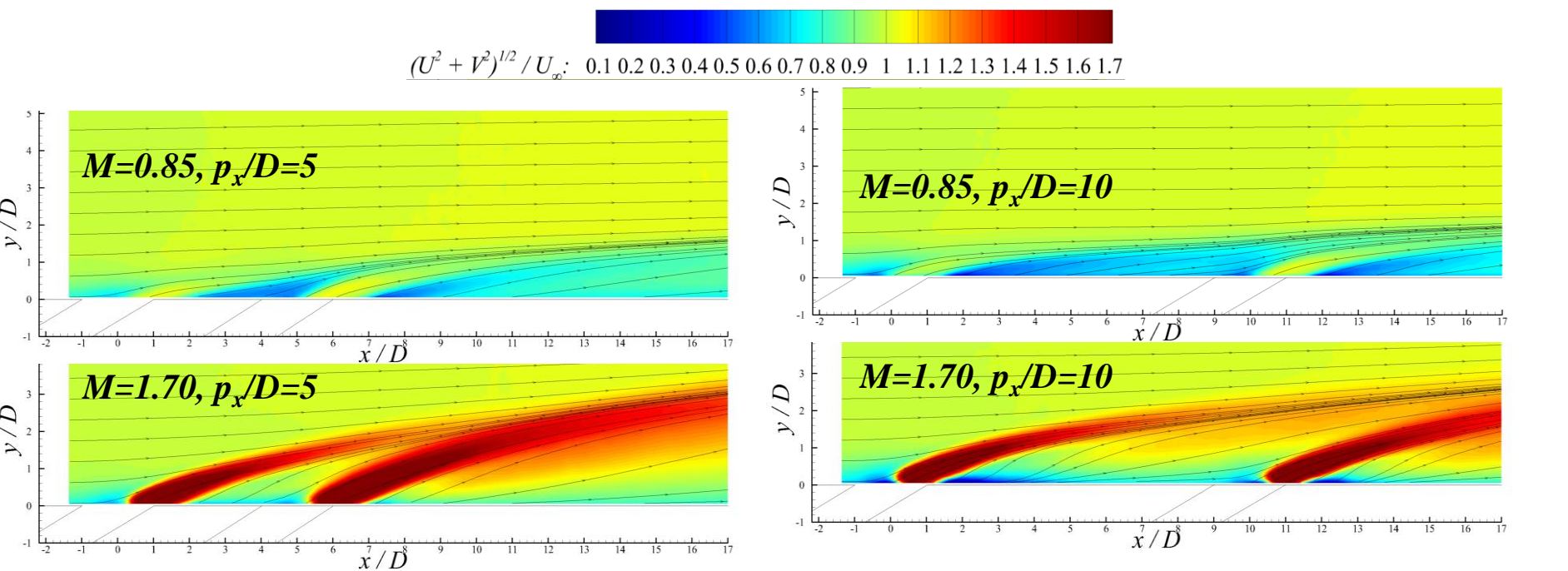
Kinematics
↑
Dynamics

- Quantities that give more weight to P (I and then M) have more success to collapse data for varying P at low coolant flow rates.
- Bulk velocity ratio V_r may be used with some success to scale the cooling effectiveness from jets of higher velocities.

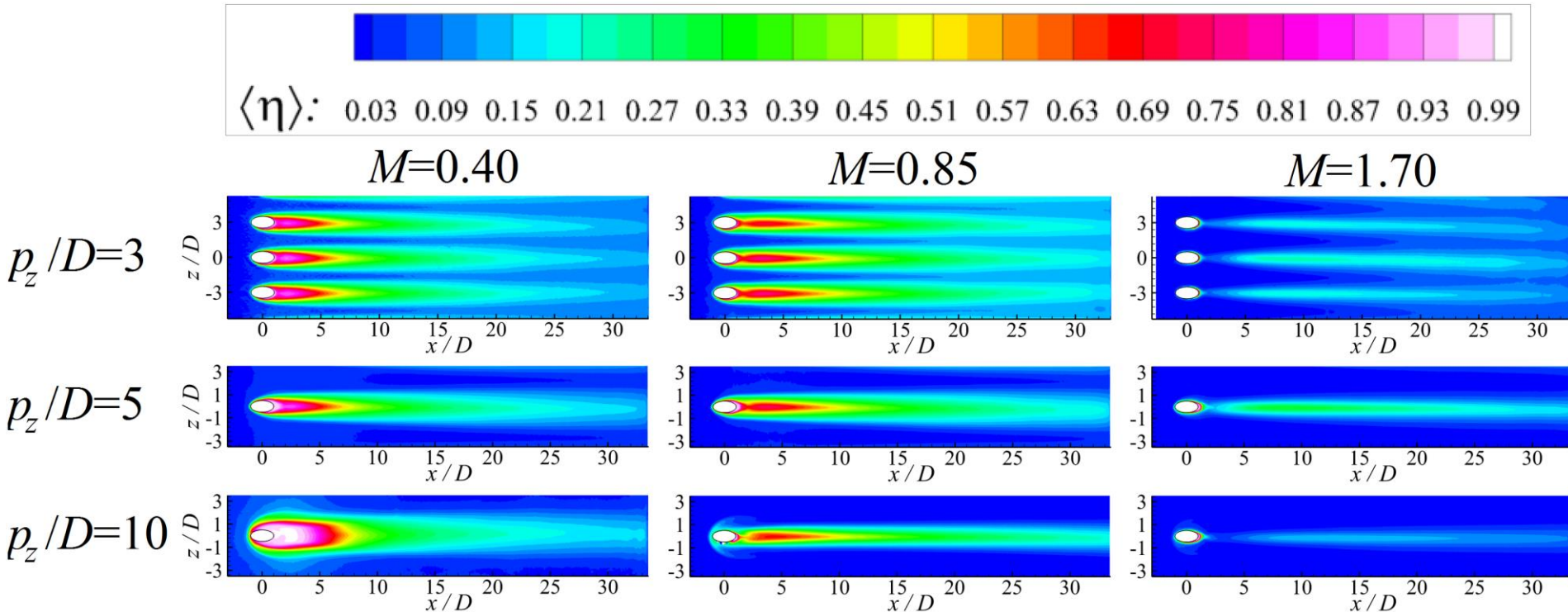
Effects of Injection Angle of the Coolant Injection Holes



Effects of Streamwise Spacing Between the Coolant Injection Holes

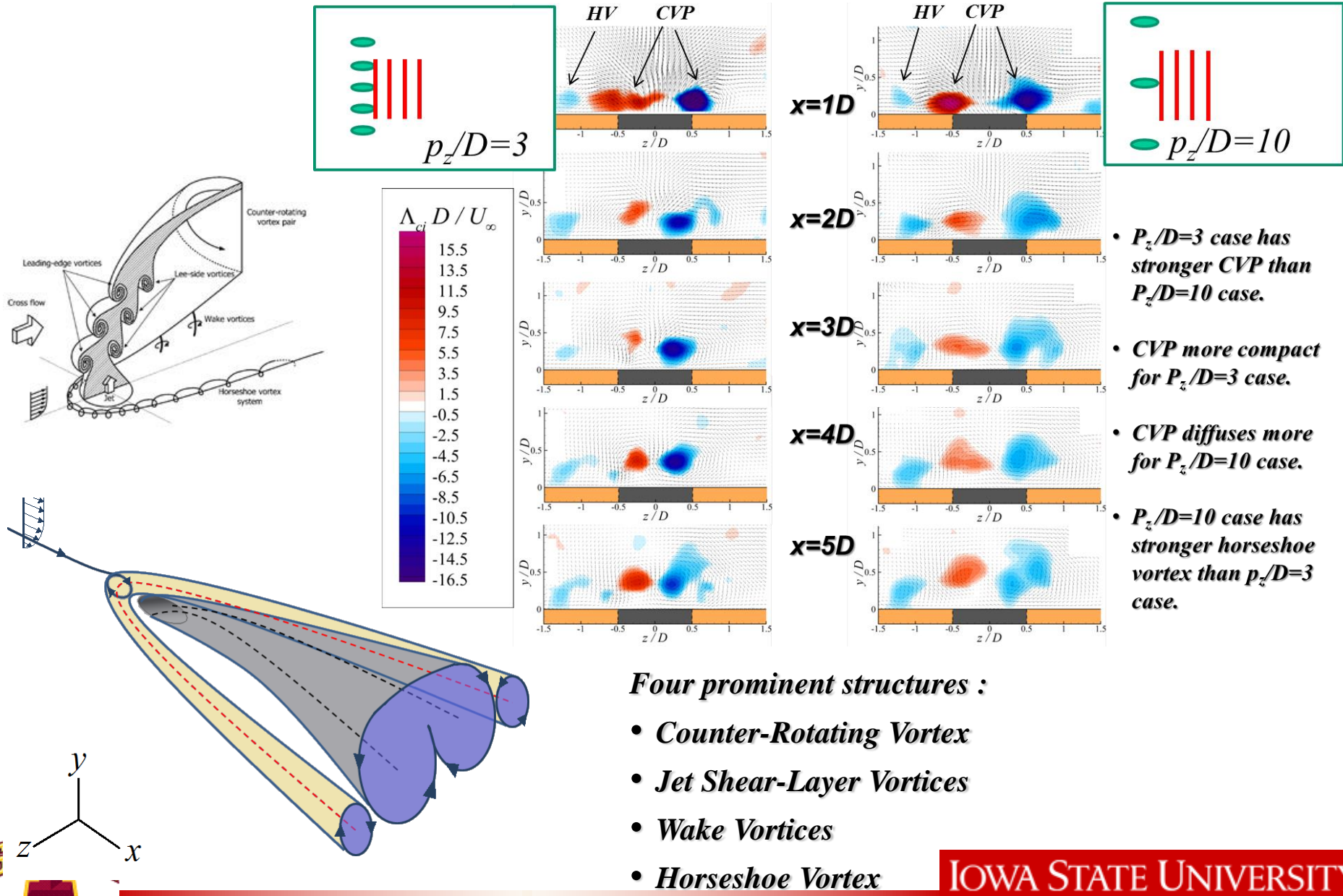


Effects of Spanwise Spacing Between the Coolant Injection Holes



- $p_z/D=3$ and $p_z/D=5$ hole spacings have similar behavior regardless of M .
- A qualitative difference is noted for $p_z/D=10$.
 - Much higher effectiveness around the hole.
 - $M=0.85$ case suggests that the horseshoe vortex may contribute to this increase in spanwise effectiveness.

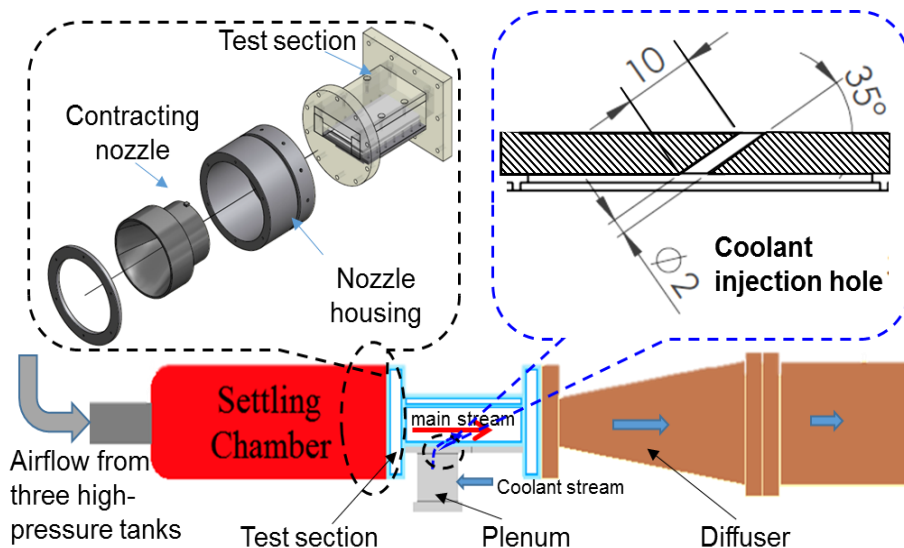
Basic Flow Structure: Jet in Cross-Flow



Compressibility Effects on the Film Cooling Effectiveness



- Most of previous studies were conducted at relatively *low Mach number* ($Ma < 0.15$), while *flow passing turbine blade* is usually *transonic*, little can be found in the literature that examines *effects of compressibility* of incoming flow on film cooling performance.



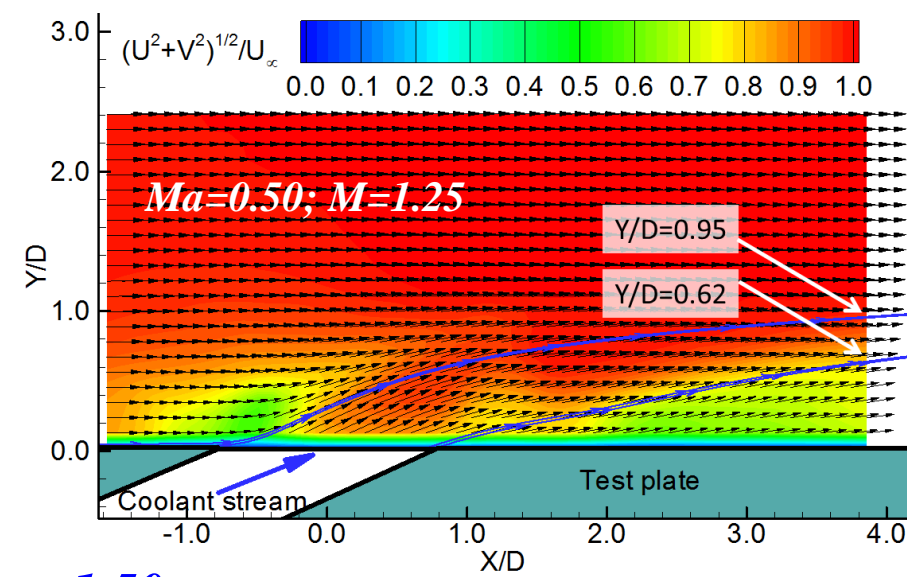
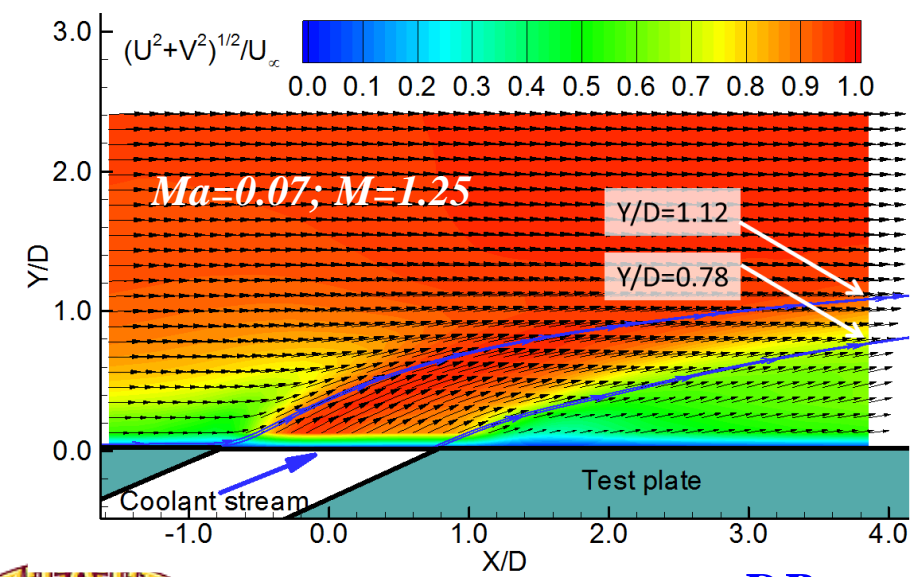
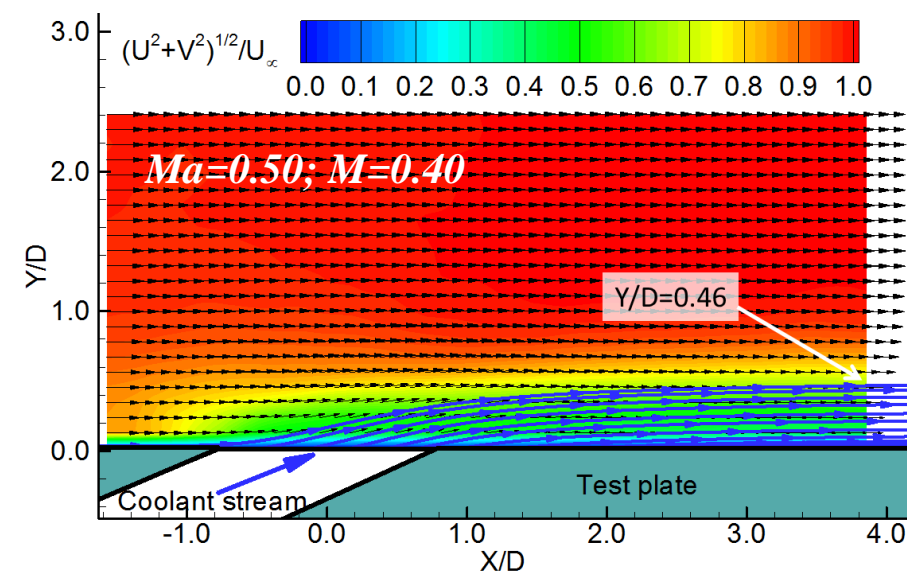
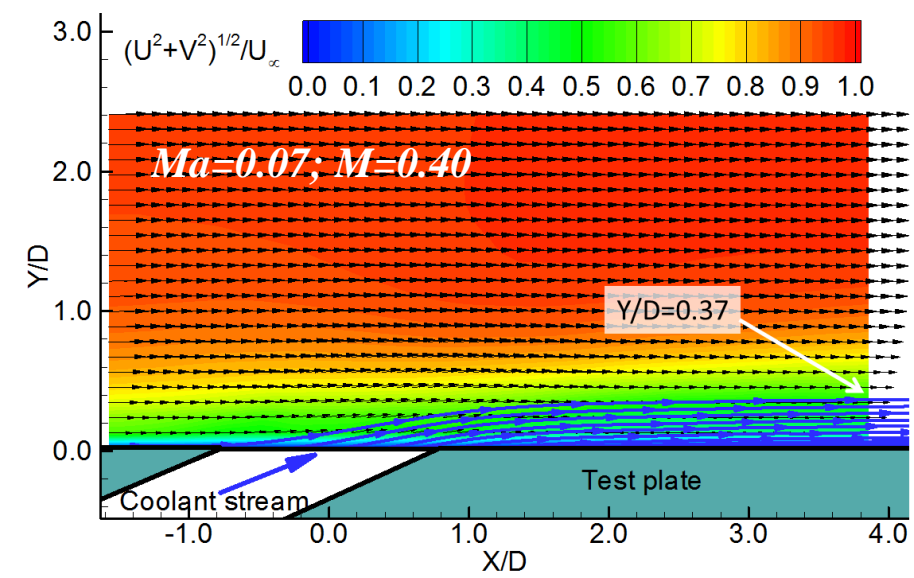
- $Ma = 0.7$ can be sustained for ~5 minutes.
- Test section: $63.5 \times 25.4 \text{ mm}^2$
- The temperature variation during the test $< 5K$.
- Uni-FIB paint temperature sensitivity is $0.5\%/deg$.

Mach number of the mainstream flow, Ma	Density Ratio $DR = \rho_c / \rho_\infty$	Blowing Ratio $M = \rho_c V_c / \rho_\infty V_\infty$
0.07	1.5	0.40, 0.85, 1.25
0.30	1.5	0.40, 0.85, 1.25
0.50	1.5	0.40, 0.85, 1.25
0.70	1.0	0.40, 0.85
0.70	1.5	0.40, 0.85, 1.25
0.70	2.0	0.40, 0.85



Laterally-averaged cooling effectiveness profiles

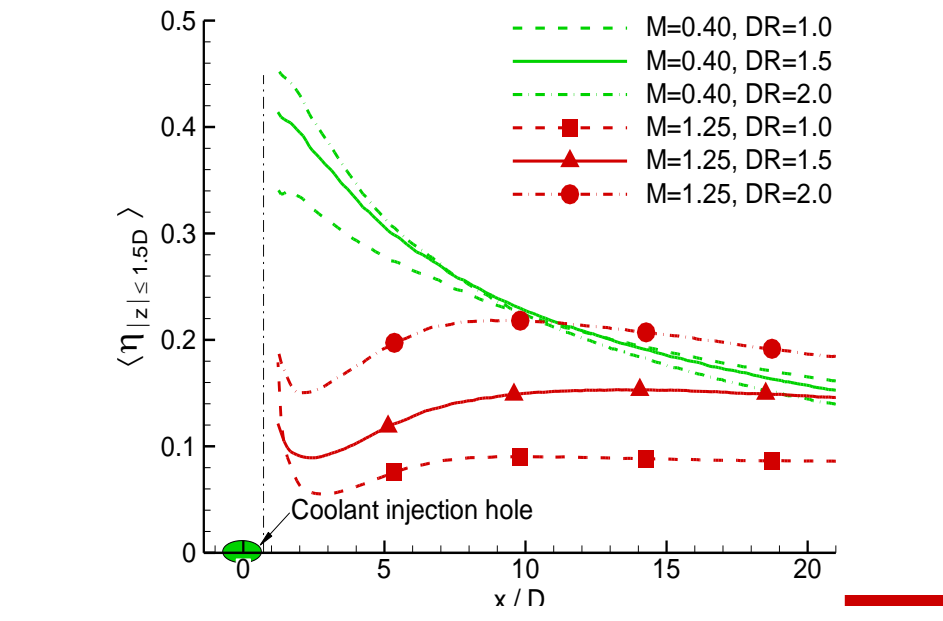
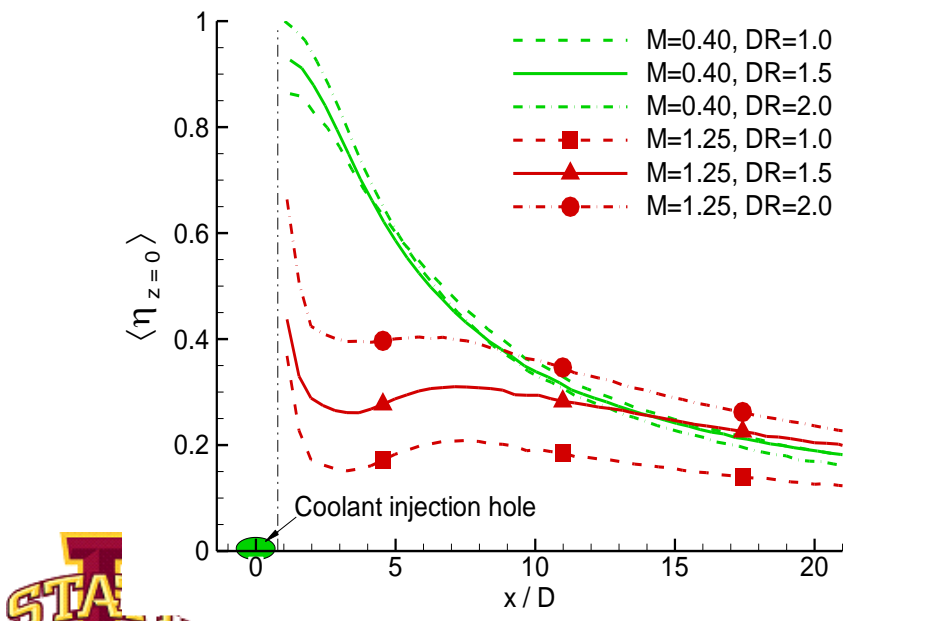
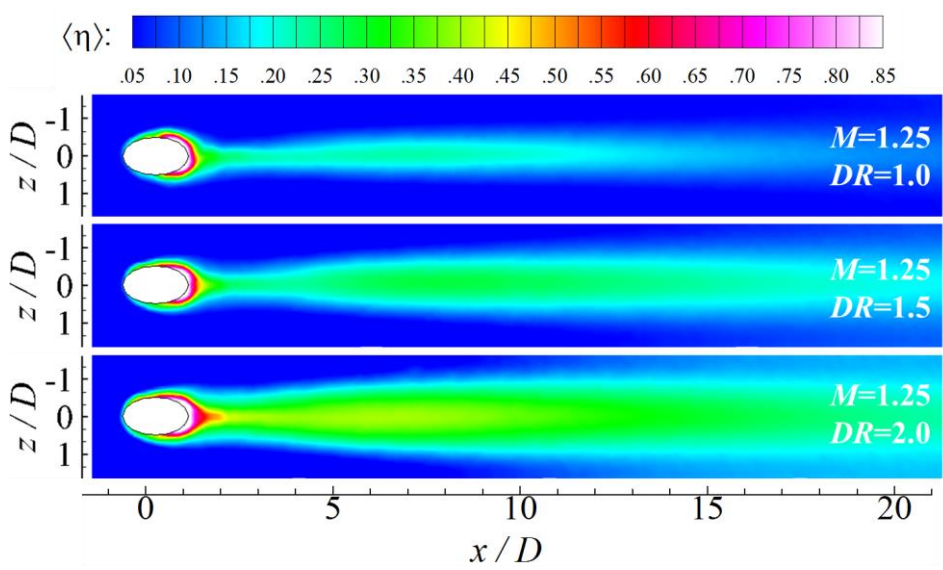
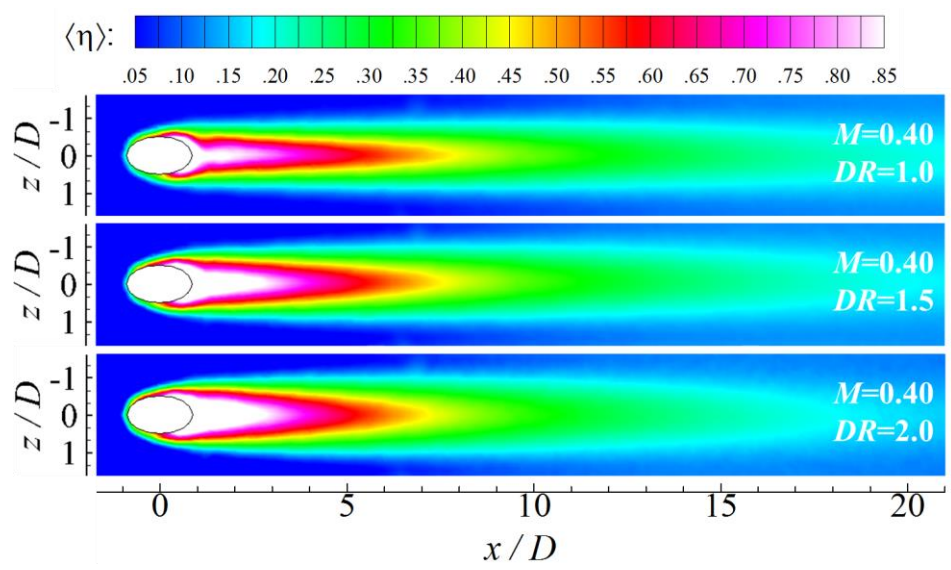
PIV Measurement Results with $DR = \rho_c / \rho_\infty = 1.50$



$DR = \rho_c / \rho_\infty = 1.50$



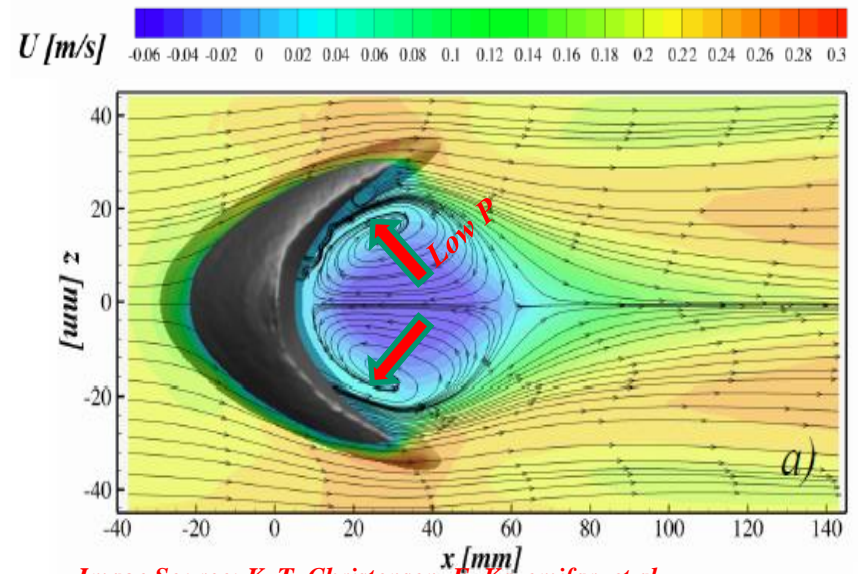
Effects of Density Ratio on Film Cooling @ Transonic condition



Centerline cooling effectiveness profiles

Laterally-averaged cooling effectiveness profiles

Barchan Dune Inspired Film Cooling Designs for Improved Cooling Effectiveness





Shaped Film Cooling Holes

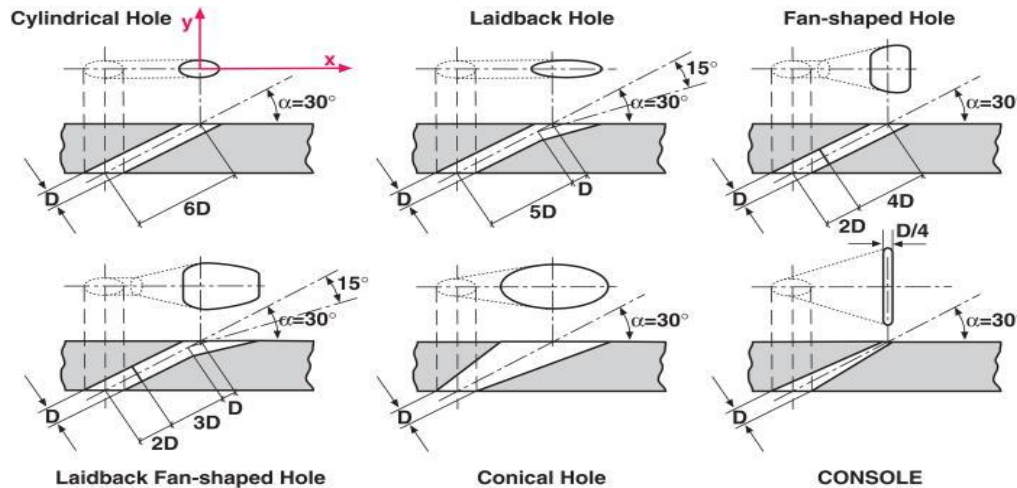


Image Source: Saumweber, et al. (2012).

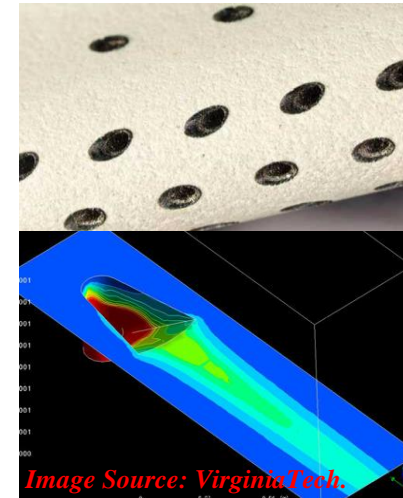
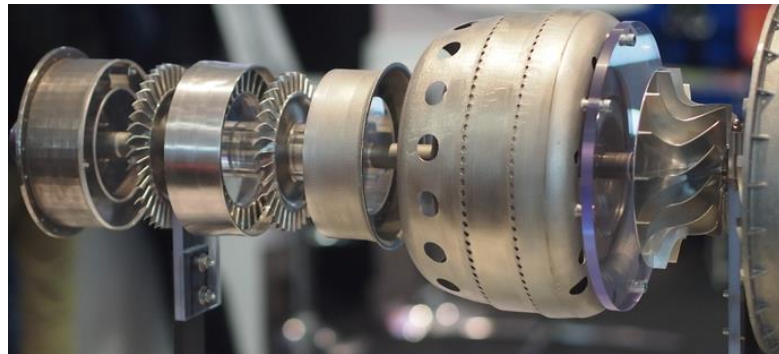


Image Source: VirginiaTech.

- 3D printing technique promotes the development of innovative cooling design.

3D Printed titanium blade, GE (2014).

First 3D printed jet engine, engineering.com (2015). Printed turbine blade of Morris Technologies.



- Saumweber et al, Journal of Turbomachinery, vol. 134, Aug. 2012.

Barchan Dune Shaped Ramp (BDSR)



Image Source: Sand dune search.



Image Source: Sand dune on Mars, News discovery.

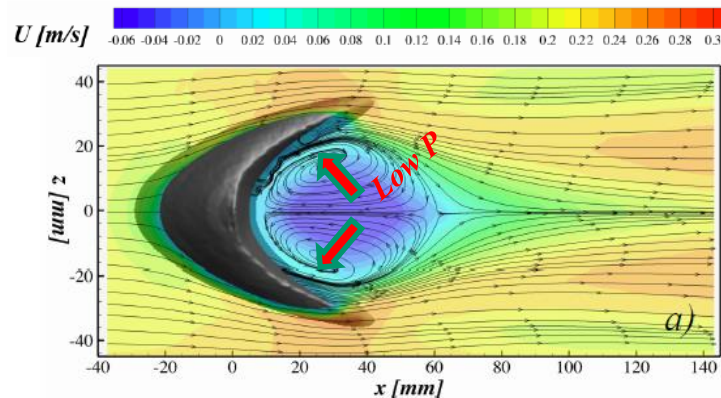


Image Source: K. T. Christensen, F. Kazemifar, et al.

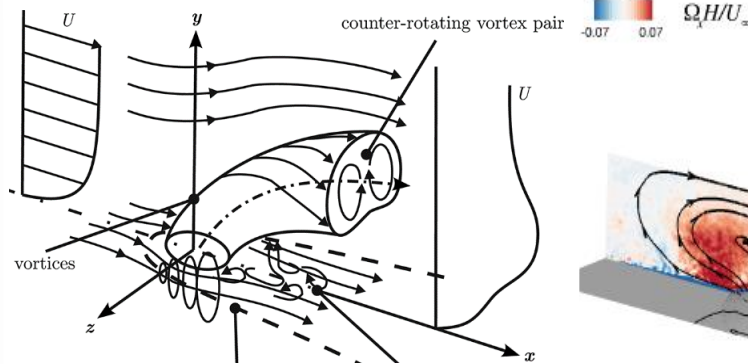


Image Source: Herbst et. al (2013).

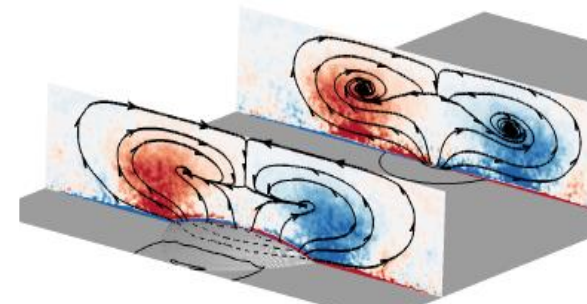


Image Source: K. T. Christensen, et al (2015).

- **Stable wake** right behind dune, sand stayed on the ground.
- Streamline shape **minimize the friction loss** since it is the evolution of nature wind effect.
- **Suction** behind the dune, and **Anti-CRV** formed above the dune.



Barchan-dune-shaped ramp (BDSR)

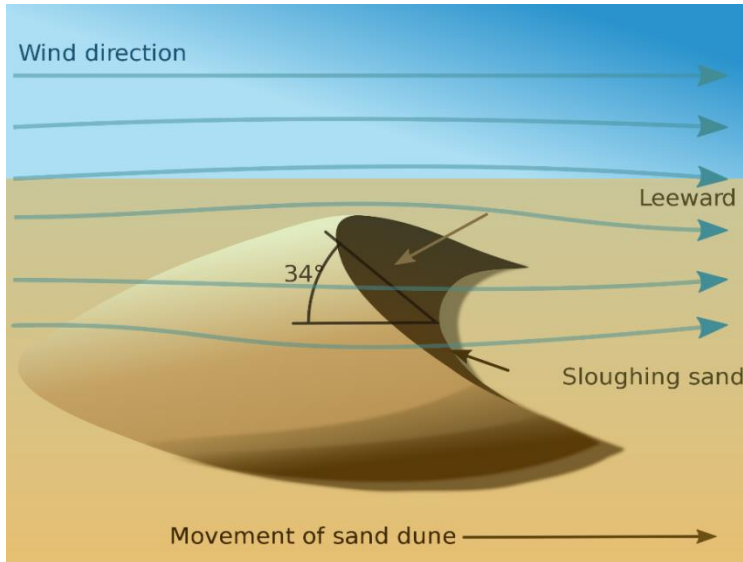


Image Source: <https://commons.wikimedia.org>

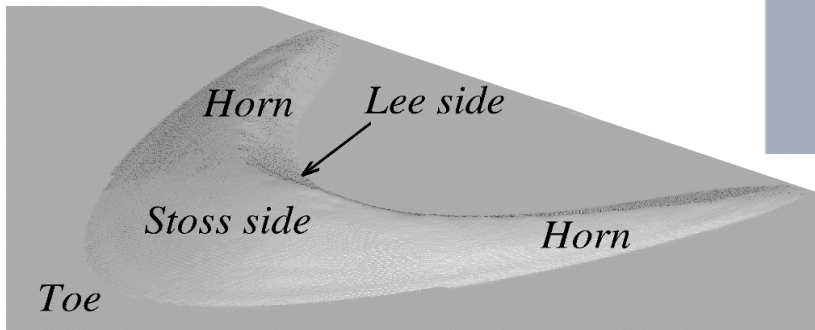
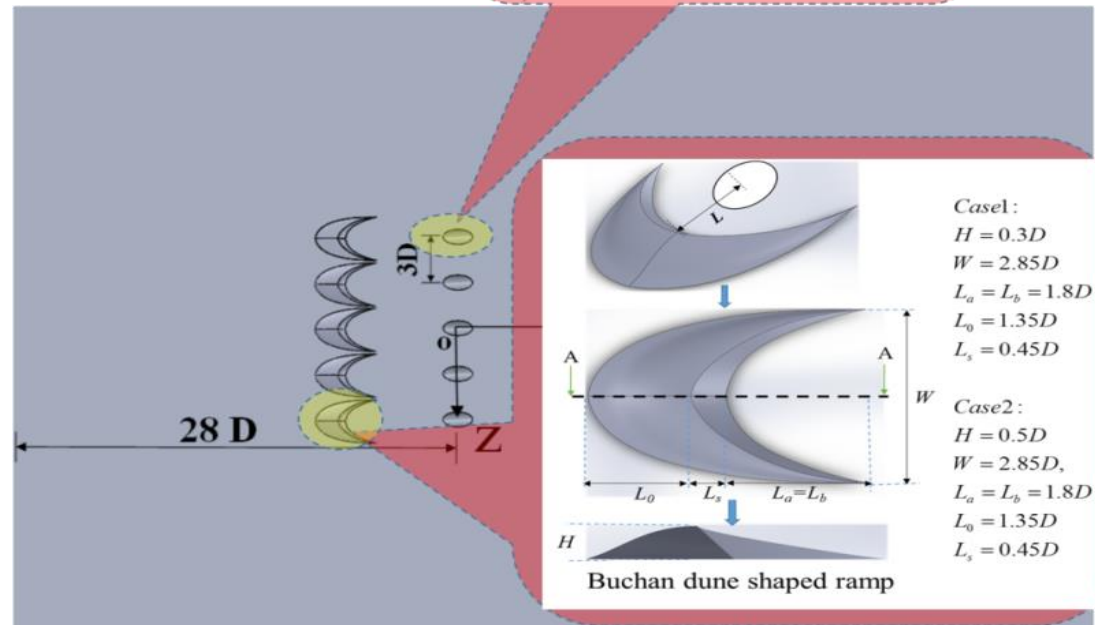
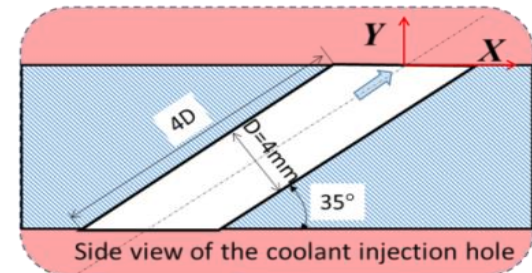
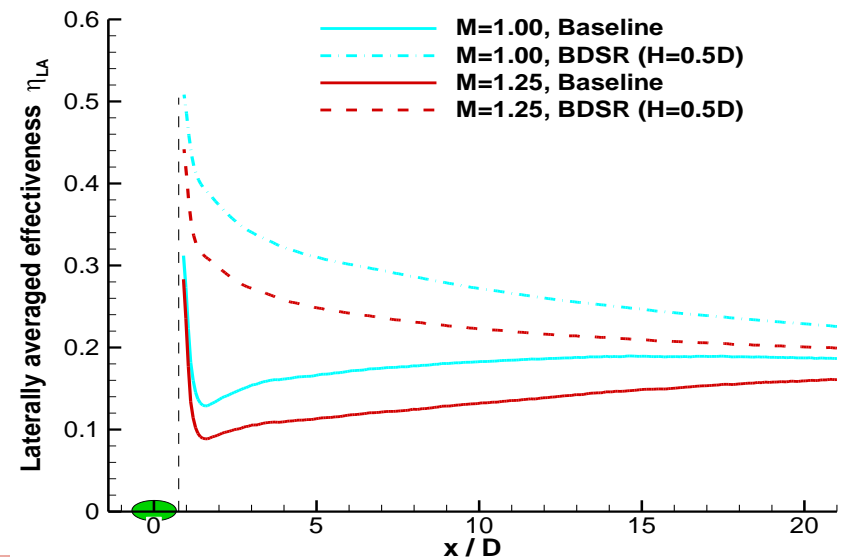
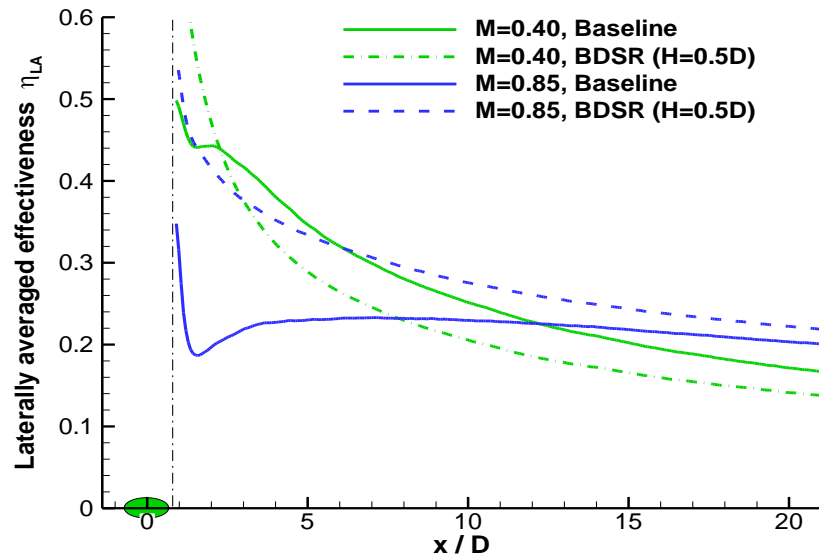
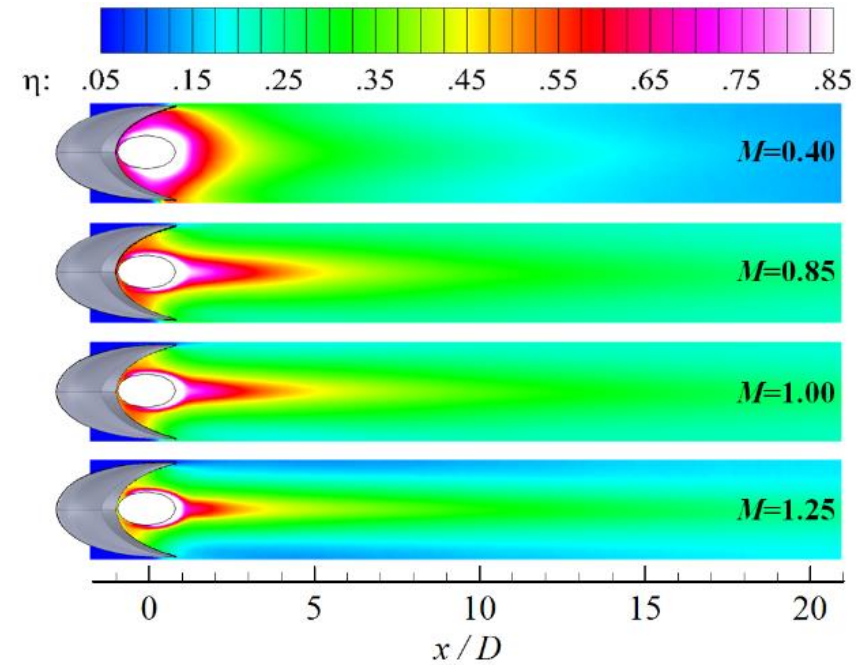
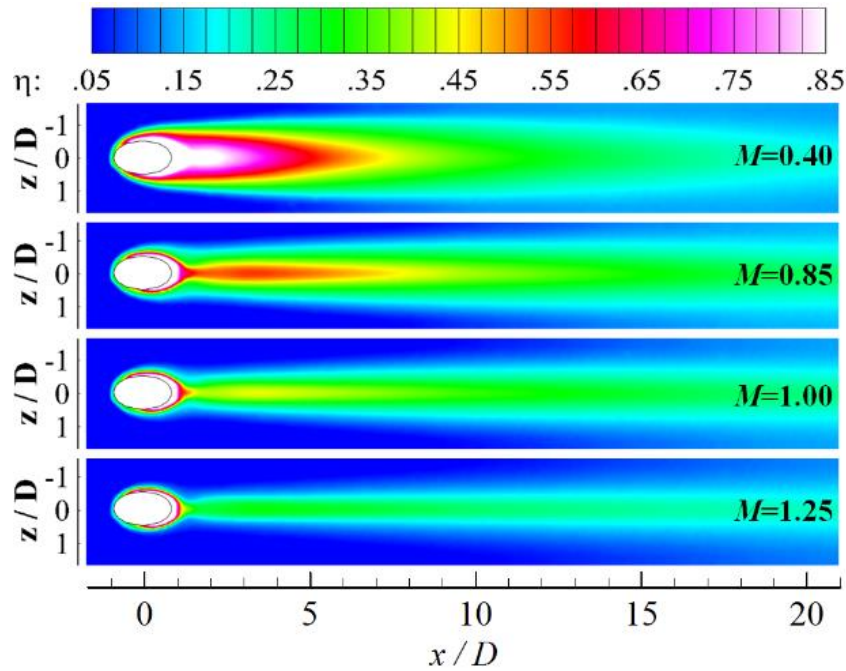


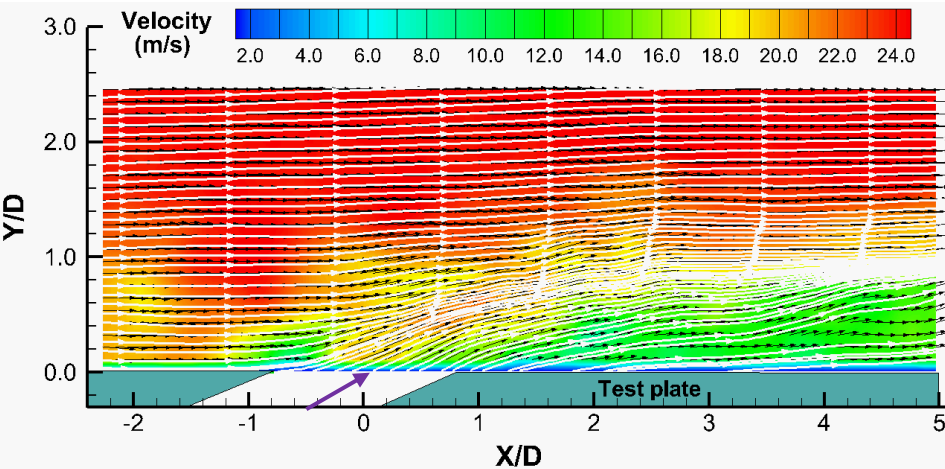
Image Source: Omidyeganeh, et al (2013).



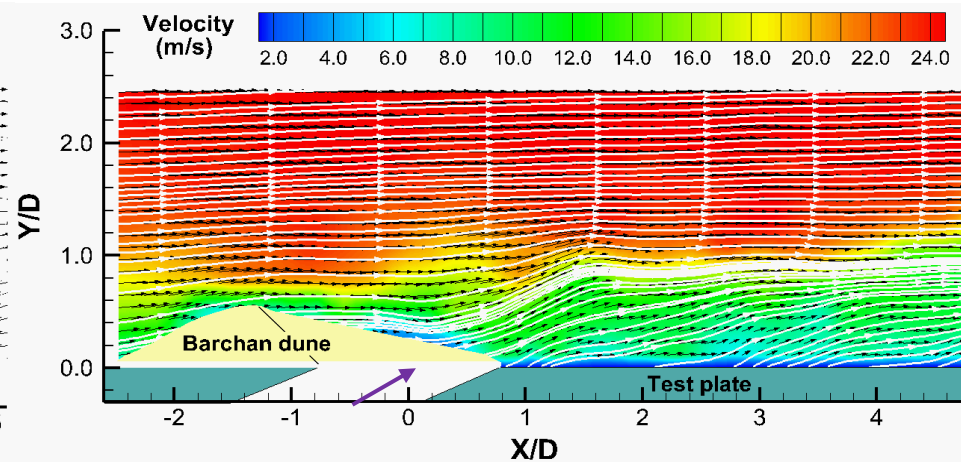
Measured Film Cooling Effectiveness with PSP Technique



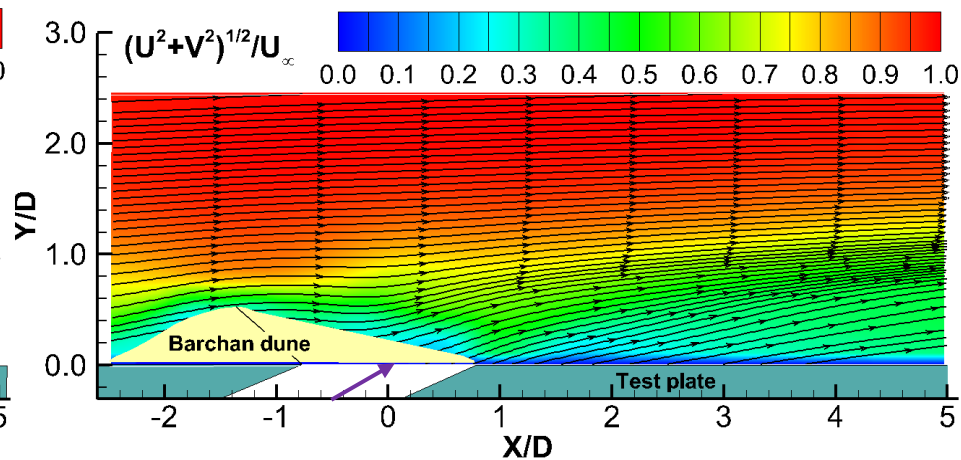
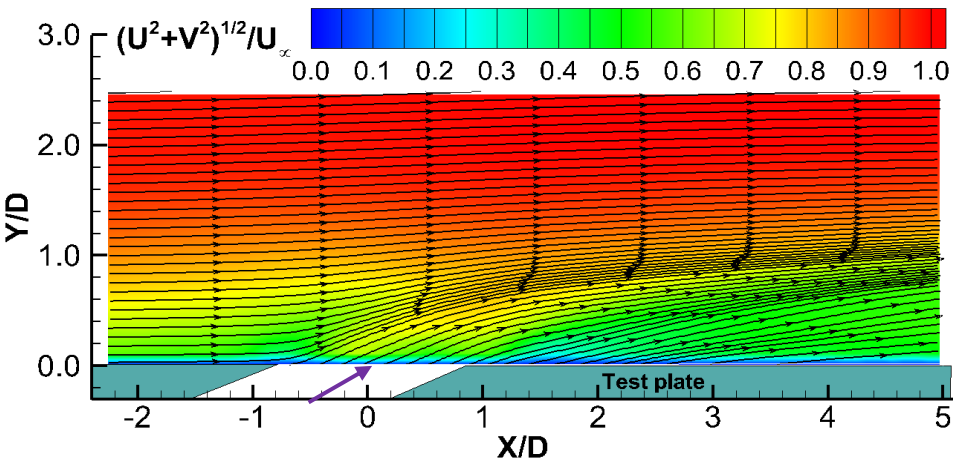
PIV Measurement Results [$M=1.00$]



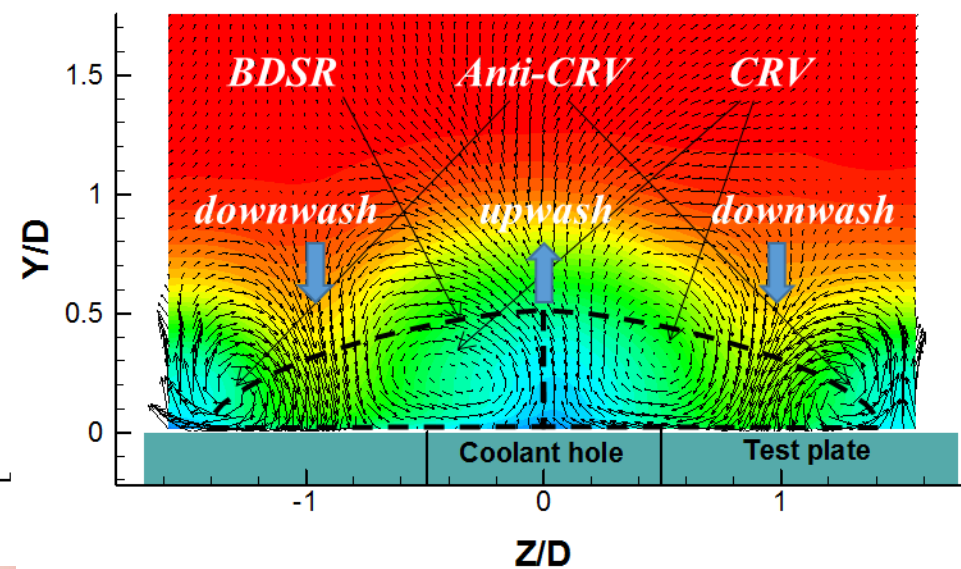
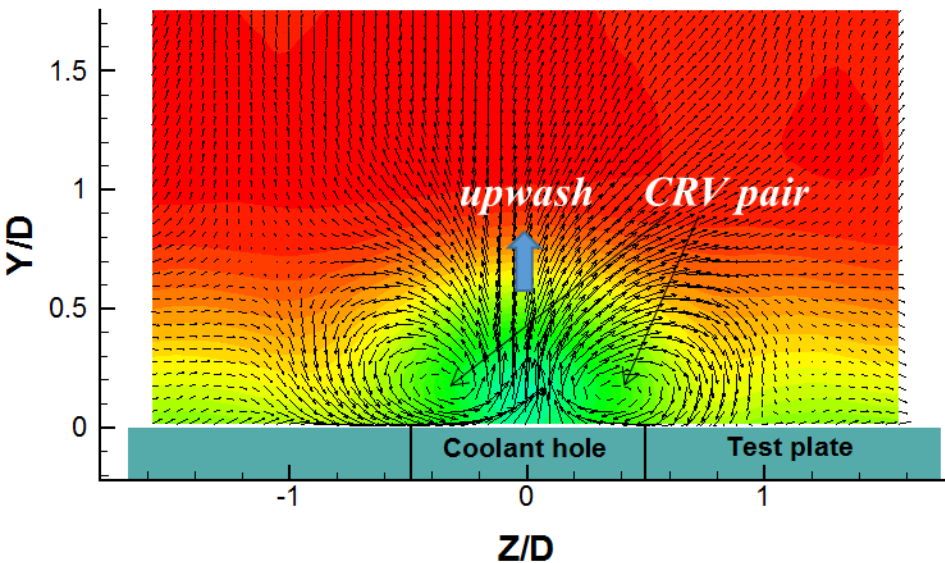
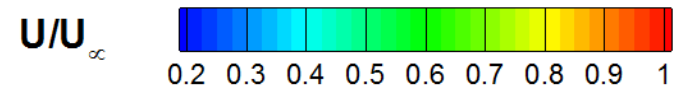
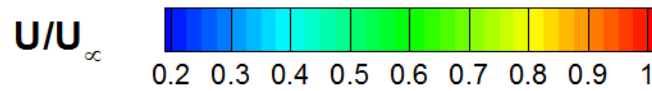
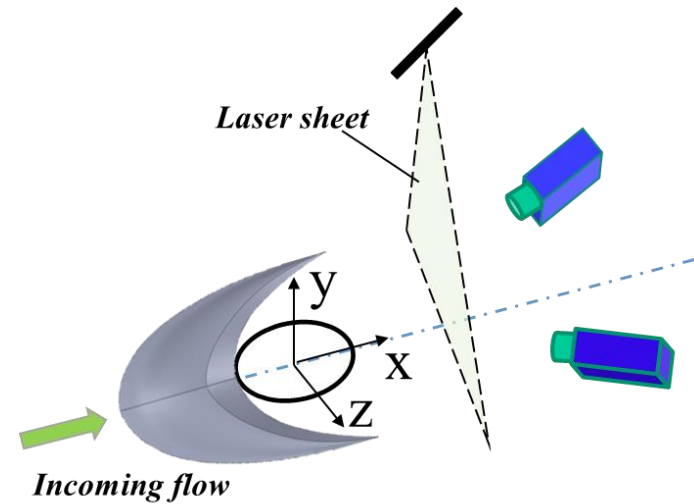
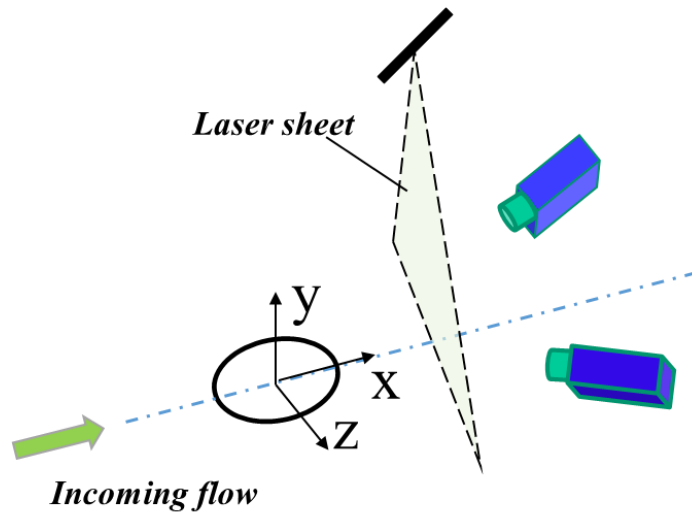
(a) *Baseline case, $M=1.00$*



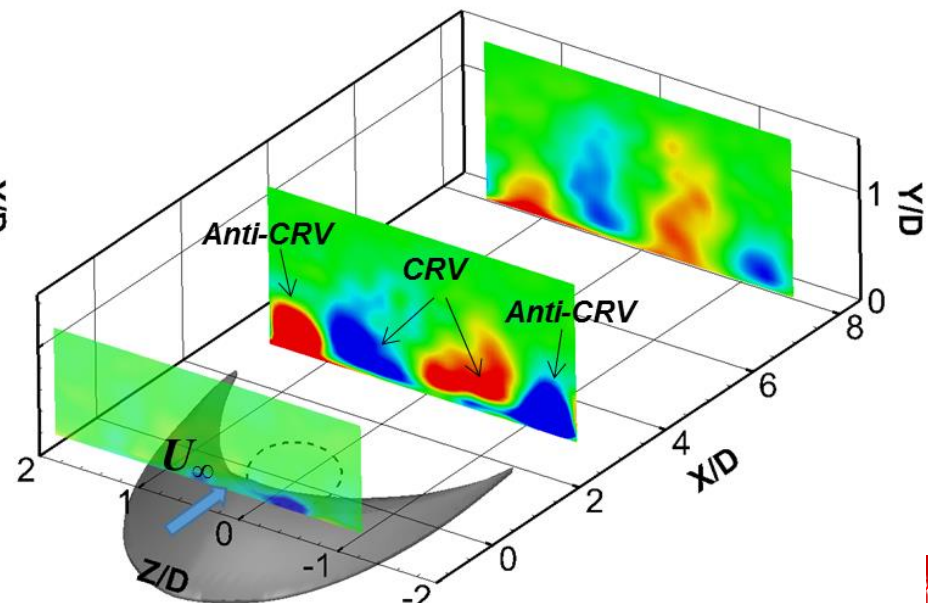
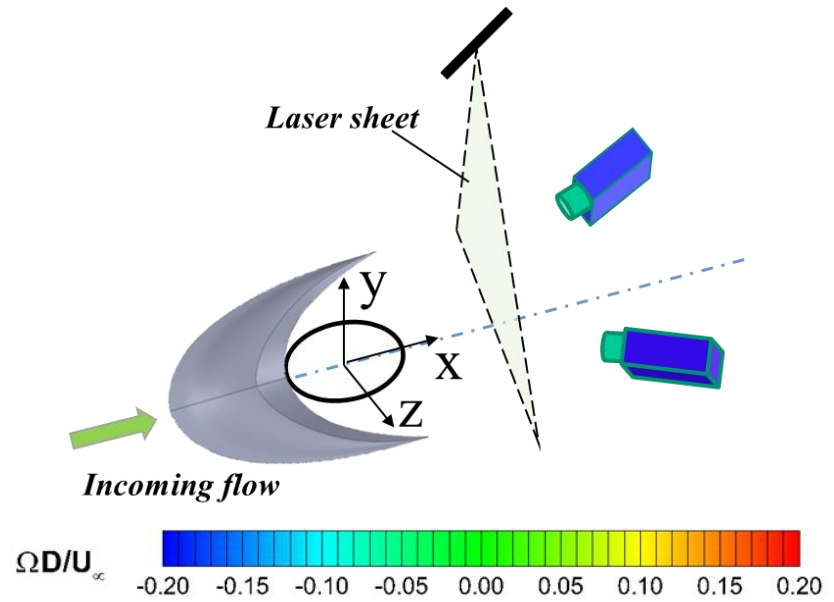
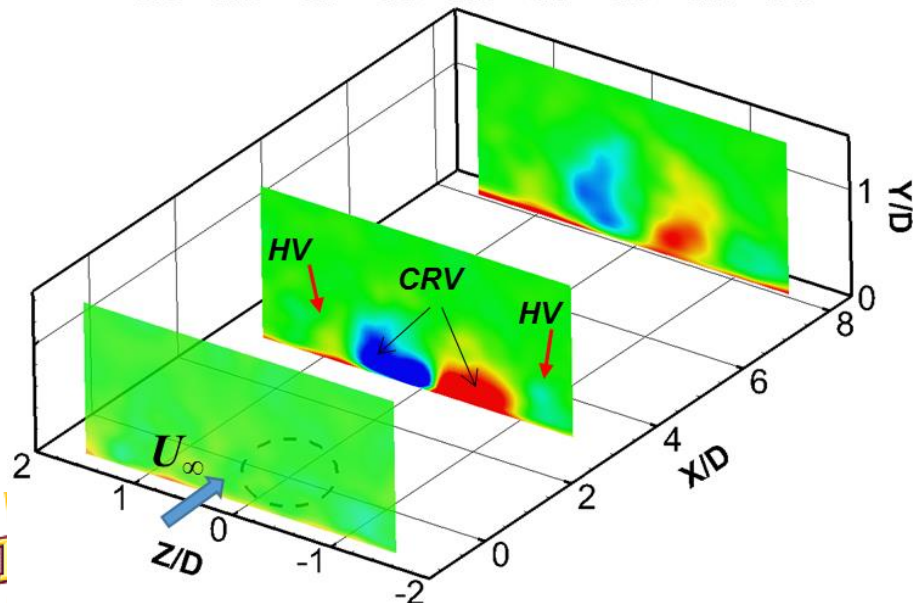
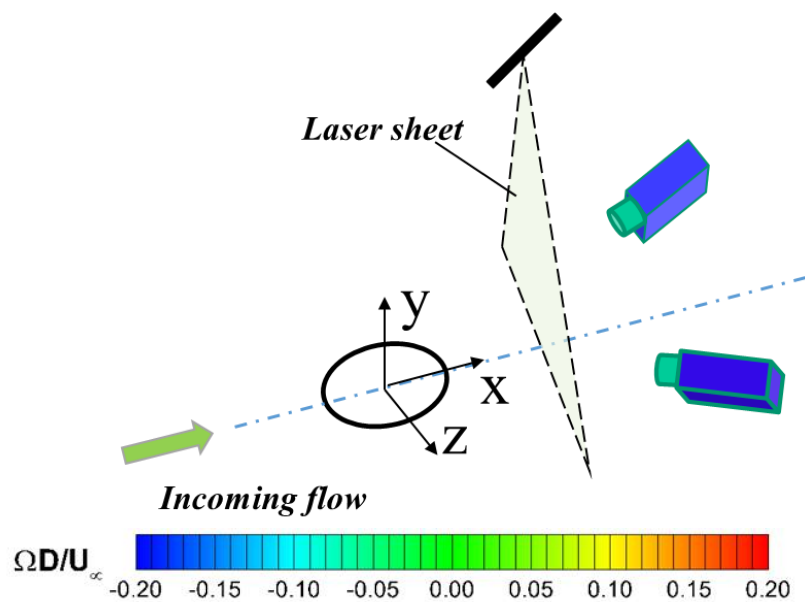
(b) *BDSR, $M=1.00$*



Stereo PIV Measurement (2D3C) [M=1.00]



Stereo PIV Measurement (2D3C) [M=1.00]





Flow over Barchan Dune

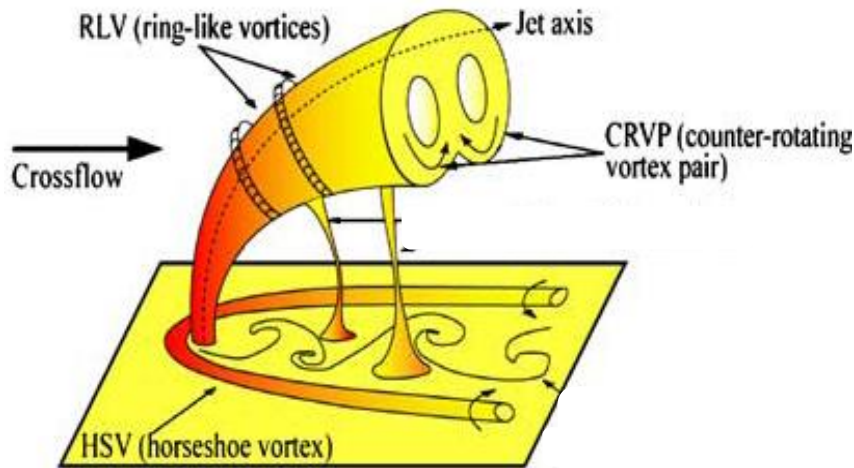
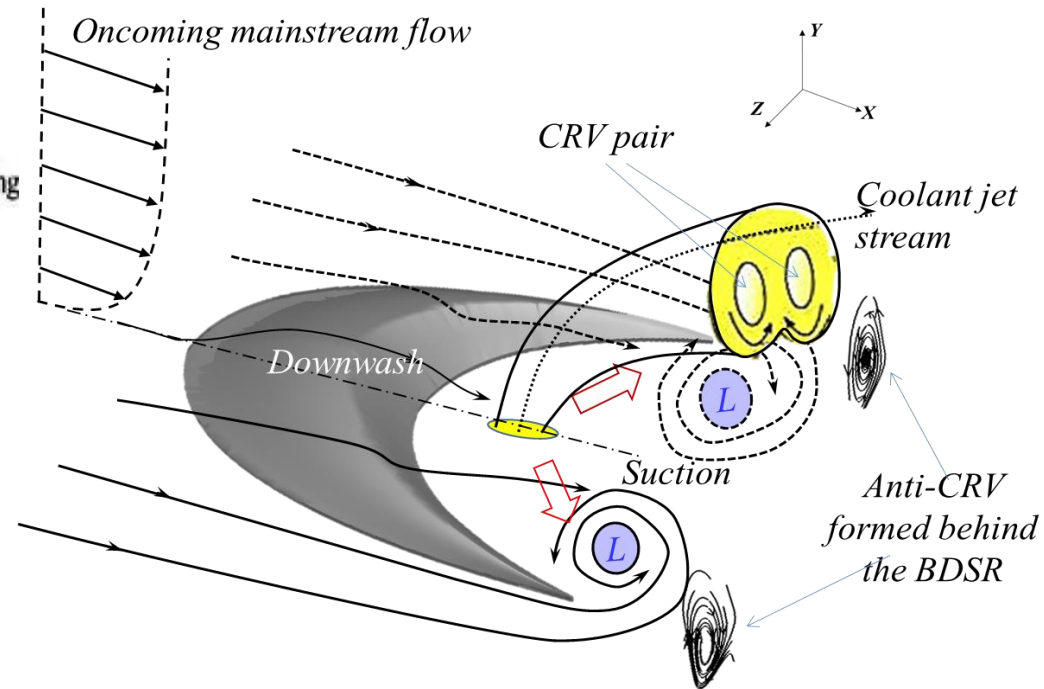


Image Source: Lehrstuhl für Thermodynamik.



Jet in cross flow for baseline case

- **CRV** in Y-Z plane generates detrimental vortex induction and promotes the jet separation.
- **Circulation** in X-Z plane generates continuous suction and force the coolant to spread uniformly.
- **Anti-CRV** in Y-Z plane is able to counteract the vorticity effect, and retards the jet separation.

Concept of Barchan-Dune-Shaped-Injection-Compound (BDSIC)

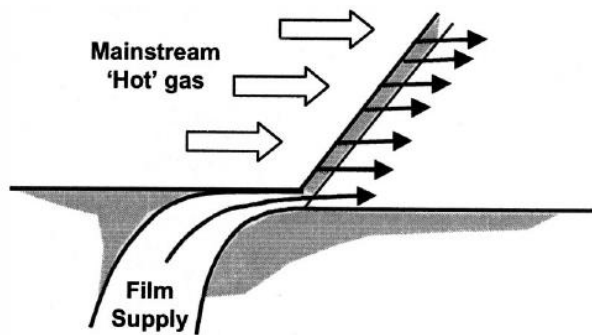
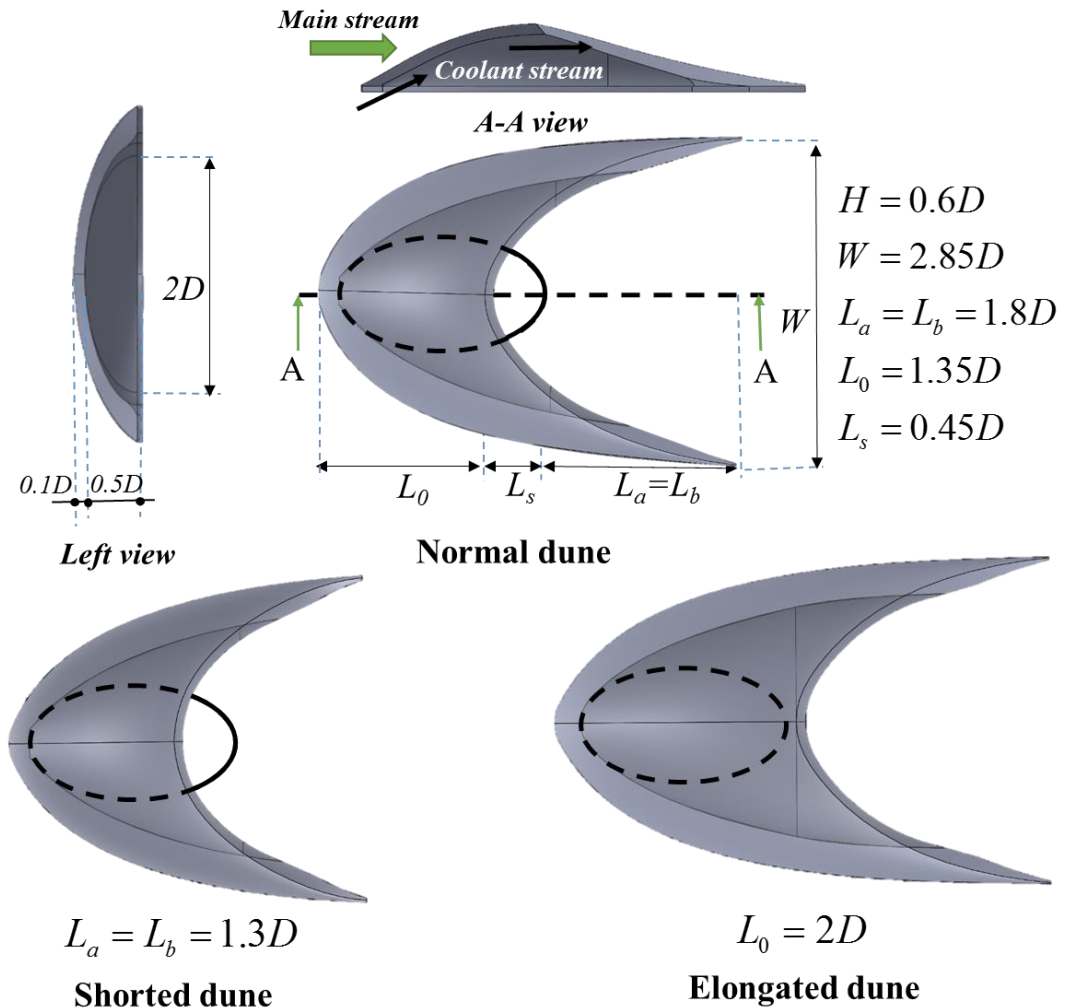


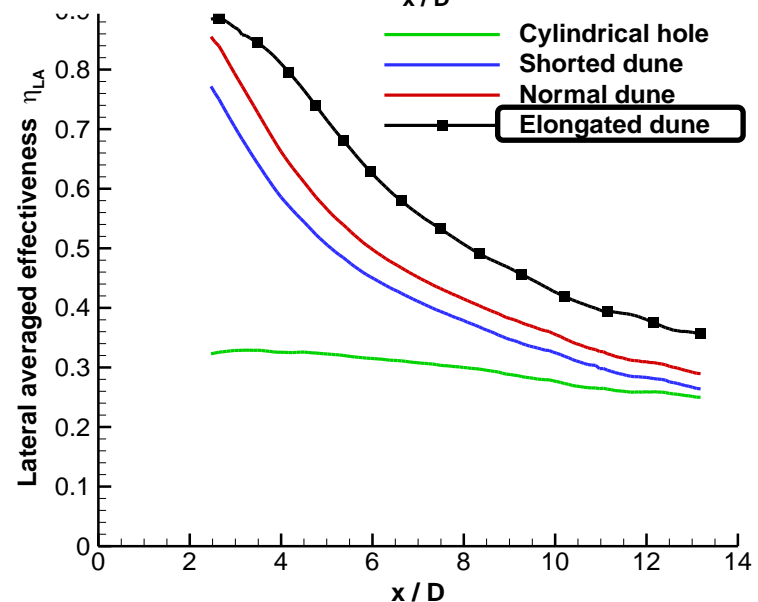
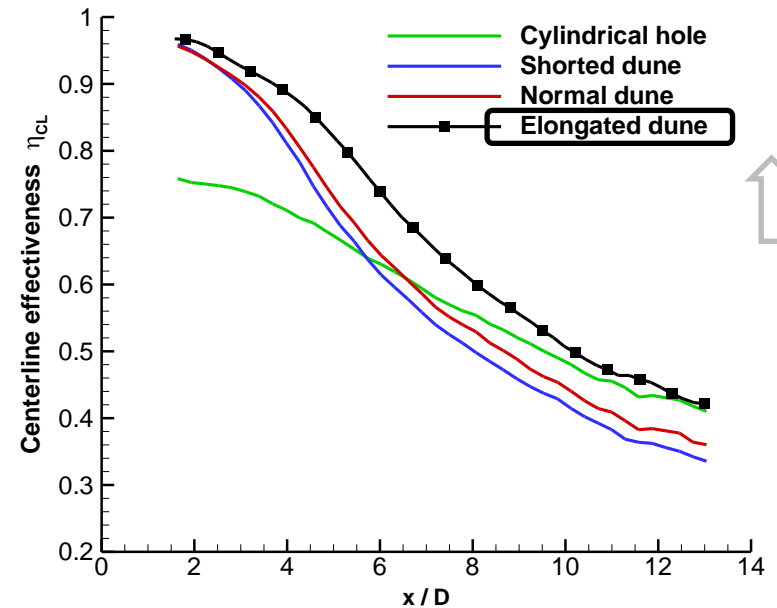
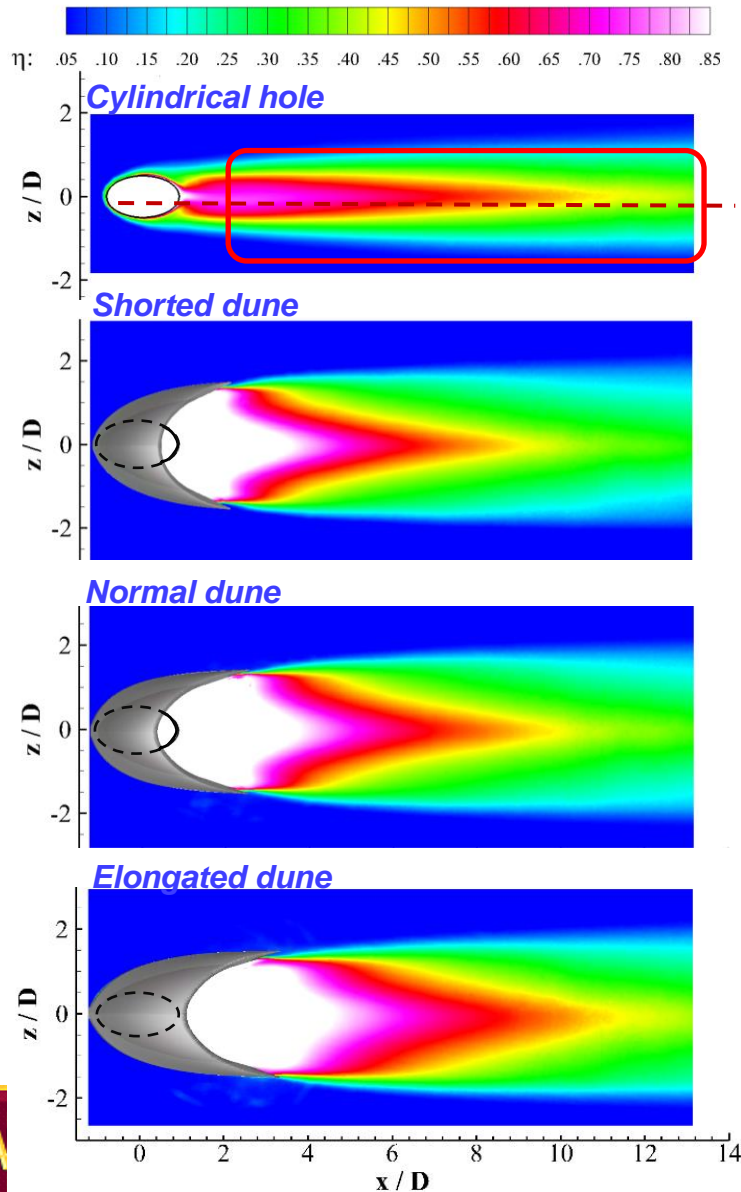
Fig. 1 Ideal tangential slot film cooling
Image Source: Goldstein (1971)

Exit area ratios remained same

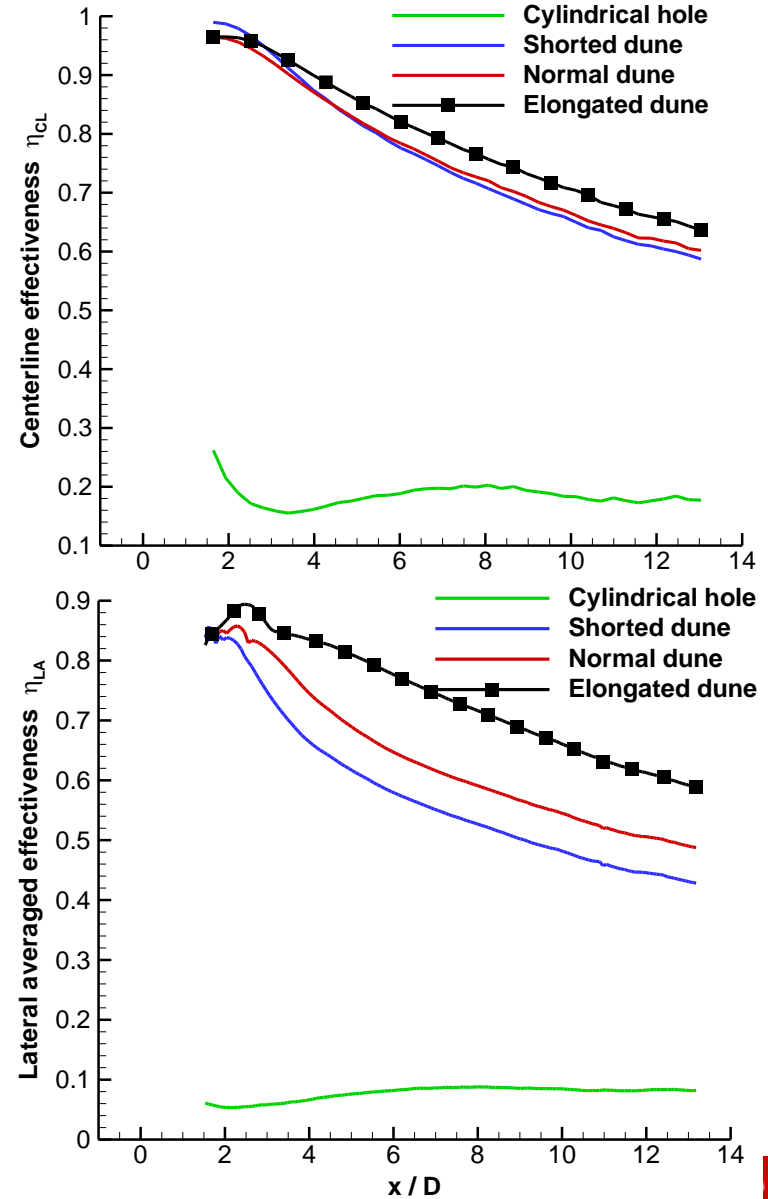
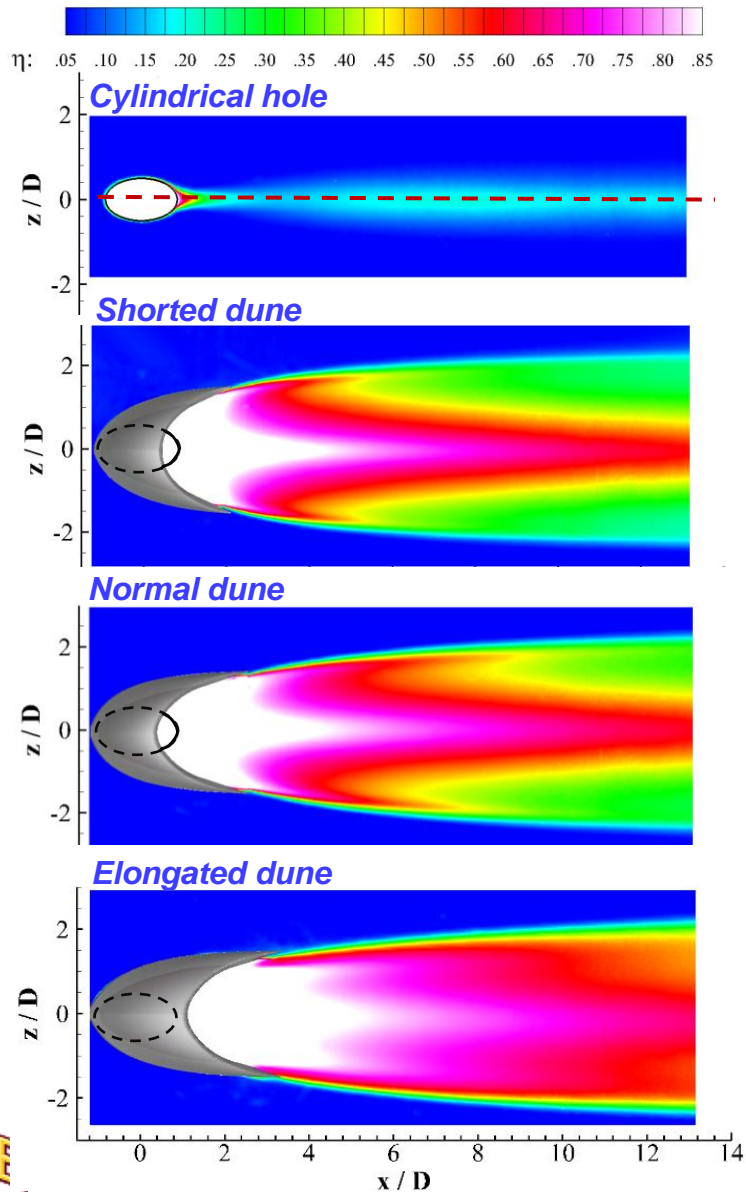


$D=12\text{ mm}$
Single hole

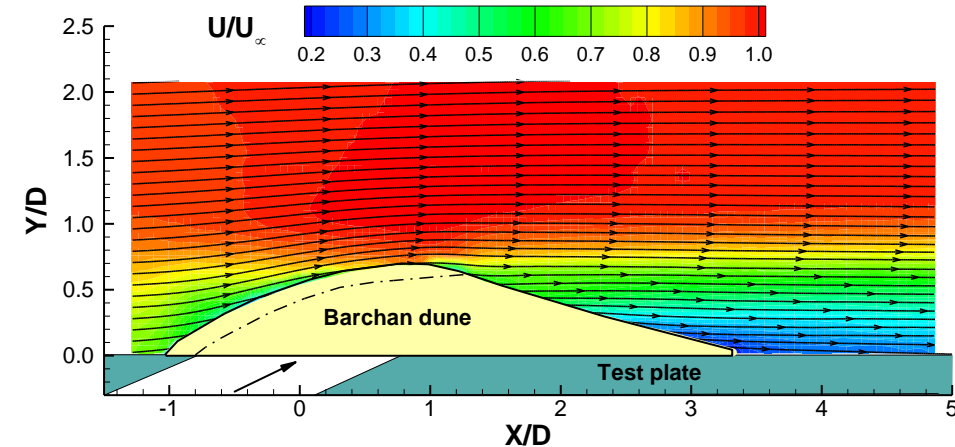
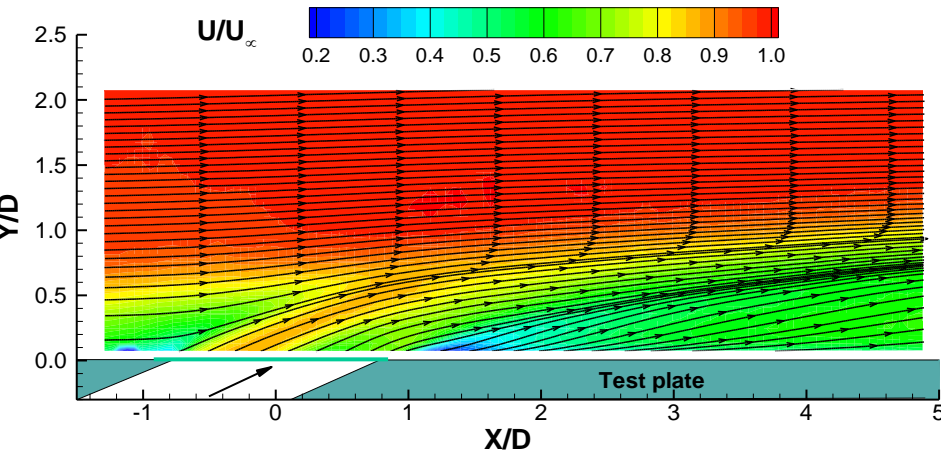
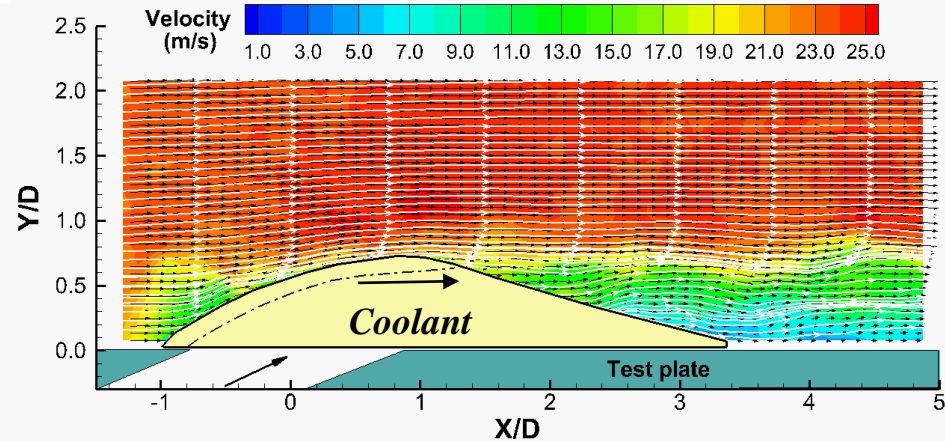
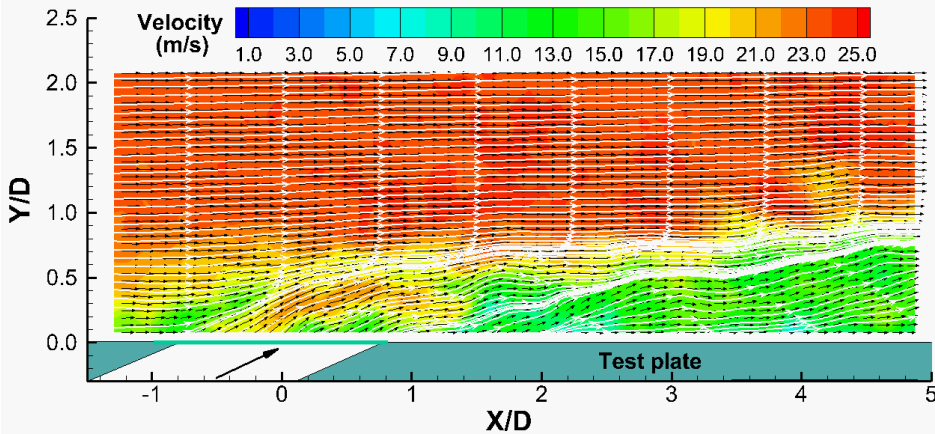
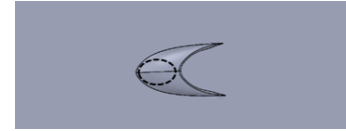
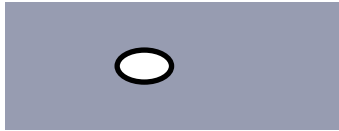
PSP Measurement Results $M=0.6$



PSP Measurement Results [M=1.5]

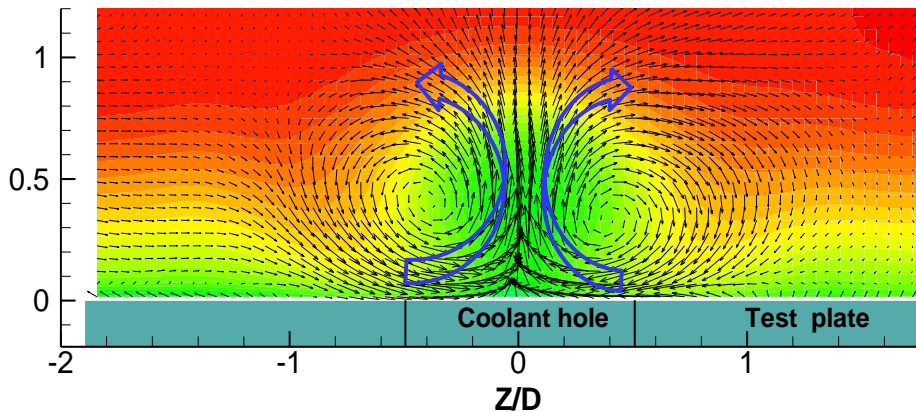
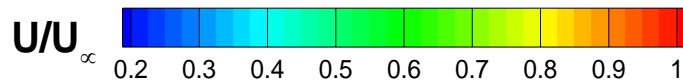
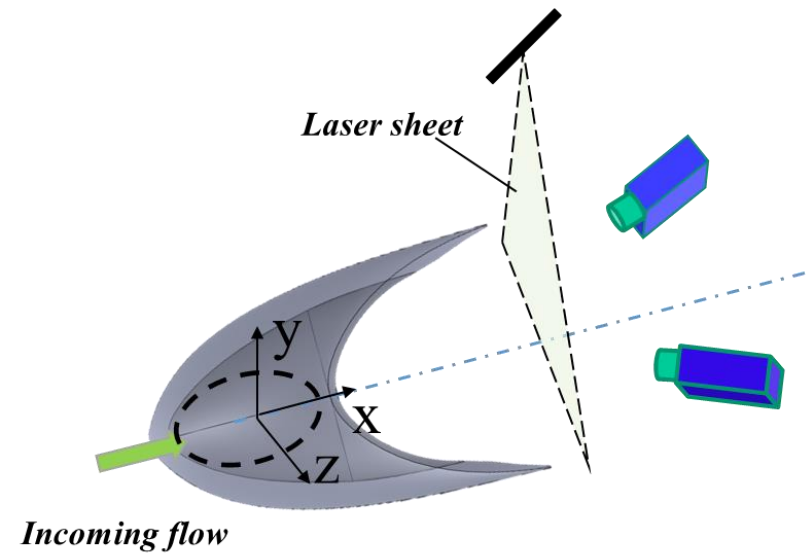
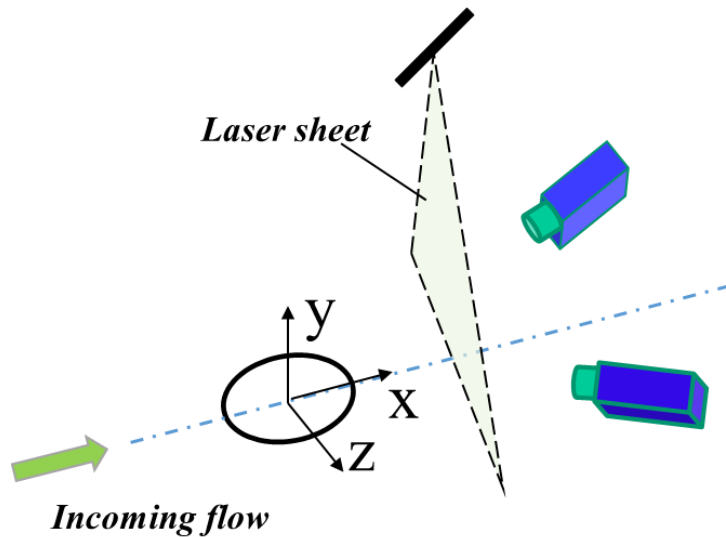


PIV Measurement Results $M=0.9$

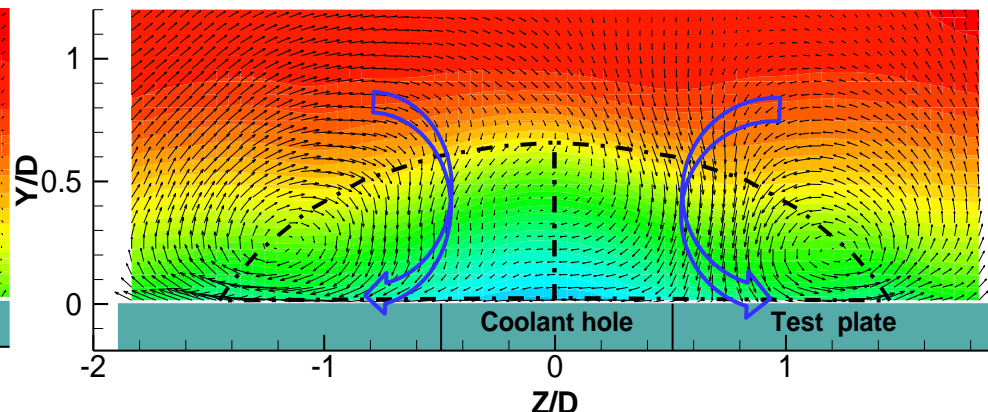
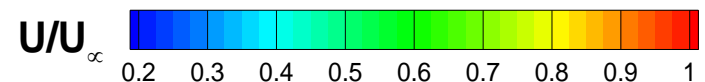


- Circular coolant jet was found to lift off, while the BDSIC jet stayed on the surface.

Stereo PIV Measurement (2D3C) [M=0.9]

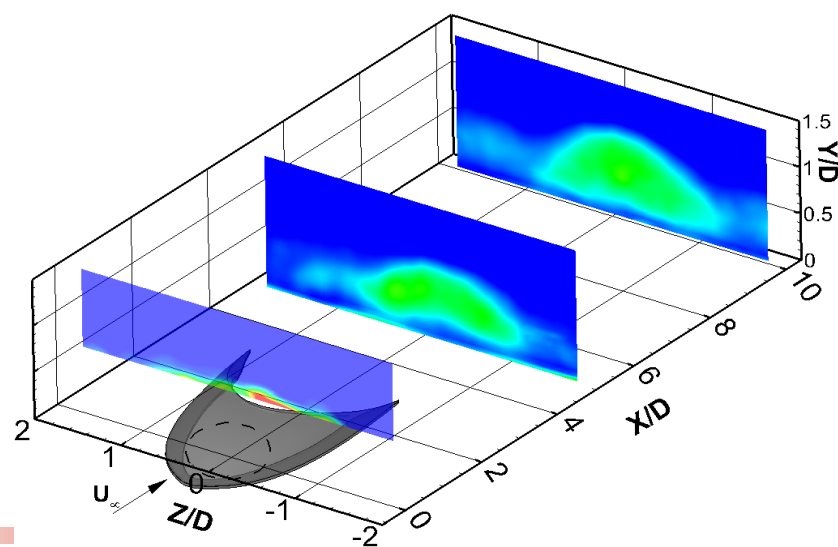
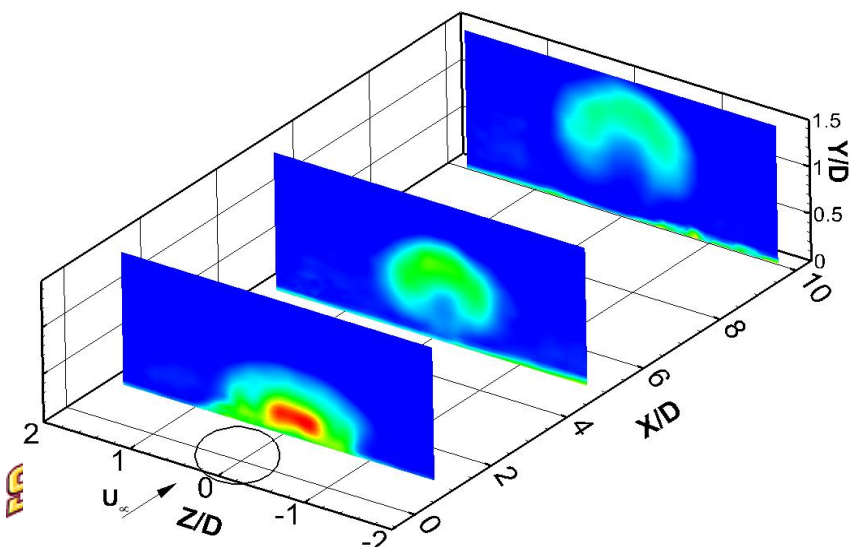
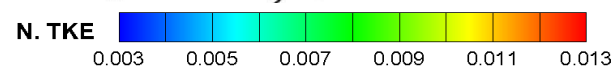
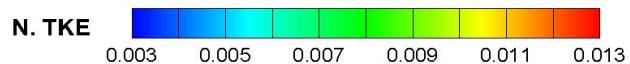
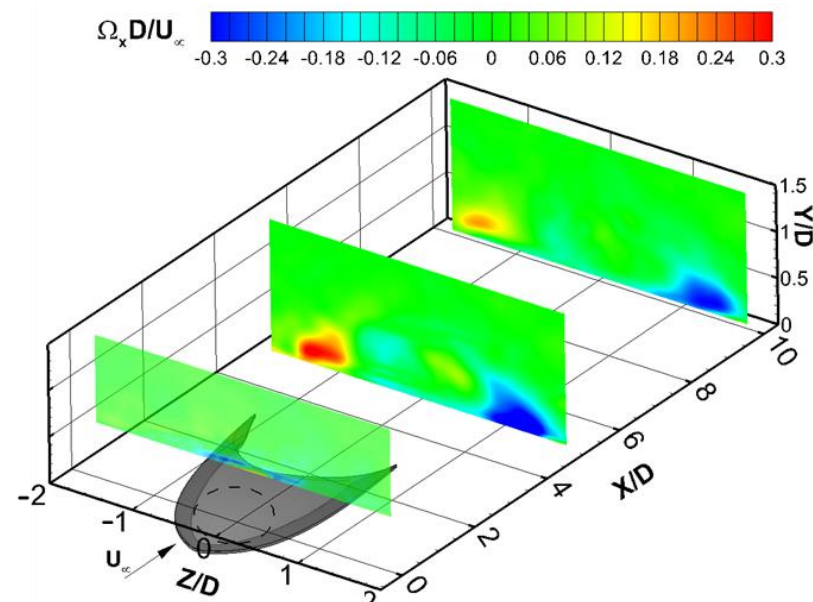
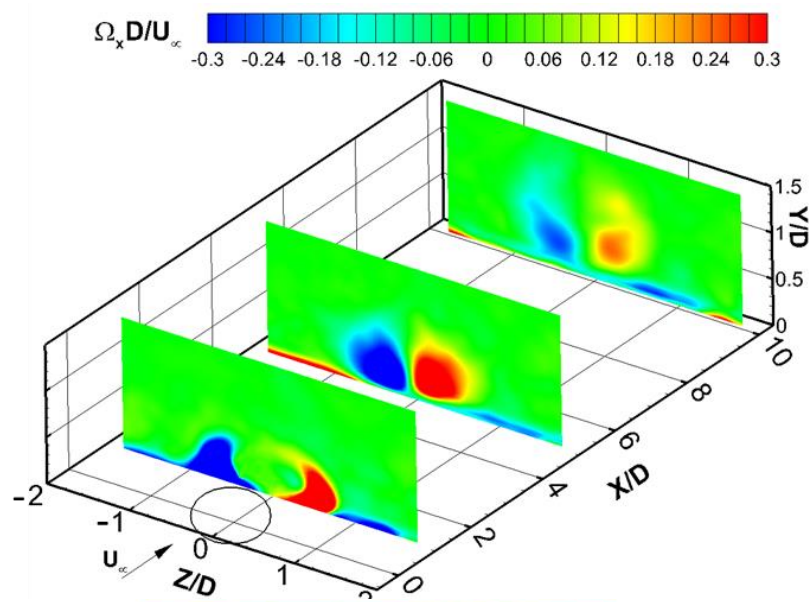


Circular hole, $x/D=5$

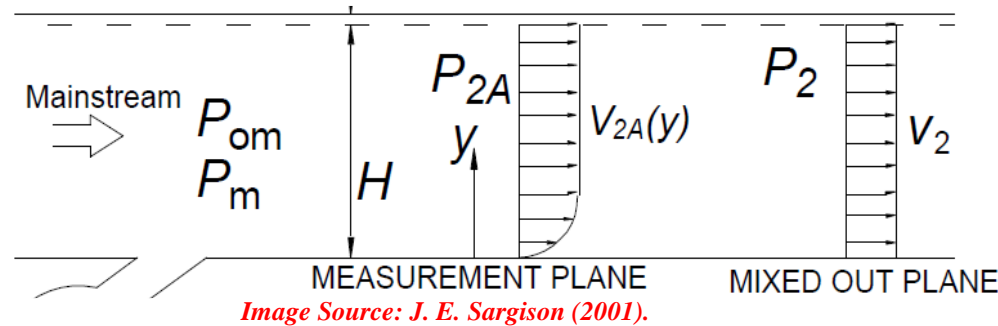


BDSIC, $x/D=5$

Stereo PIV Measurement (2D3C) [M=0.9]

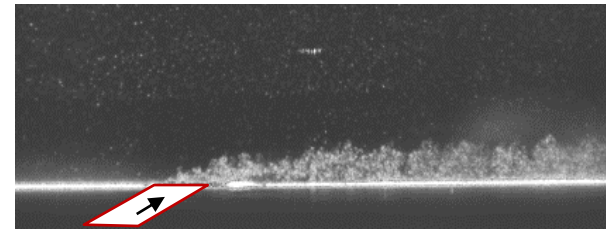
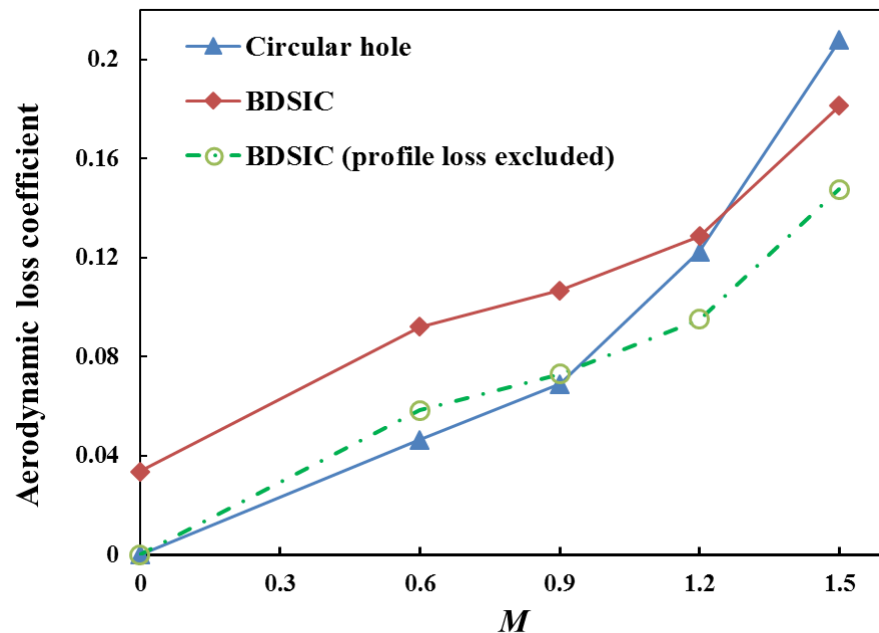


Aerodynamic loss



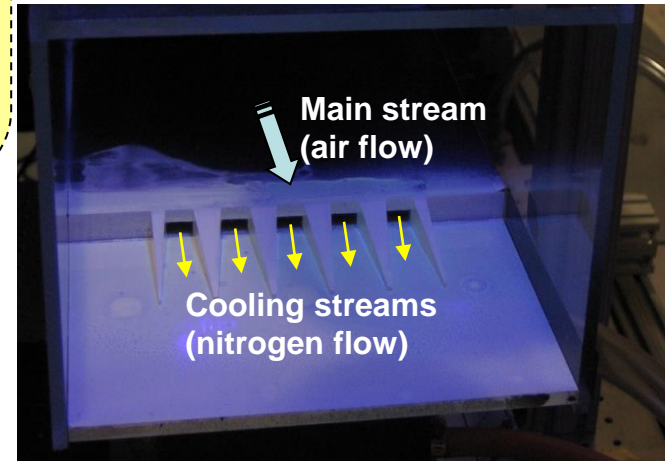
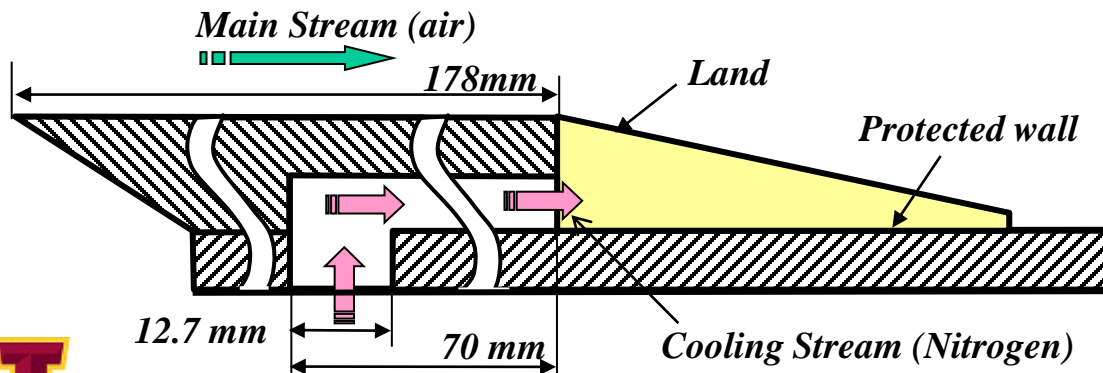
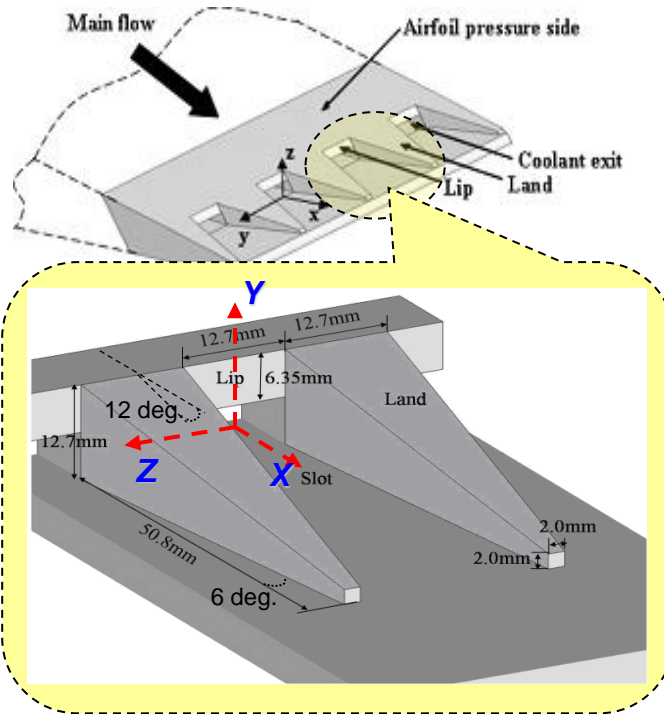
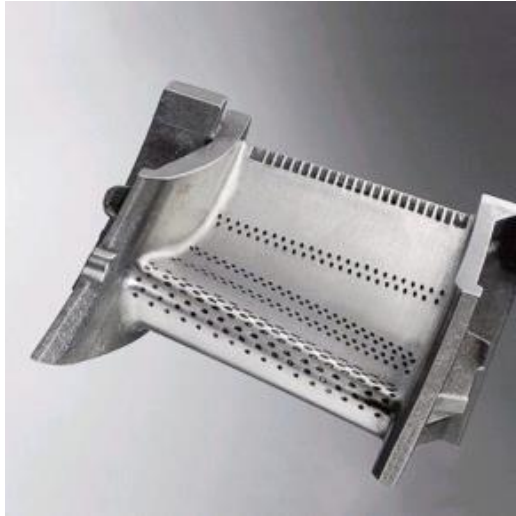
$$Loss = 1 - \frac{0.5 \rho v_2^3 A}{\frac{\dot{m}_m}{\rho_m} (P_{om} - P_2) + \frac{\dot{m}_c}{\rho_c} (P_{oc} - P_2)}$$

- *CV* ($-2D < x < 10D$, $0 < y < 2.5D$, and $-3D < z < 3D$);
- *Air served as coolant.*

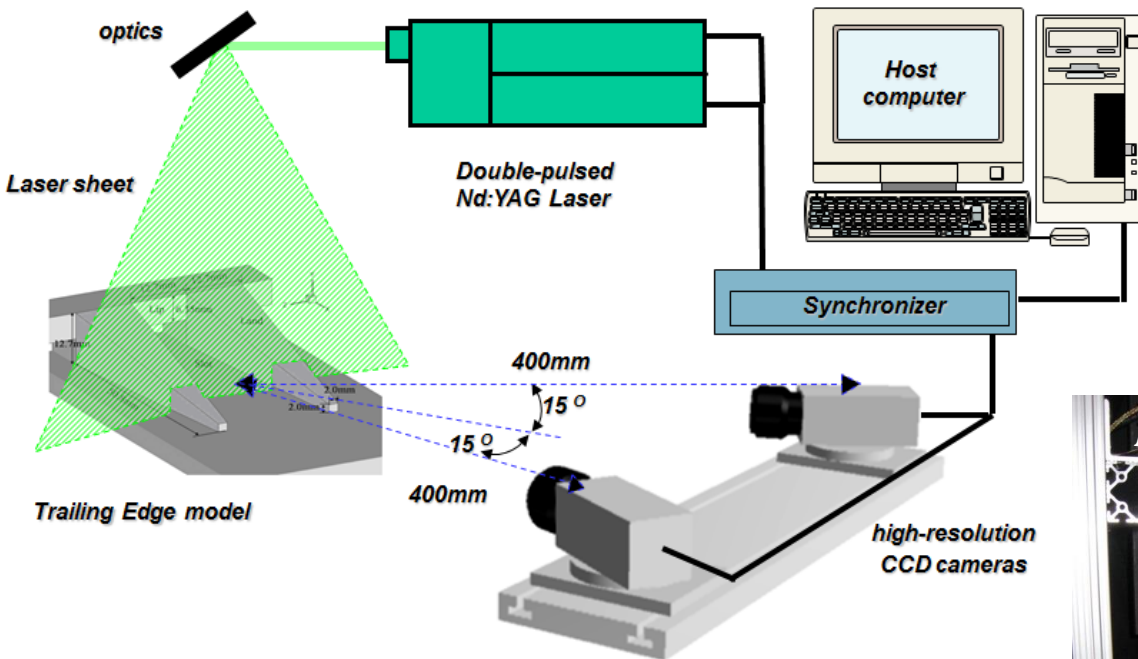


- *Boundary layer mixing is the primary loss for low M.*
- *The circular jet took off and penetrated into the mainstream at high M.*
- *The BDSIC does help alleviate the turbulent mixing between jet and mainstream at relative high M.*

Trailing Edge Cooling: Test Model and Flow Conditions



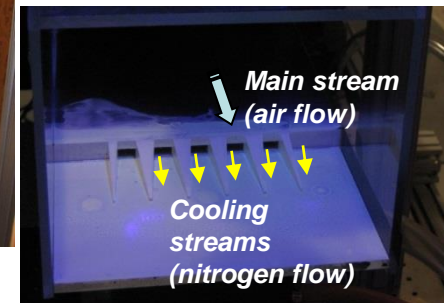
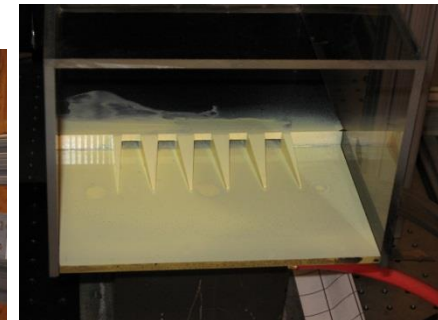
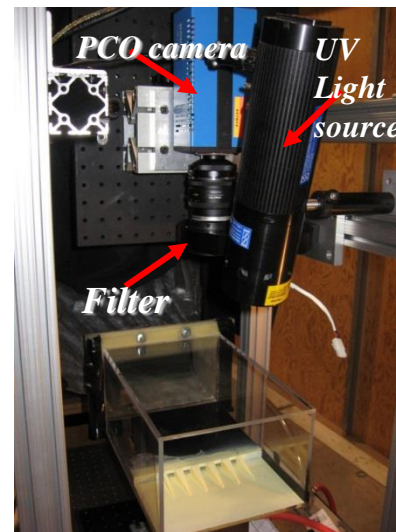
Experimental Setup: Stereo PIV and PSP Measurements



Experimental Setup for SPIV measurements

Test conditions:

- Flow velocity of main stream: $V_0 = 16.2 \text{ m/s}$
- Blowing ratio : $M = 0 \sim 1.6$.
- $Re_m = 190K$ based on model length.
- $Re_s = 2,800 \sim 10,500$ based on tip thickness
- Turbulence intensity for main stream: $< 1.0\%$
- Turbulence intensity for coolant streams: $\sim 5.0\%$.

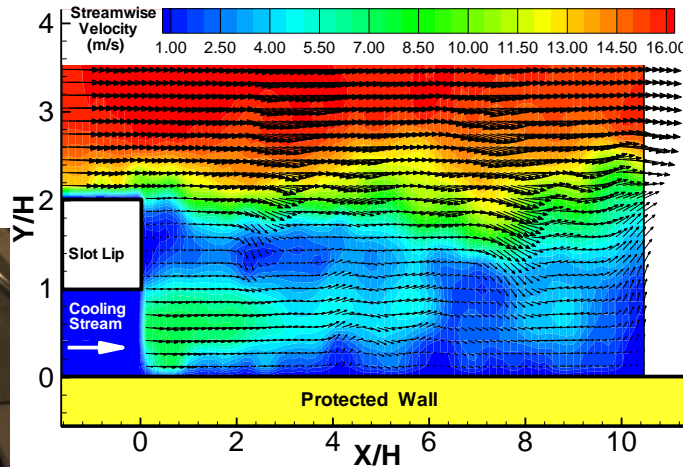


Experimental Setup for PSP measurements

PIV measurement Results in the Cross Plane Along Flow Direction

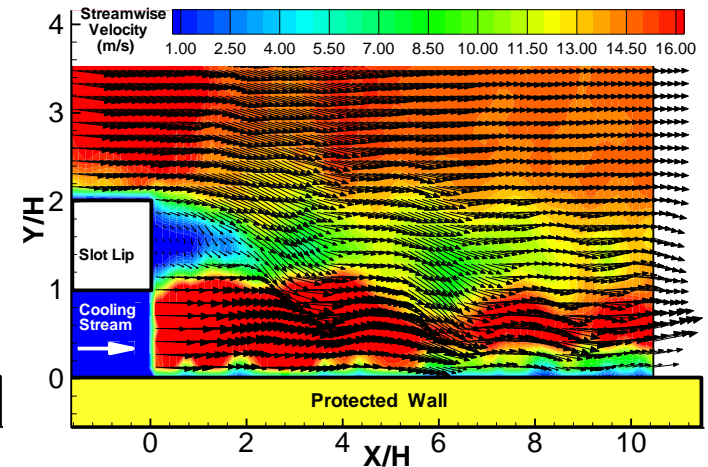


Blowing ratio $M=0.45$

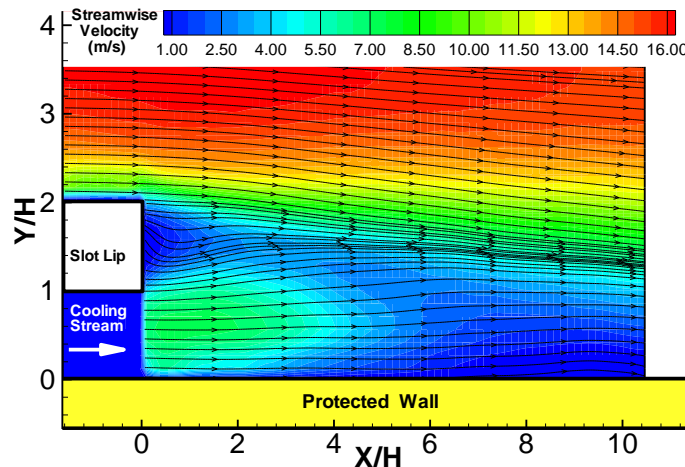
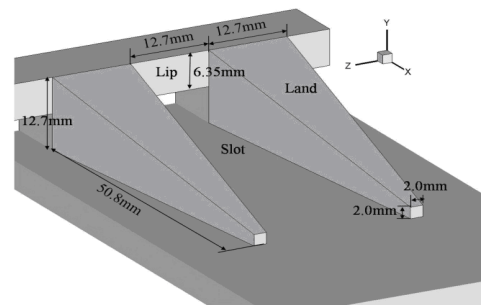
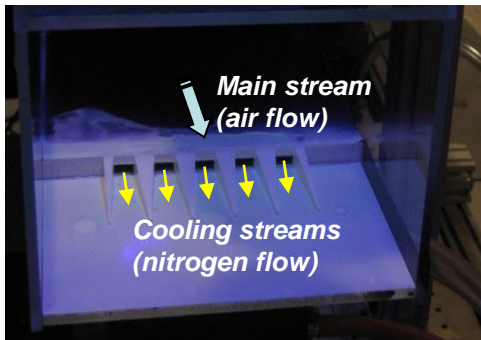


Instantaneous velocity distributions

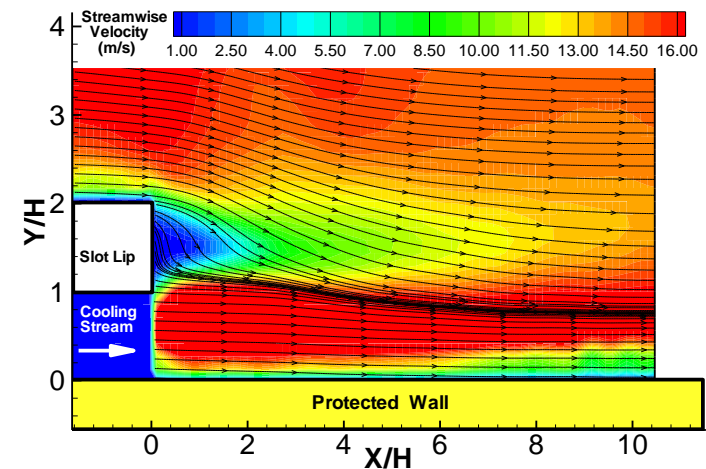
Blowing ratio, $M=1.60$



Instantaneous velocity distributions



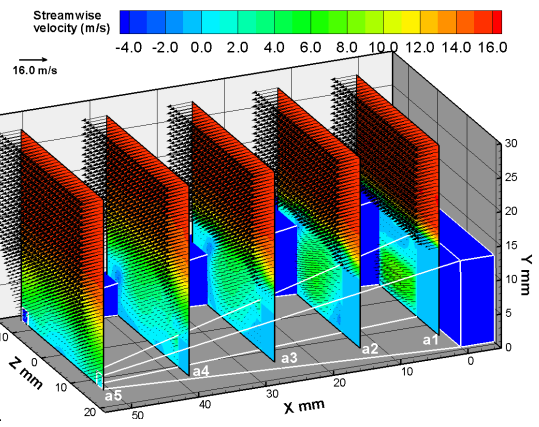
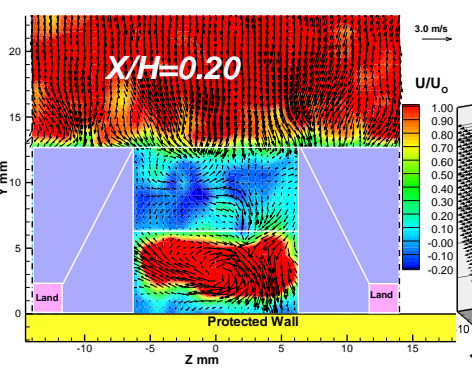
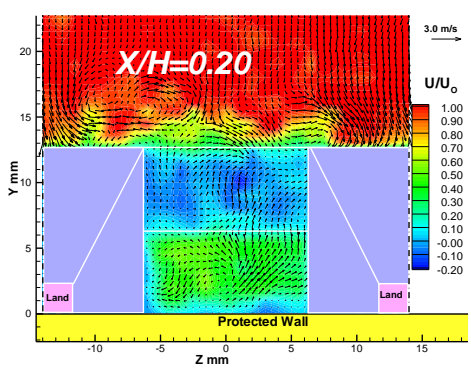
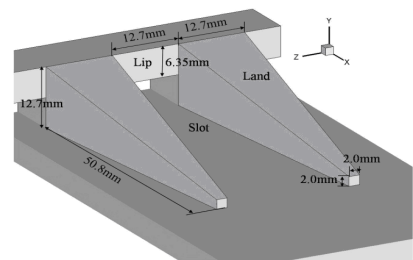
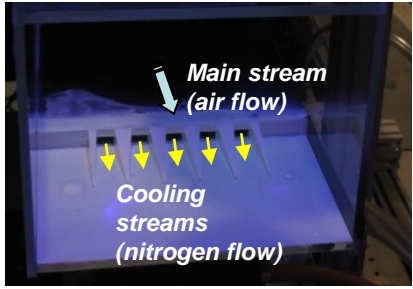
Time-averaged velocity distribution



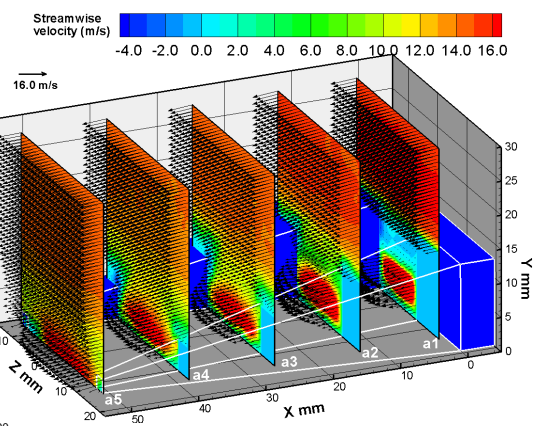
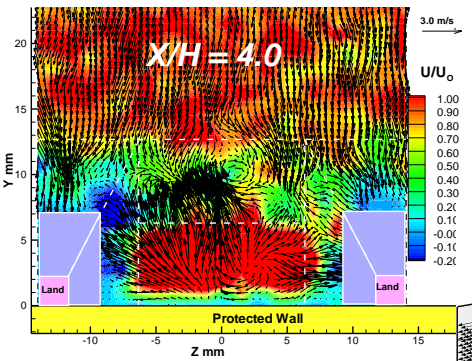
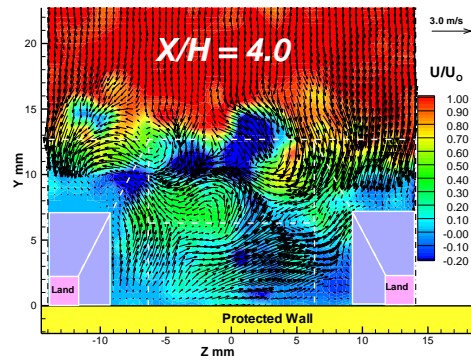
Time-averaged velocity distribution



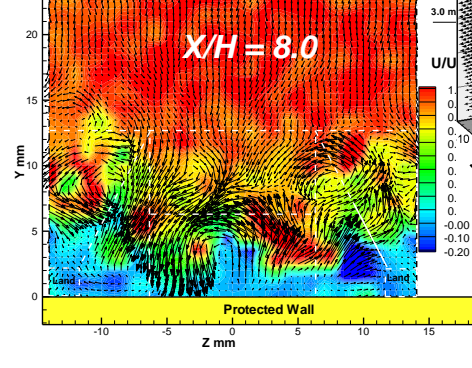
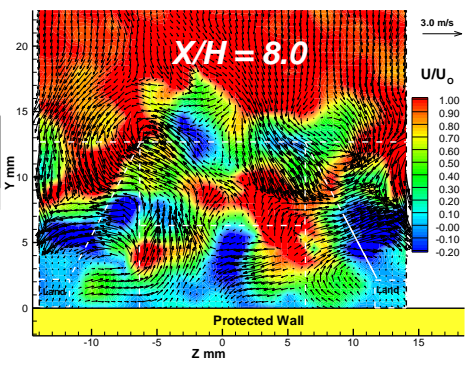
Stereoscopic PIV measurement Results



Blowing ratio, $M = 0.45$



Blowing ratio, $M = 1.60$



Blowing ratio, $M = 0.45$

Blowing ratio, $M = 1.60$



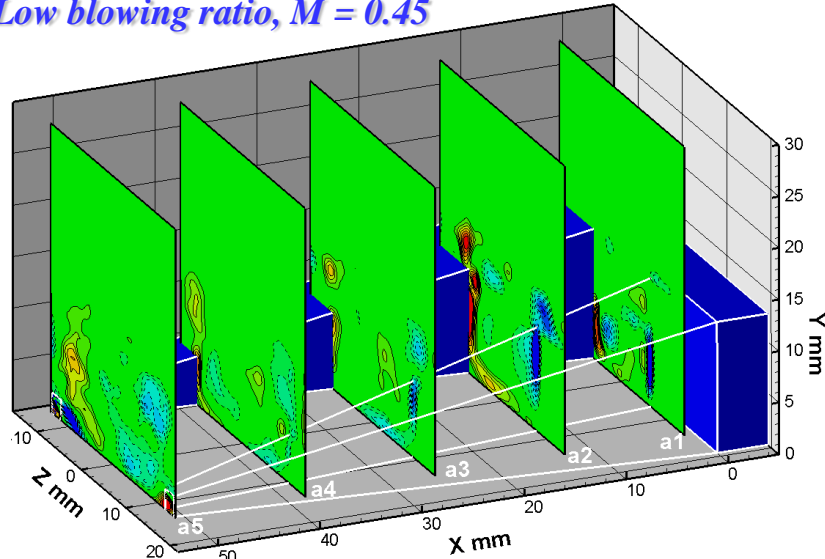
Flow Patterns of the Slot Jets near the Trailing Edge of a Turbine Blade



Vorticity (1/s)

-0.40	-0.35	-0.30	-0.25	-0.20	-0.15	-0.10	0.10	0.15	0.20	0.25	0.30	0.35	0.40
-------	-------	-------	-------	-------	-------	-------	------	------	------	------	------	------	------

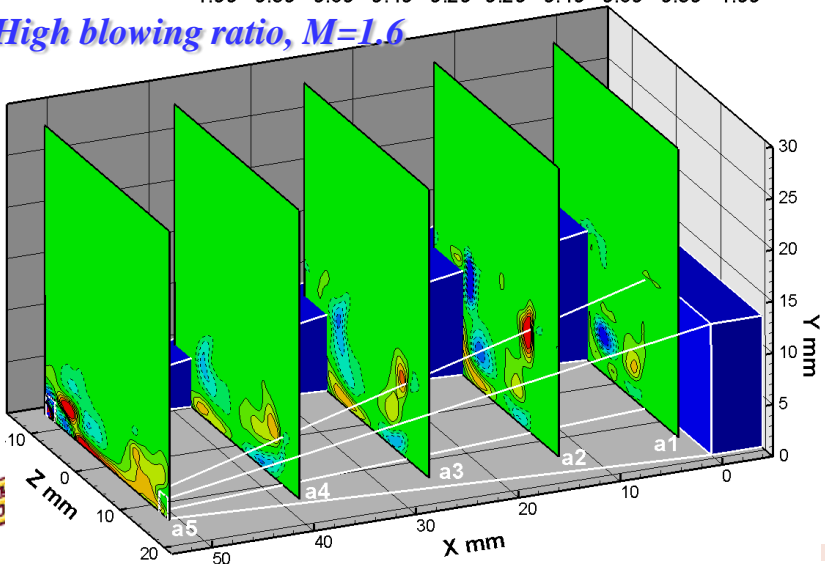
Low blowing ratio, $M = 0.45$



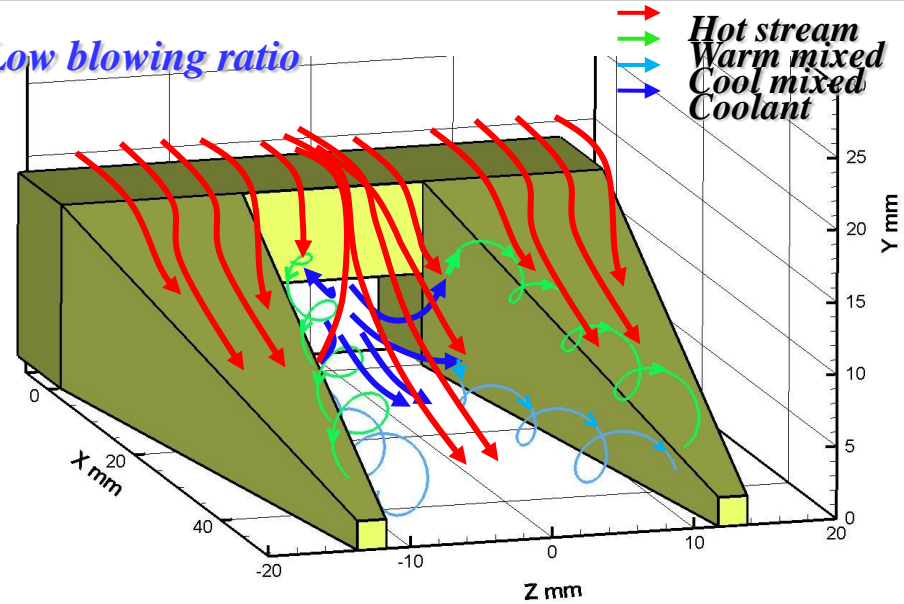
Vorticity (1/s)

-1.00	-0.80	-0.60	-0.40	-0.20	0.20	0.40	0.60	0.80	1.00
-------	-------	-------	-------	-------	------	------	------	------	------

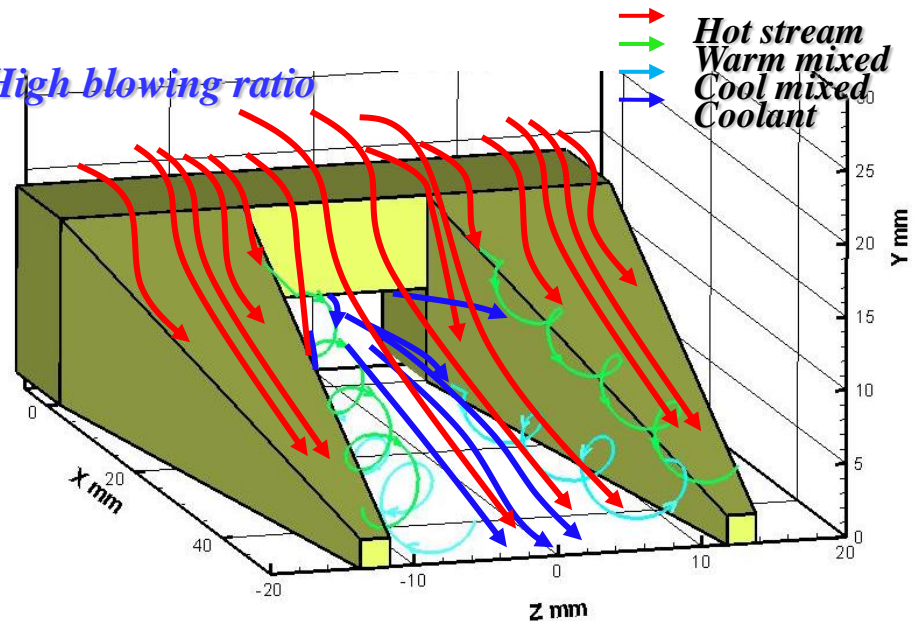
High blowing ratio, $M=1.6$



Low blowing ratio



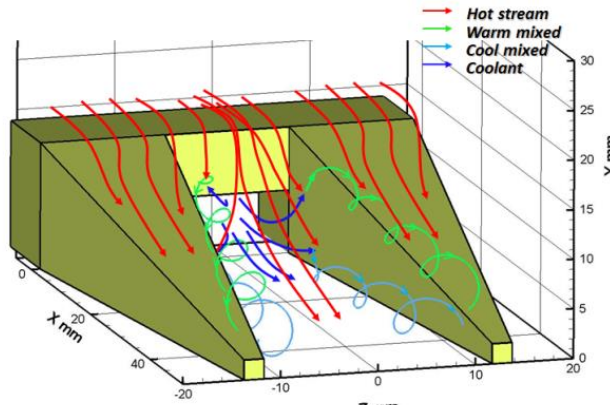
High blowing ratio



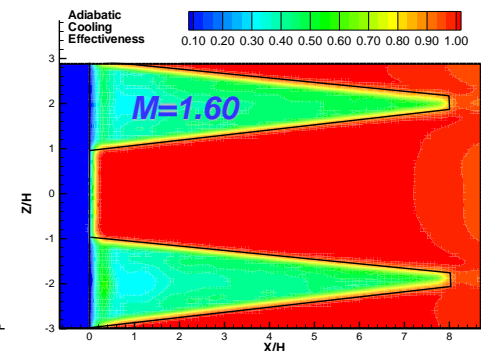
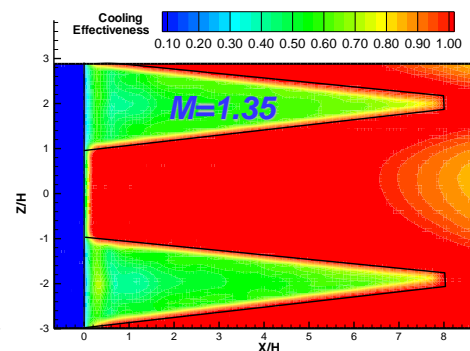
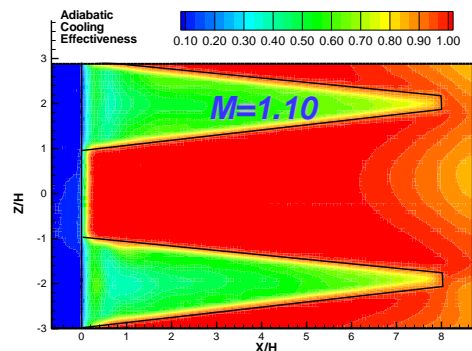
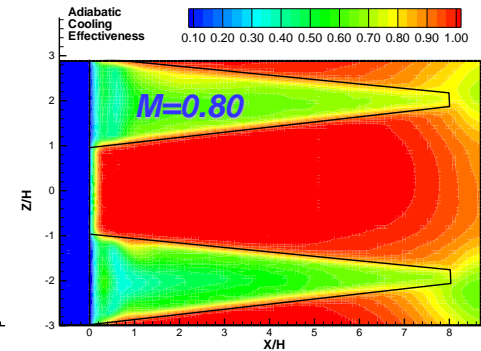
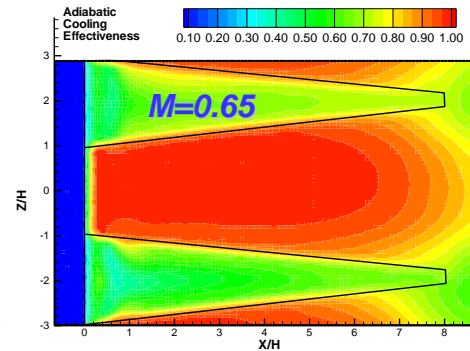
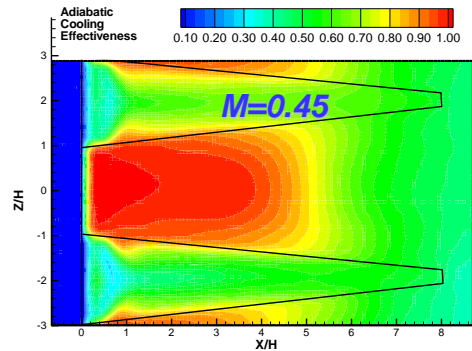
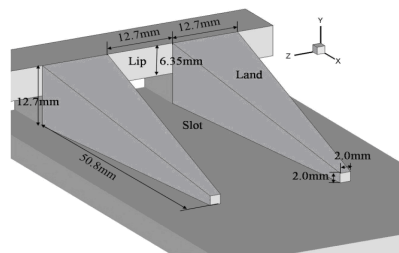
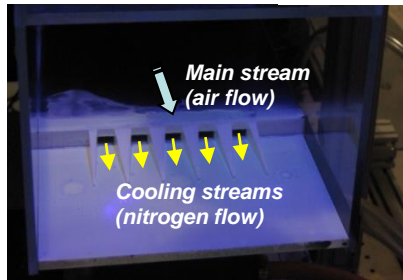
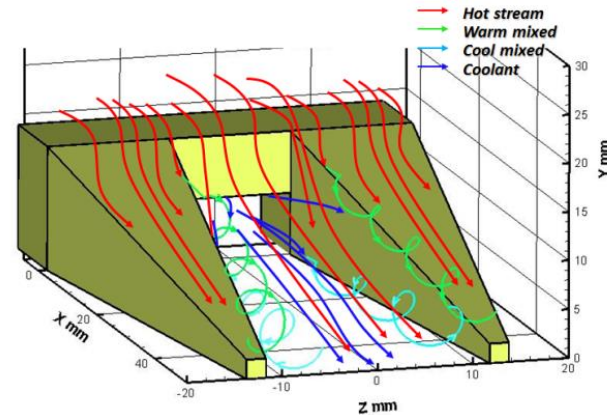


PSP Measurement Results – Blow Ratio, $M = 1.60$

At a lower
blowing ratio,
 $M < 1.0$



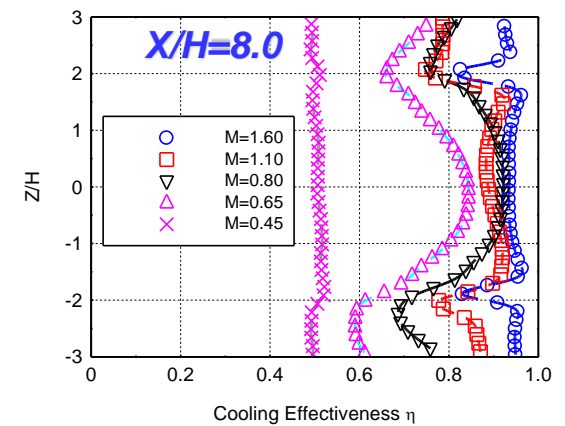
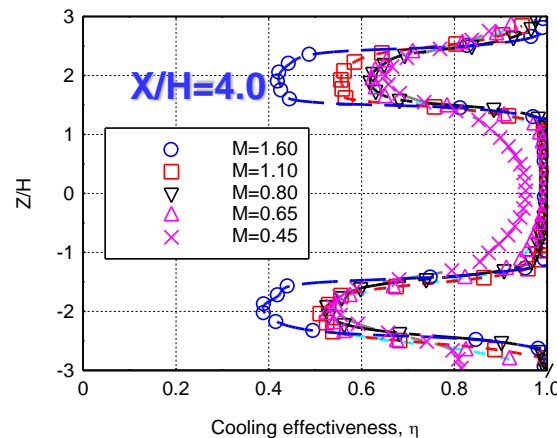
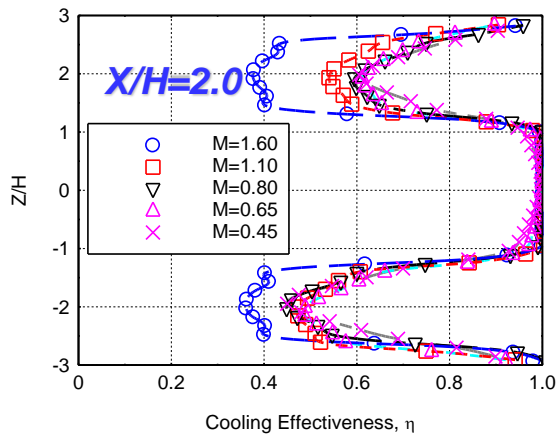
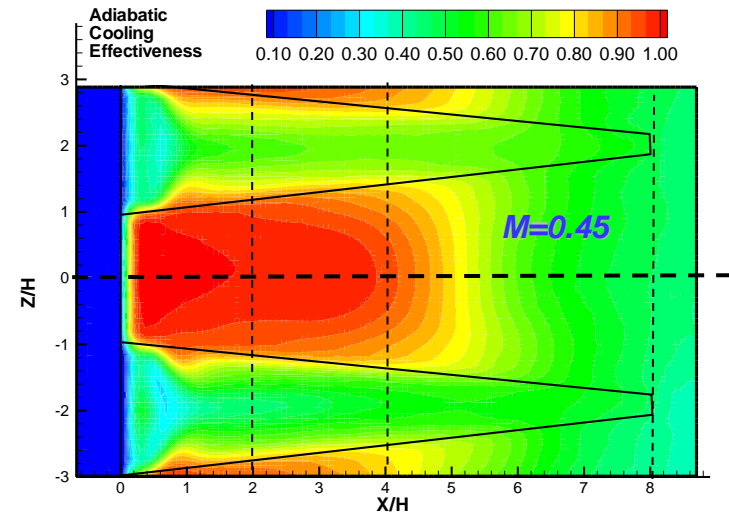
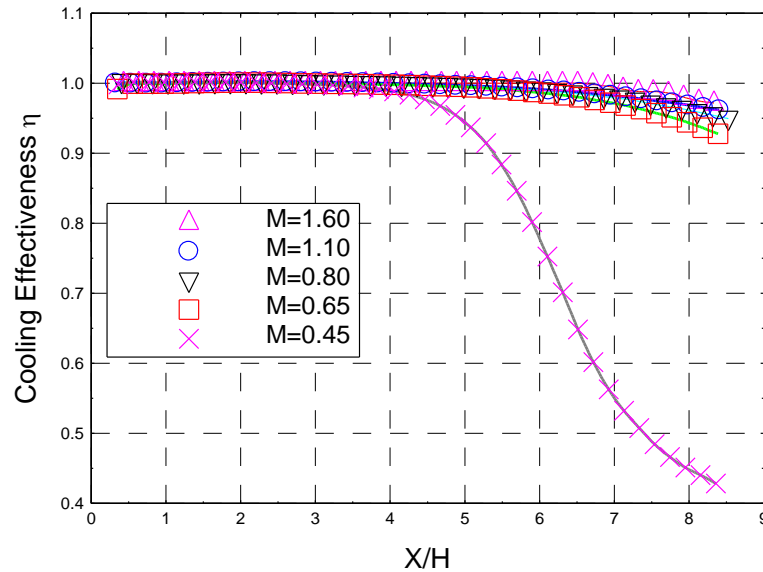
At a higher
blowing ratio,
 $M > 1.0$



(Yang and Hu, AIAA J. of Power and Propulsion, Vol.27, No.3, pp700-709, 2011)

IOWA STATE UNIVERSITY

Cooling Effectiveness Measurements by using PSP technique



Internal Cooling of Turbine Blades



Internal heat transfer:

- *Impinging cooling along the leading edge and trailing edge*
- *Rib turbulator in the middle range to enhance force convective heat transfer*
- *Near trailing edge utilizing pin-fin cooling*

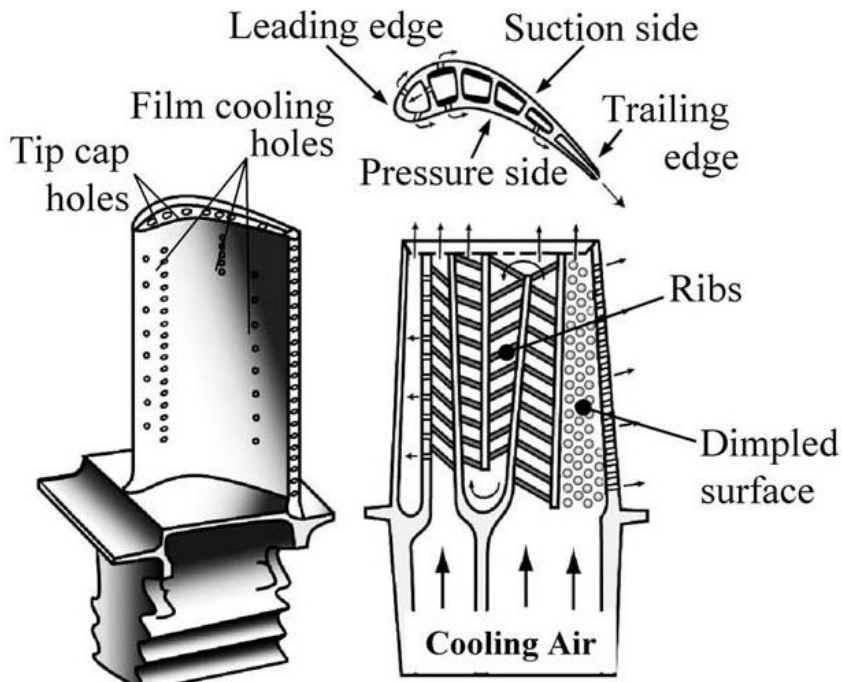


Image Source: Murata Lab

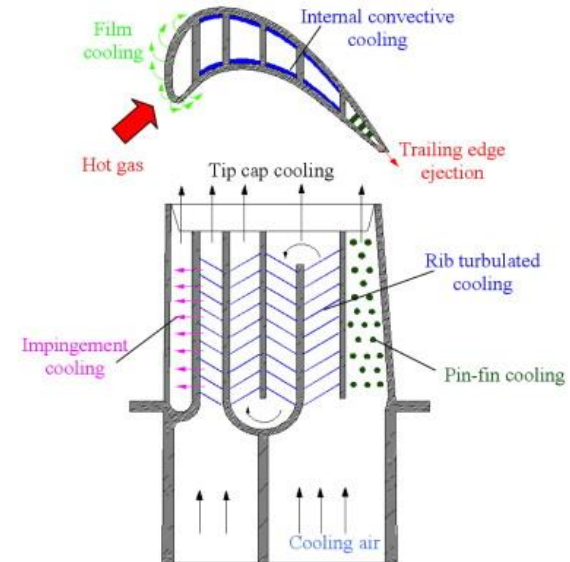


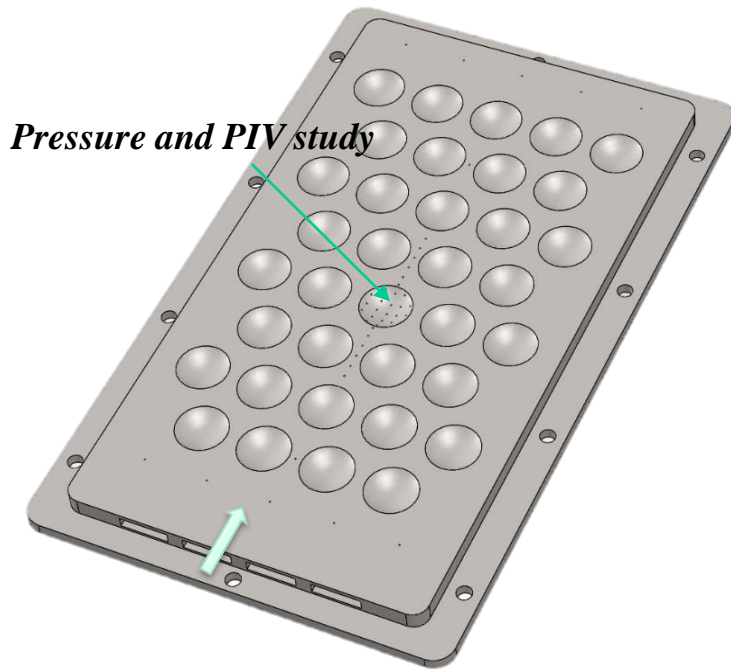
Image Source: Gongnan Xie, Bengtsunden

What about replacing the cylinder pin with dimples?

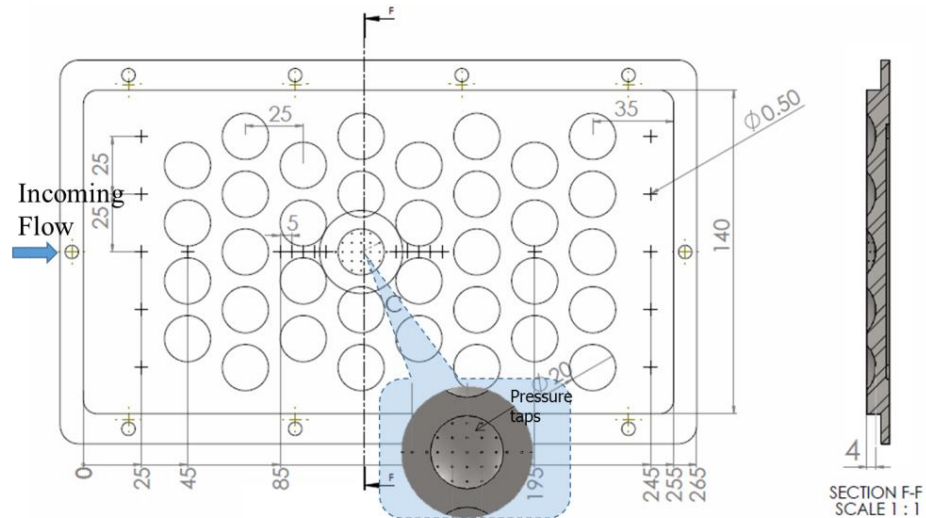
Dimples

- *Modest heat transfer enhancement*
- *Lower pressure loss penalty than fins*

Experimental Setup

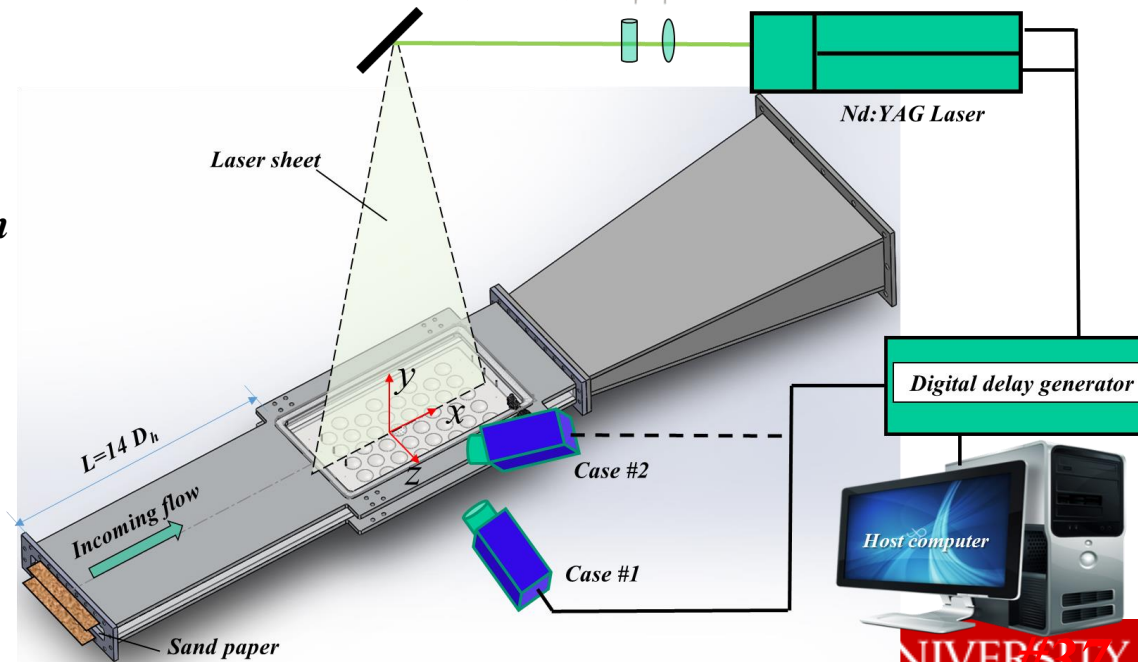


Pressure and PIV study



Hydraulic diameter: $D_h = 35.36 \text{ mm}$

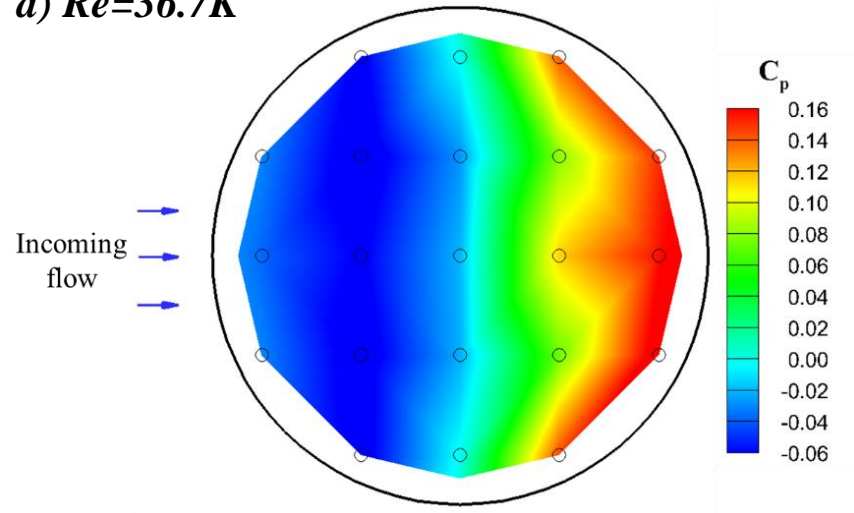
1. Dimple diameter $D = 20 \text{ mm}$
2. Dimple depth $h = 4 \text{ mm}$
3. 21 pressure taps inside dimple
4. Channel height $H = 20 \text{ mm}$
5. $H/D = 1$
6. $h/D = 0.2$



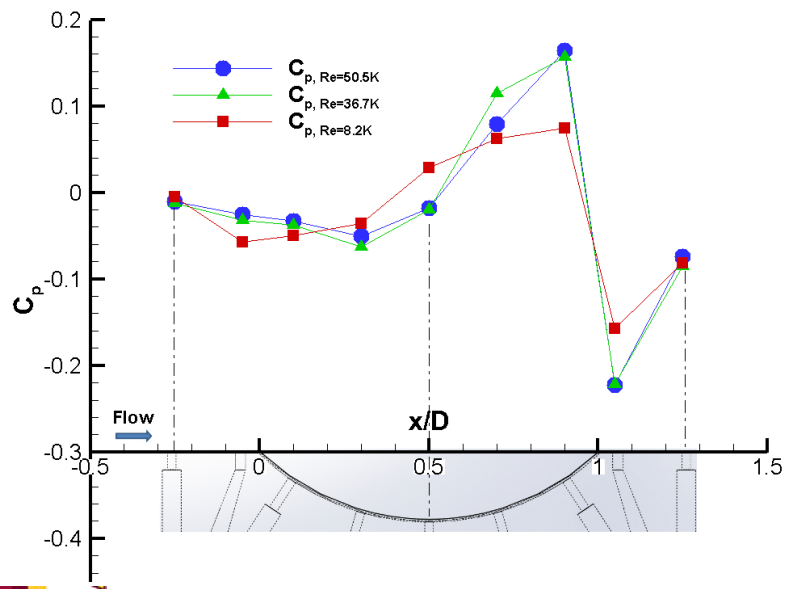
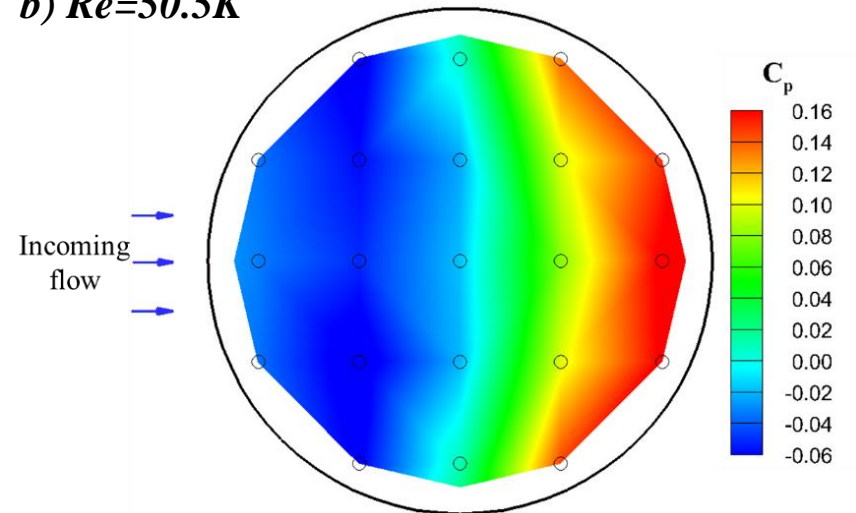


Pressure Distribution inside Dimple

a) $Re=36.7K$



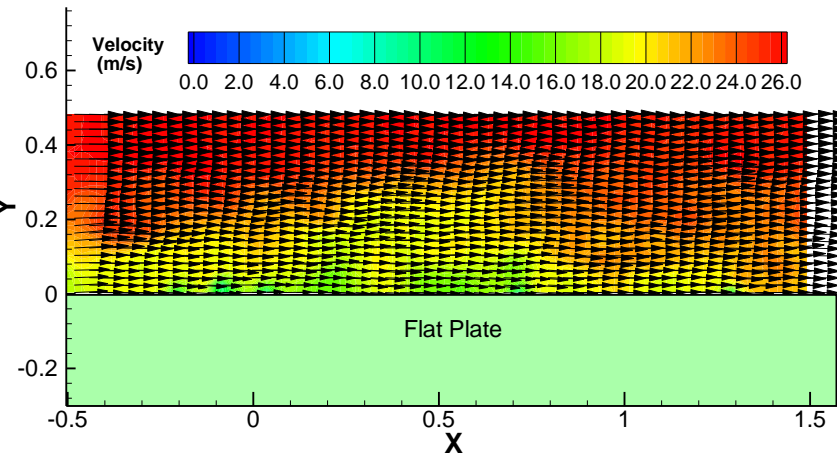
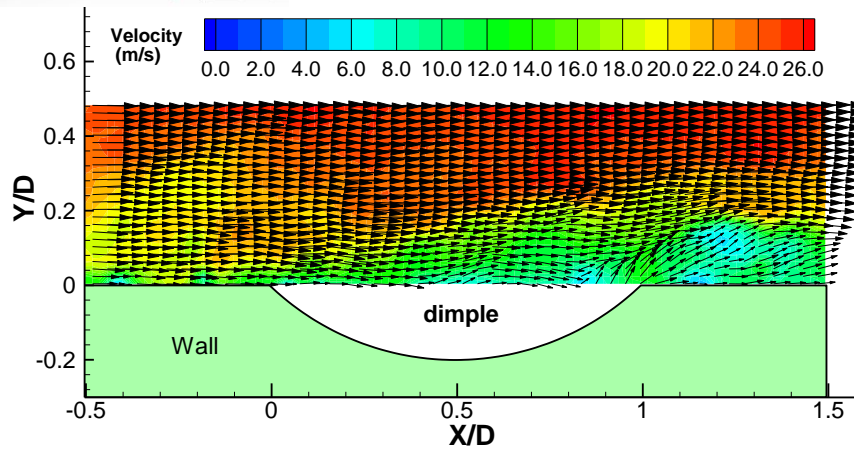
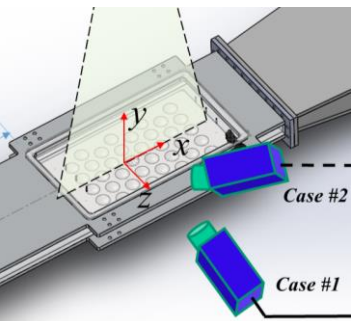
b) $Re=50.5K$



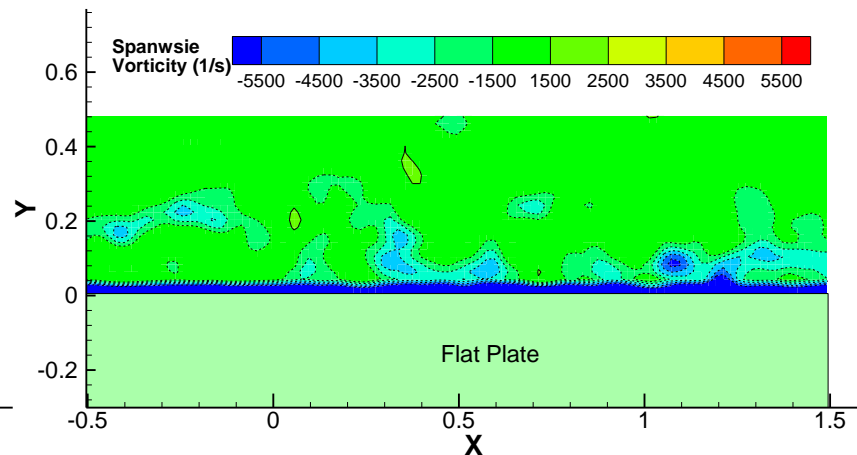
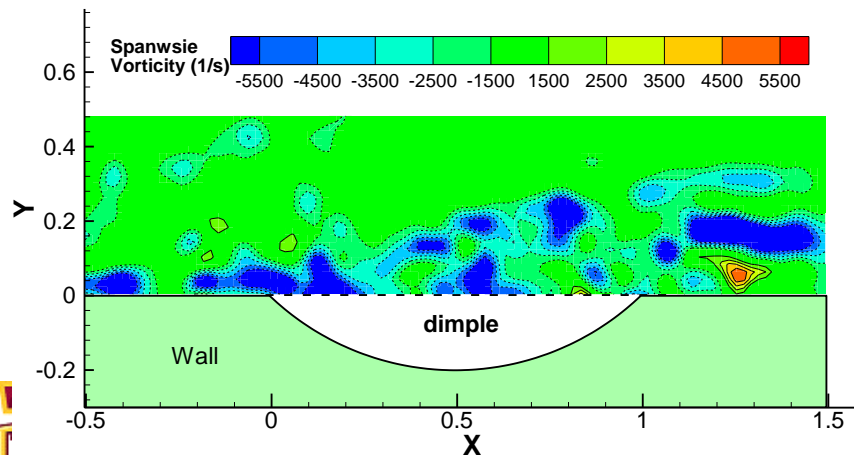
- *Similar pressure distribution for tested cases*
- *Separation at the front, impinging at the back of dimple*
- *Insensitive to Reynolds number*



PIV Measurement Results ($Re=50.5K$)

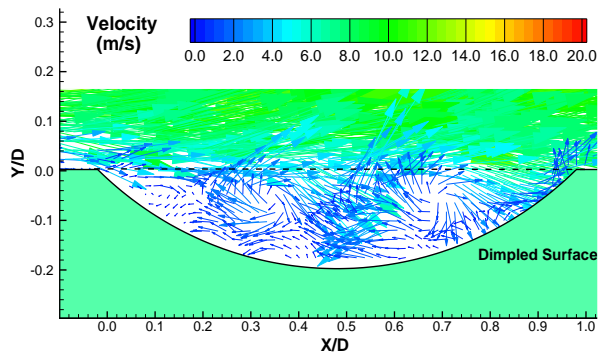
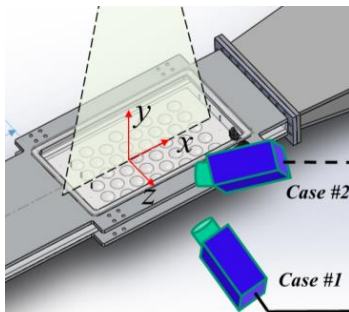


(a). Instantaneous velocity field

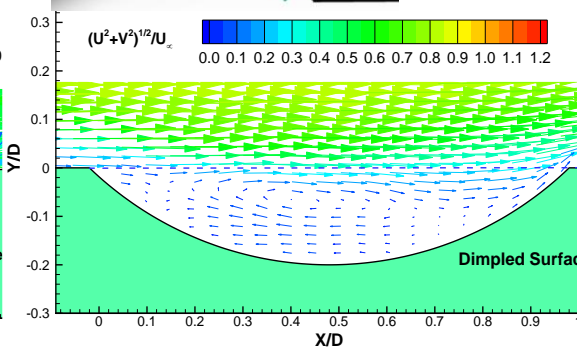


(b). Instantaneous vorticity distributions

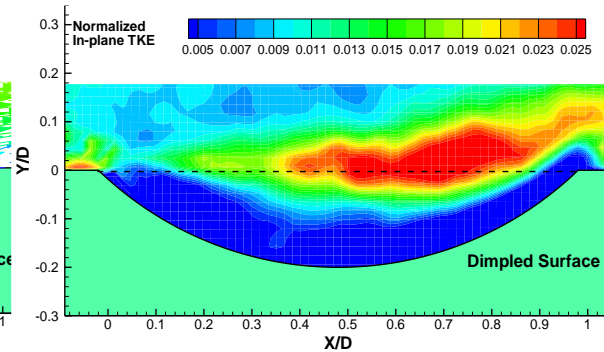
PIV Measurement Results (Inside the dimple, $Re=36.7K$)



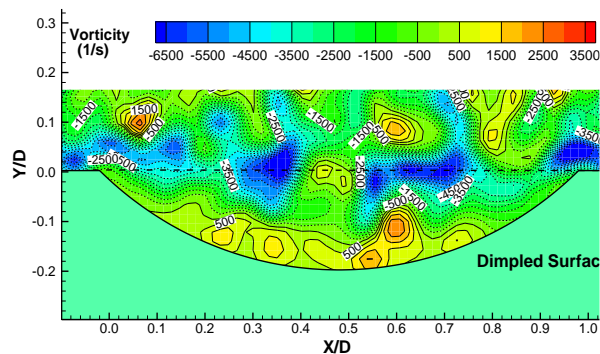
(a). Instantaneous velocity



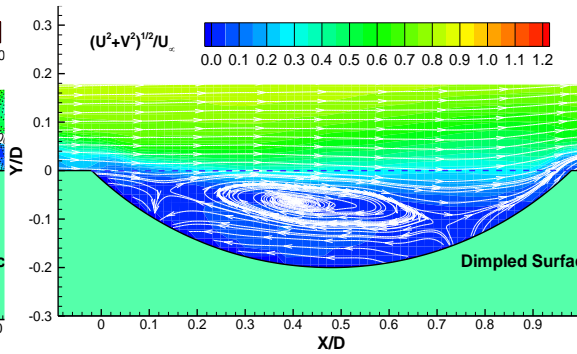
(c). Ensembles-averaged velocity



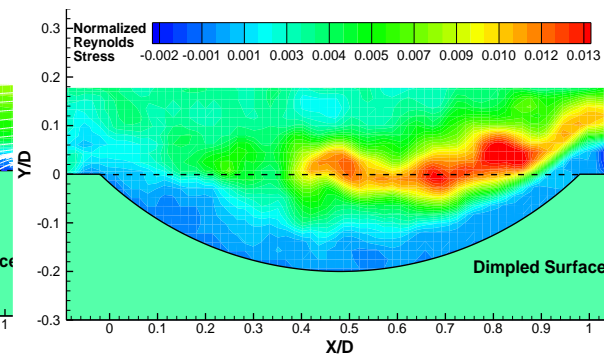
(e). In-plane TKE



(b). Instantaneous vorticity



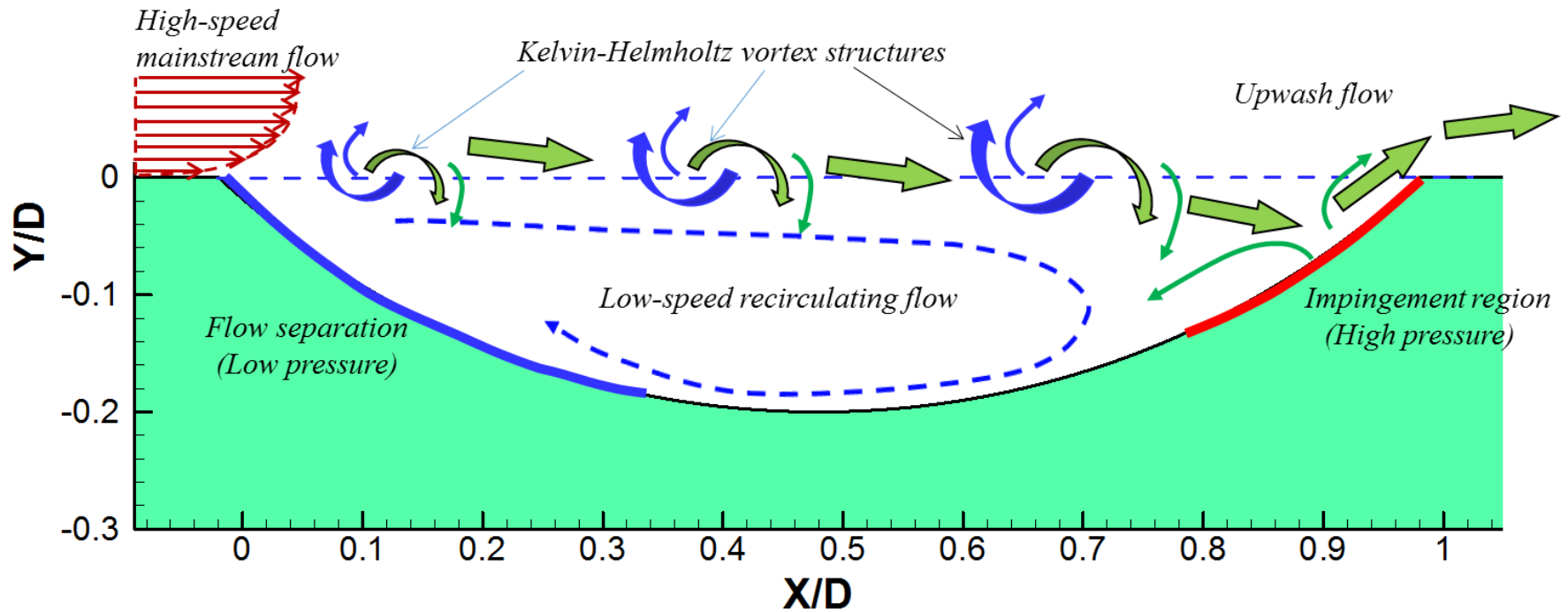
(d). Streamlines of the mean flow



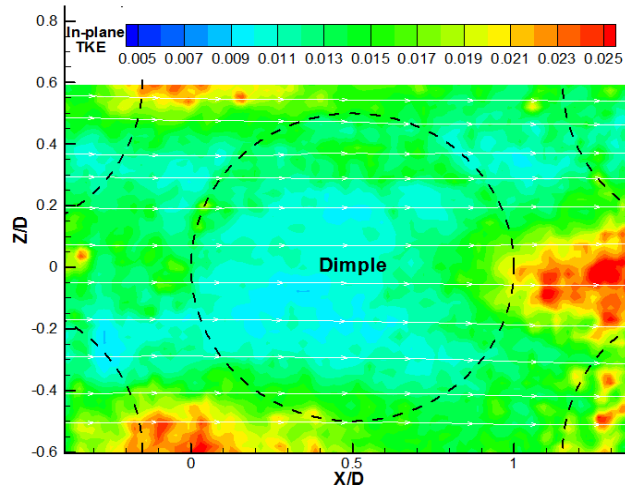
(f). N. Reynolds stress

Similar results for different Reynolds numbers

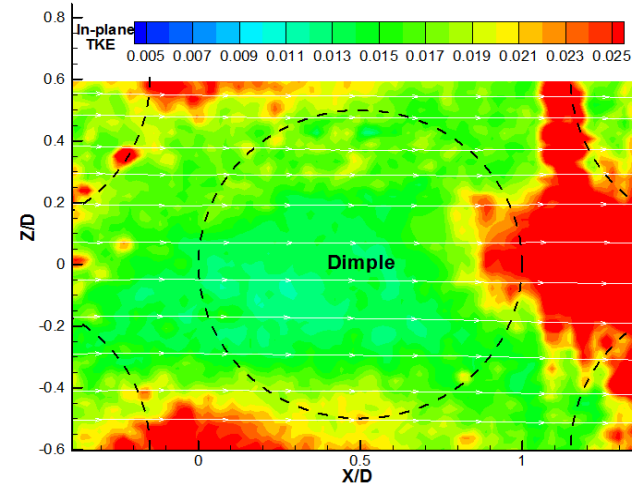
Results and Discussion



PIV Measurement Results

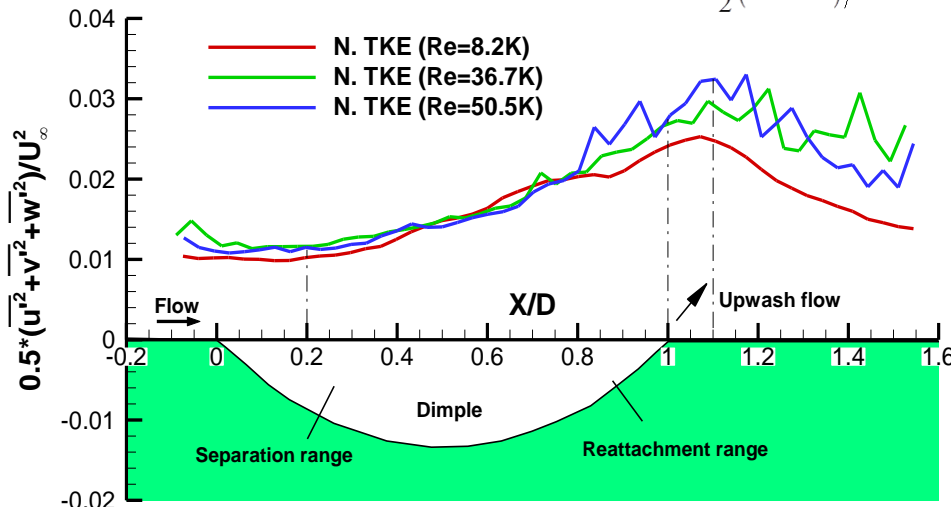


(a) $Re = 36.7K$

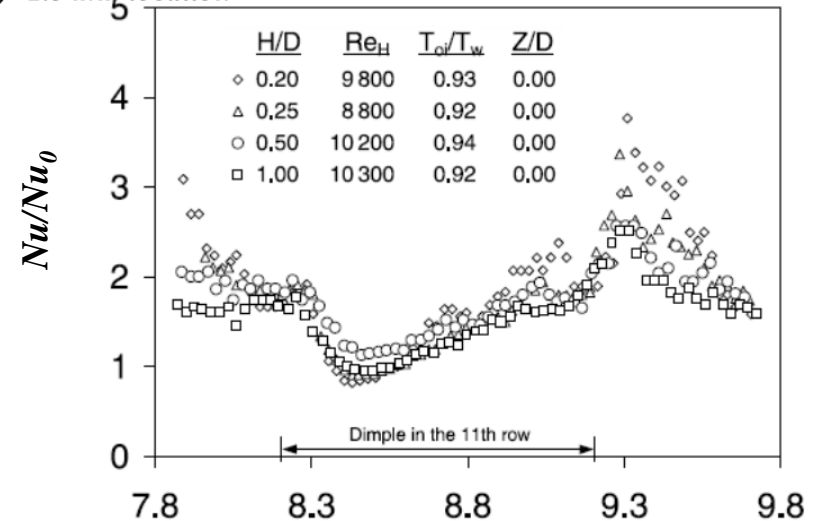


(b) $Re = 50.5K$

In-plane TKE $\frac{1}{2}(\overline{u^2} + \overline{w^2})/U_\infty^2$ at $y = 1.5 \text{ mm}$



(a) Measured TKE profiles of the present study



(b) Local Nu distribution (*Mahmood et al. (2002)*)

Thank You Very Much for Your Time!

Questions?

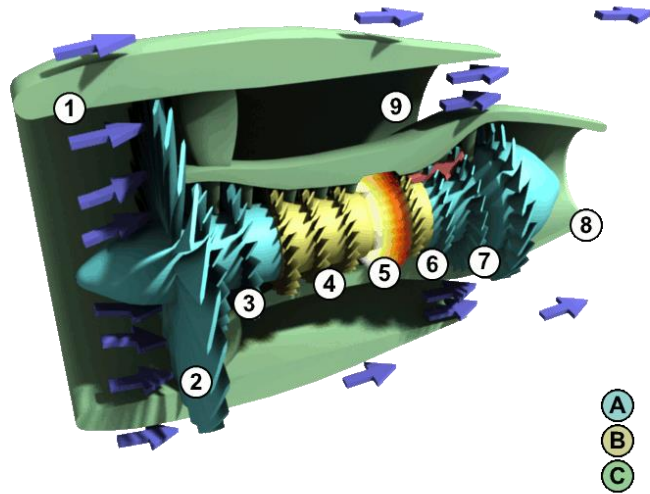
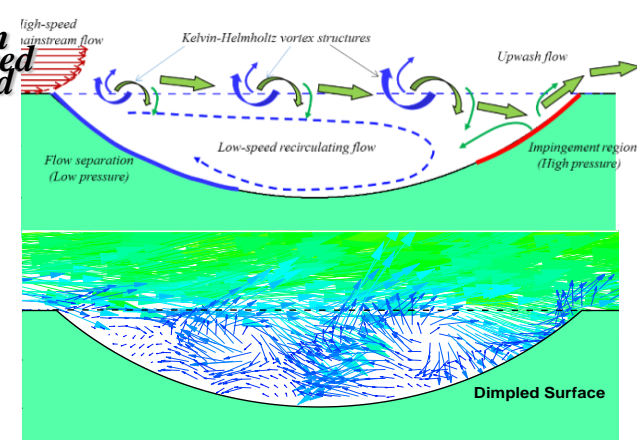
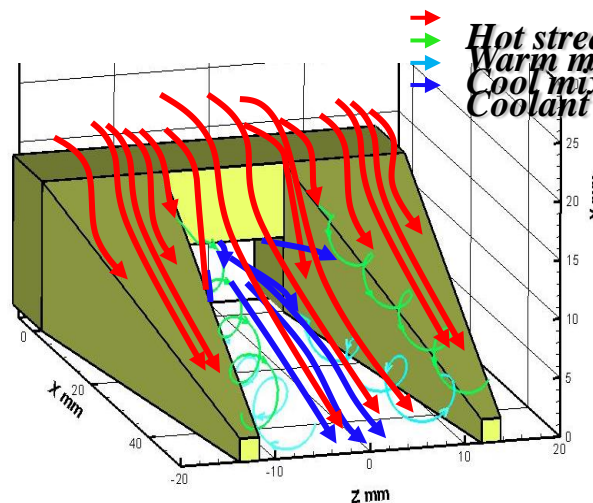
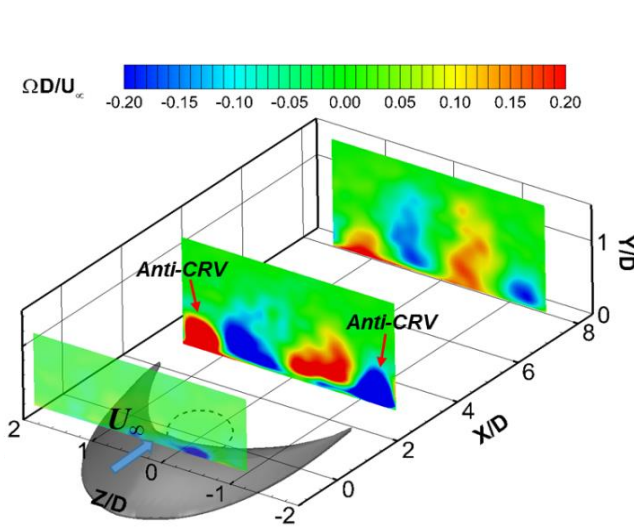


Image Source: Wikipedia.



IOWA STATE UNIVERSITY